Vol. 2.

STRAIN HARDENING AND SOFTENING OF METALS PRODUCED BY CYCLES OF PLASTIC DEFORMATION

by

P. W. J. OLDROYD

B.Sc.(Eng.), A.C.G.I., D.I.C., A.M.I.Mech.E..

Thesis submitted for the degree of Doctor of Philosophy in the Faculty of Engineering of the University of London

Mechanical Engineering Department
City and Guilds College
Imperial College of Science and Technology

January 1968

LIST OF FIGURES

1 Contact-bend-stretch rolling process.

2 Basic circuit showing the principle on which the microformer-operated recording system works.

3 Strain measuring system.

4 The specimen.

5 The end-fitting.

6 The diametral extensometer.

7 Spring bracket mounting for extensometer.

8 Calibration graph for the three strain scales.

9 Stress-strain curves for a cold-worked copper specimen.

10 Diagramatic representation of the strain cycling control system.

11 Stress-strain curves for cold-worked copper cycled at $\pm$1% axial plastic strain, showing the softening caused by cycles of plastic deformation.

12 Location of annealed copper specimens in 3 in. diameter bar.

13 Location of bars for cold drawing in the 3 in. diameter bar.

14 Location of bars for swaging in the 3 in. diameter bar.

15 Location of aluminium specimens in the 2.312 in. diameter bar.

16 Location of stainless steel specimens in 2 3/4 in. diameter bar.

17 Stress-strain curves for annealed copper cycled at $\pm$1% axial plastic strain, showing the hardening caused by cycles of plastic deformation.

18 Effect of plastic strain range on the cyclic hardening of annealed copper.

19 Cyclic hardening and softening of cold-worked copper.

20 Effect of method of cold-working on cyclic hardening and softening of copper: $\pm$1% axial plastic strain.

21 Effect of degree of cold-working on cyclic hardening and softening of copper: $\pm$1% axial plastic strain.

22 Comparison of step and constant strain amplitude behaviour of annealed copper.

23 Cyclic and static stress-strain curves for copper.

24 Effect of direction of initial loading on cyclic hardening of annealed copper.

25 Variation of creep rate with mean nominal streee: Annealed copper cycled at a stress range of 12.4 tons/in^2.

26 Cyclic softening of roller swaged copper: Nomonal stress limits of $\pm$15.2 tons/in^2.

27 Tension and compression tests for annealed copper.

28 Reverse loading curves for annealed copper.

29 Series of reverse loading tests on a specimen of annealed copper.

30 Tension and reverse loading curves for cold-worked copper.

31 Tension tests following sequences of cycling at progressively decreasing strain amplitudes.

32 Reduction of the Bauschinger effect in cycled annealed copper: Plastic strain range $\pm$0.5%.

33 Rates of hardening compared for cyclic and uni-directional deformation.

34 The Bauschinger effect compared for cyclic and uni-directional deformation.

35 Effect of plastic strain range on the cyclic hardening of annealed aluminium.

36 Effect of plastic strain range on the cyclic softening of cold-drawn aluminium.

37 Cyclic and static stress-strain curves for annealed aluminium.

38 Variation of creep rate with mean nominal stress: Annealed aluminium cycled at a stress range of 3.8 tons/in^2.

39 Tension and reverse loading curves for annealed aluminium.

40 Tension and reverse loading curves for cold-drawn and annealed aluminium.

41 Stress-strain curves for En25 steel, hardened from 840°C and tempered at 450°C, cycled at ±1% axial plastic strain.

42 Effect of plastic strain range on the cyclic softening of En25 steel.

43 Cyclic stress-strain loops compared for effect of tensile or compressive loading in the first cycle: (Latter is drawn with signs reversed): Annealed En25 steel at ±1% plastic strain: 1st and 40th cycles are shown.

44 Cyclic softening of hardened and tempered En25 steel: ±1% axial plastic strain.

45 Cyclic and static stress-strain curves for En25 steel.

46 The cyclic softening of cold stretched En25 steel: ±1% axial plastic strain.

47 Effect of rest periods between cycles on the stress-strain loop for hardened and tempered En25 steel.

48 Tension and compression tests on annealed En25 steel.

49 Reverse loading curves for annealed En25 steel.

50 Tension tests for En25 steel hardened at 840°C and tempered from 550°C.

51 Tension and reverse loading curves for heat treated En25 steel.

52 The Bauschinger effect in cycled annealed En25 steel: Plastic strain range ±1%.

53 Tension test following a series of cycles of progressively decreasing strain amplitude.

54 Compression test following a series of cycles of progressively decreasing strain amplitude.

55 Reduction of the Bauschinger effect in cycled annealed En25 steel: Plastic strain range ±1%.

56 The effect of plastic strain range on the cyclic hardening of austenitic stainless steel.

57 Cyclic and static stress-strain curves for austenitic stainless steel.

58 Tension and compression tests on austenitic stainless steel.

59 Reverse loading curves for austenitic stainless steel

60 Diagramatic illustration of the use of simple reverse loading curves to derive cyclic hardening stress-strain loops.

61 The settled cyclic stress-strain curve predicted from simple reverse loading tests.

62 Demonstration that the Bauschinger effect cannot be eliminated by interrupting the settled cyclic loop at a selected point.

63 Pin jointed bar analogue model for cyclic behaviour.

64 Spring-block analogue model for cyclic behaviour.

65 Typical stress-strain diagrams for anspring-block model

LIST OF PLATES
(Figures Nos. 66 to 73.)

66 The extensometer in position on the specimen.

67 The specimen and the dismantled extensometer.

68 Modification panel and plug ready for attachment to the chart drive circuit. (Front view.)

69 Modification panel and plug ready for attachment to the chart drive circuit. (Rear view.)

70 Modification panel in place on the chart drive amplifier.

71 The fixed and moving contacts on the pen recorder unit.

72 The end-fittings. (One dismantled.)

73 The Instron testing machine.

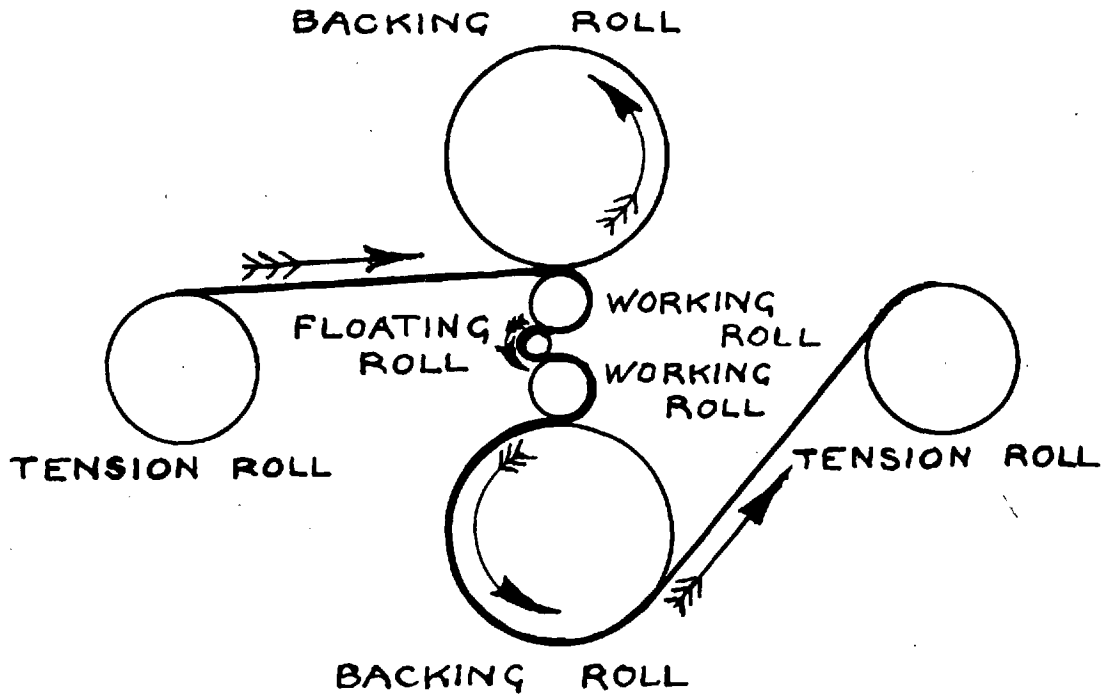

Fig. 1. Contact-bend-stretch rolling process.

Fig. 2. Basic circuit showing the principle on which the microformer-operated recording system works.

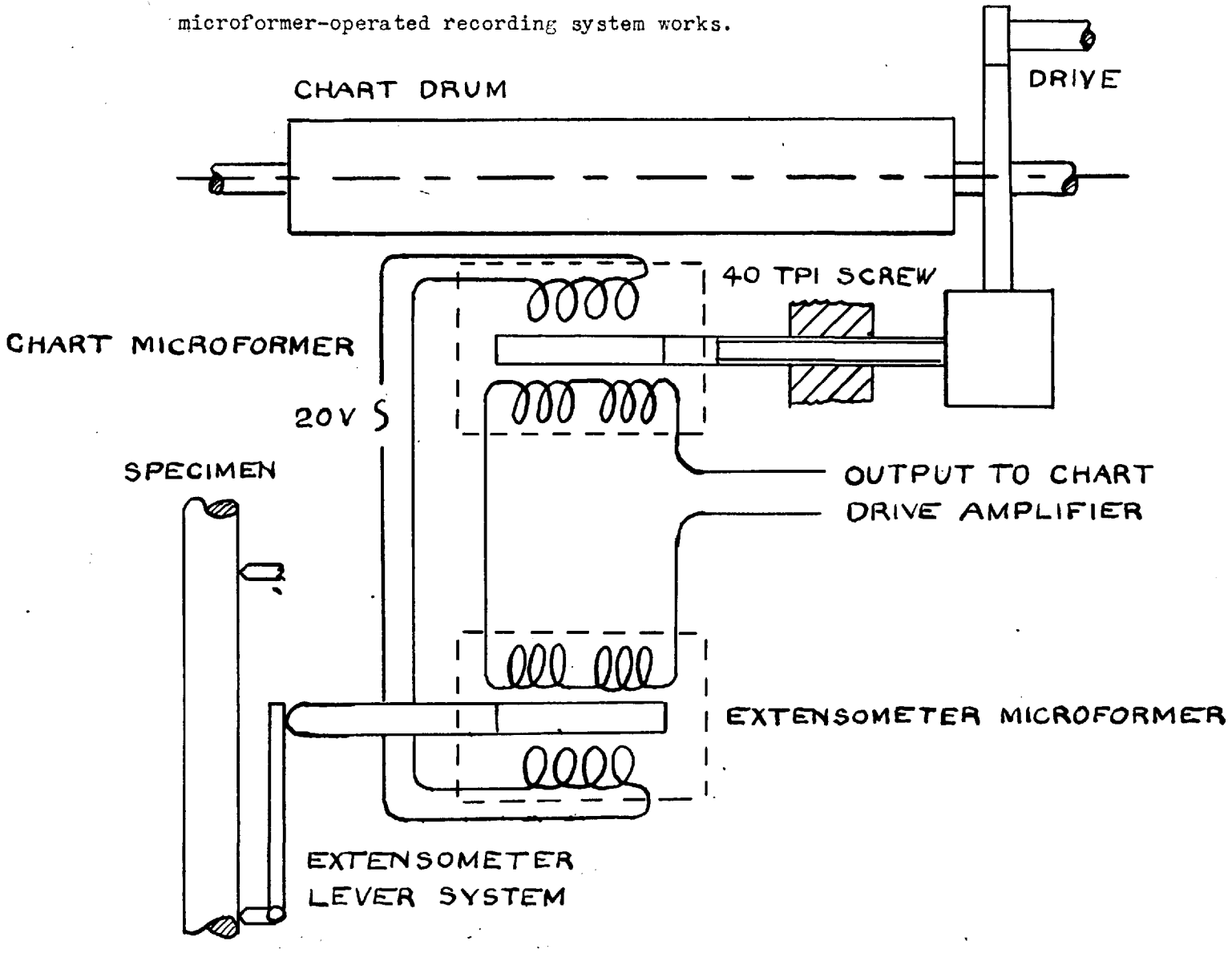

(a) Original circuit.

(b) Modified circuit.

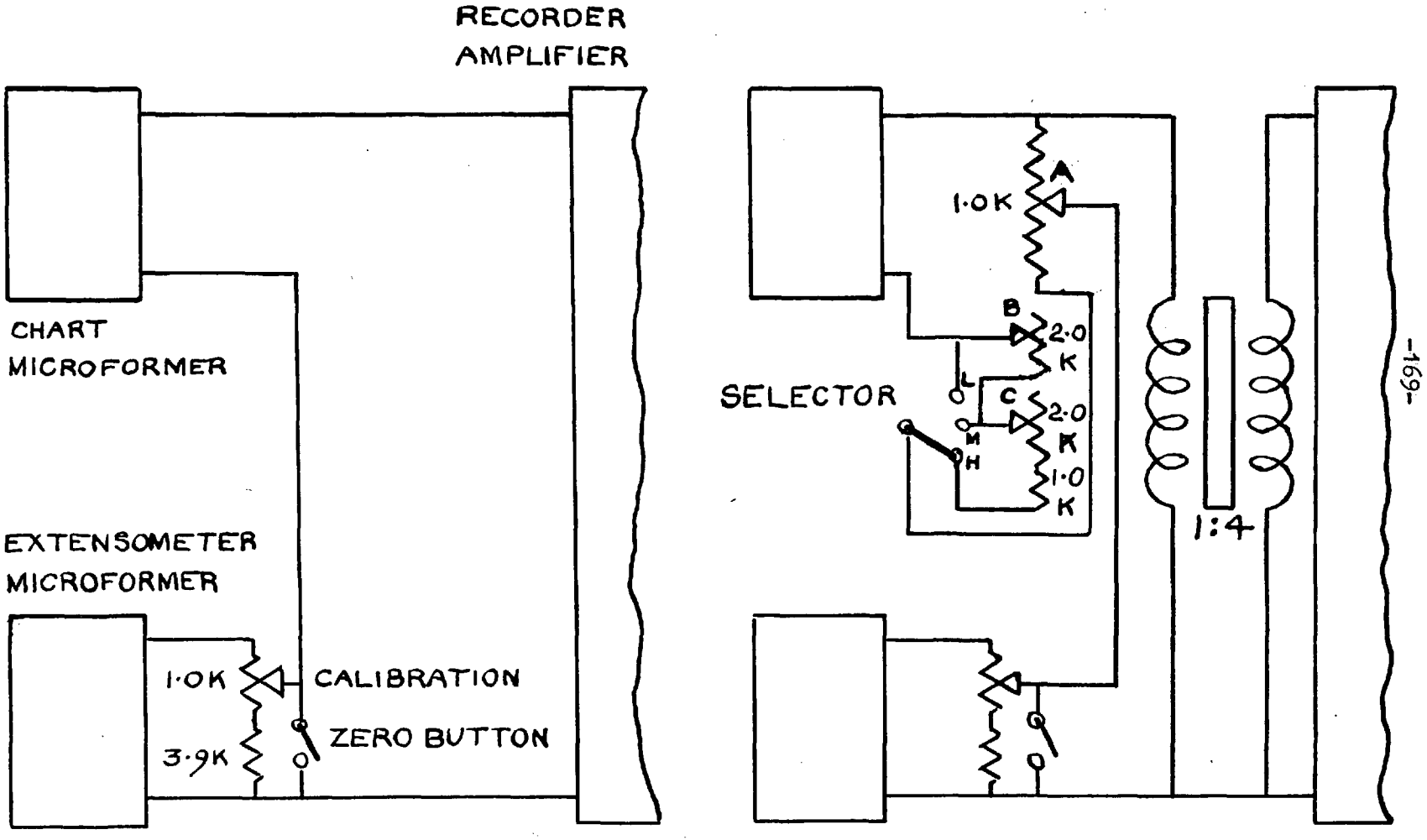

Fig.3. Strain measuring system.

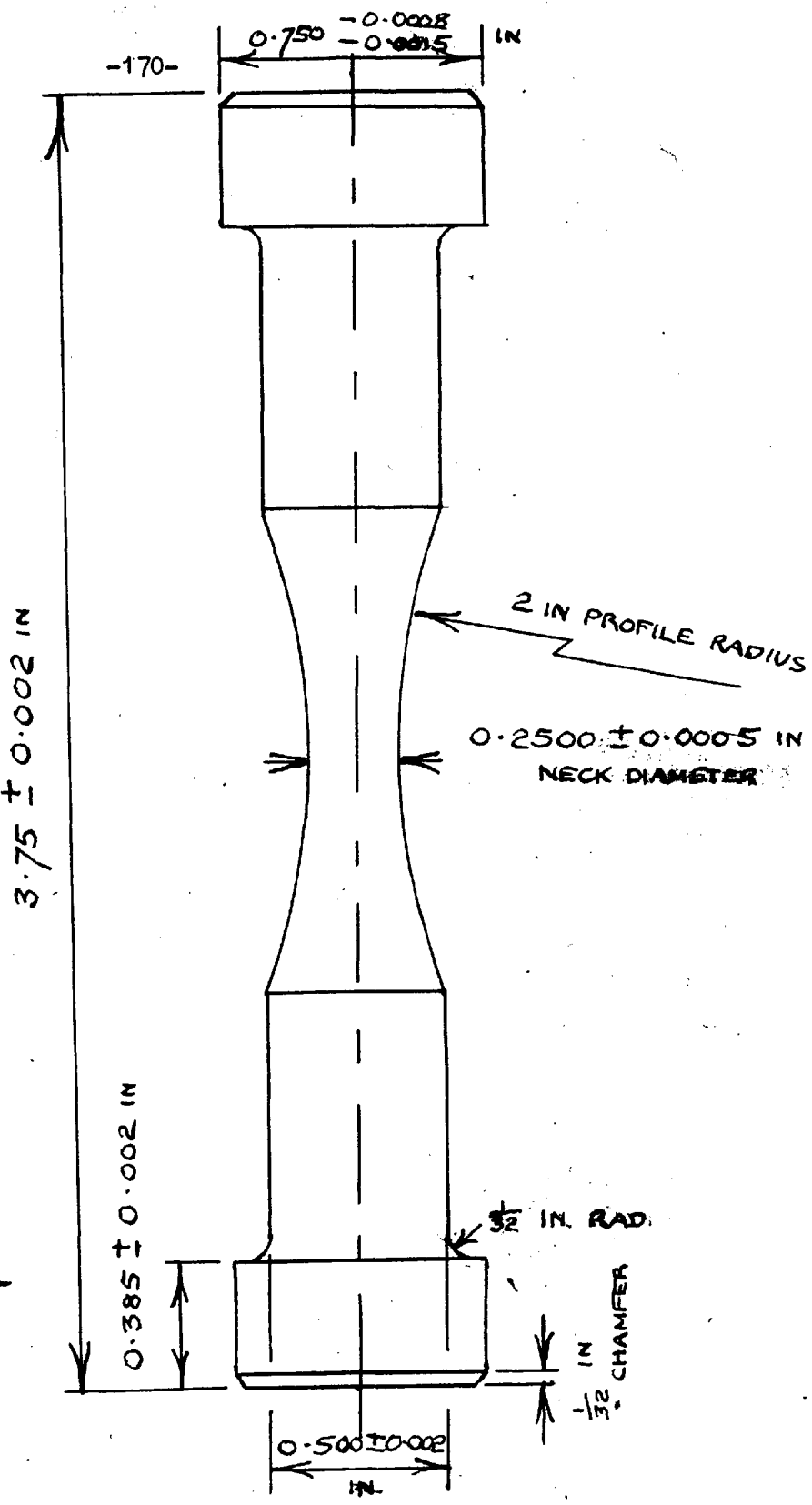

Fig. 4. The specimen.

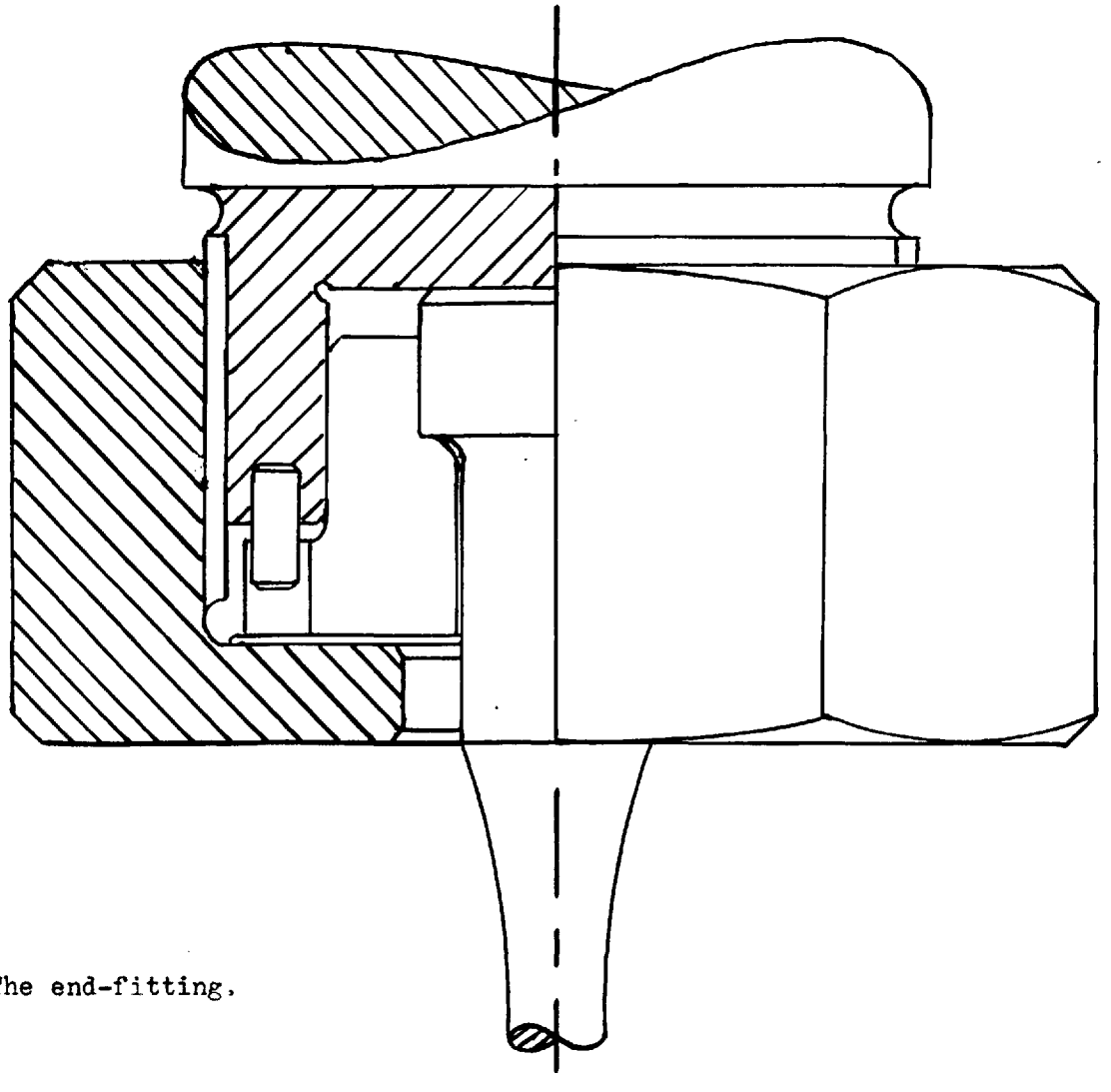

Fig. 5. The end-fitting.

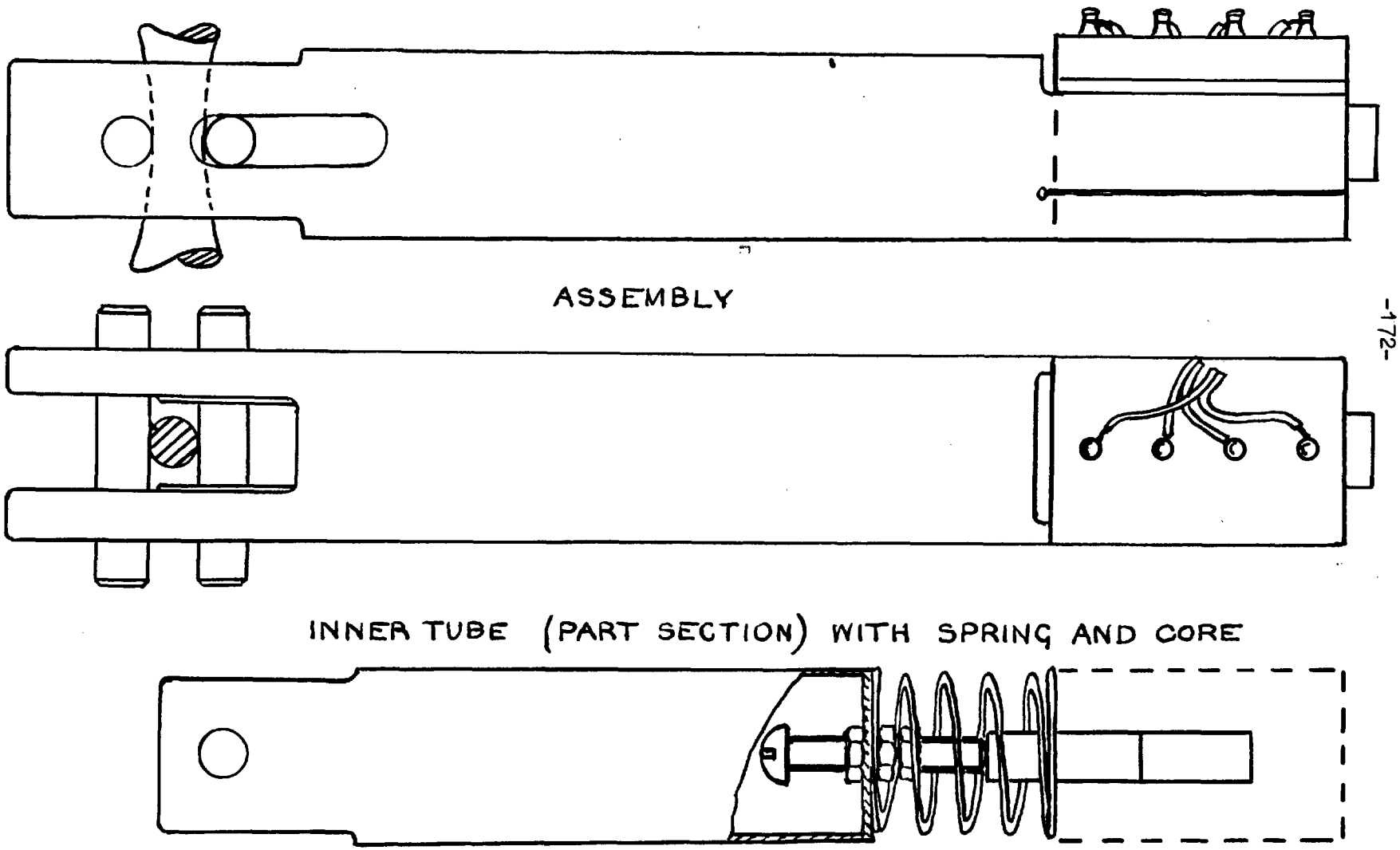

Fig. 6. The diametral extensometer, shown in position on a specimen.

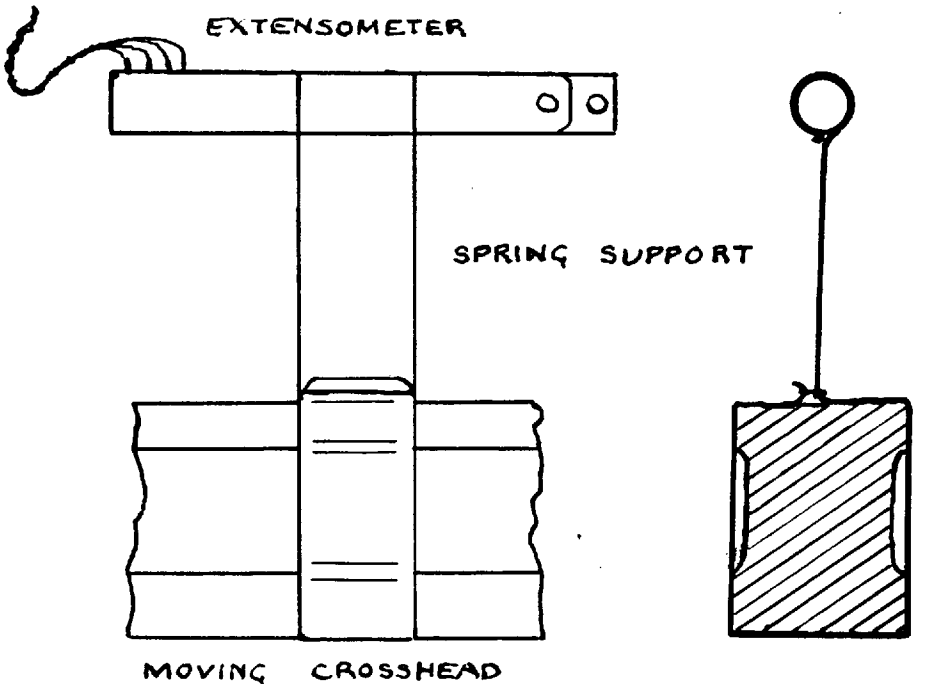

Fig. 7. Spring bracket mounting for extensometer.

Fig. 8.

Fig. 8. Calibration graph for the three strain scales.

Fig. 9.

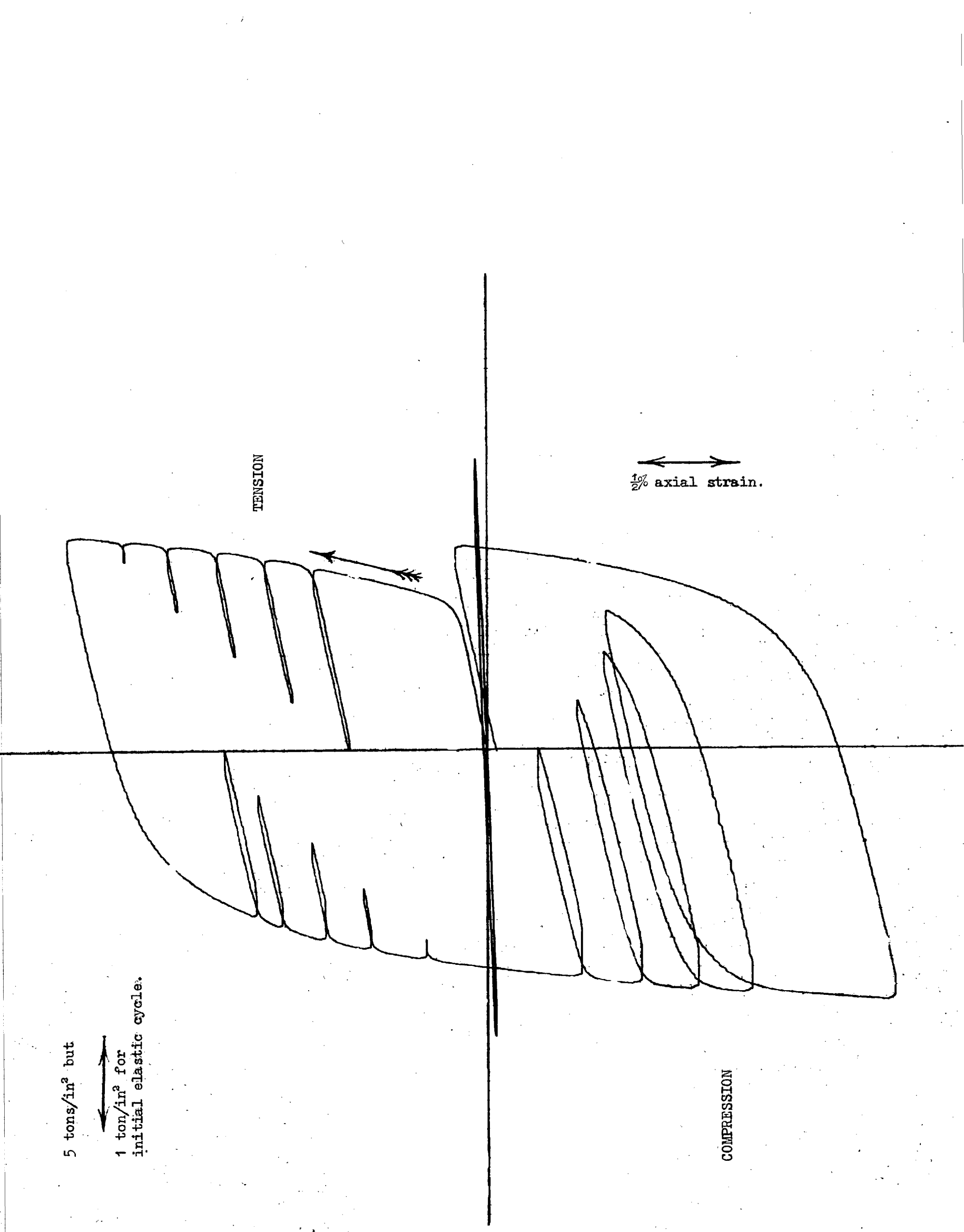

Fig. 9. Stress-strain curves for a cold worked copper specimen.

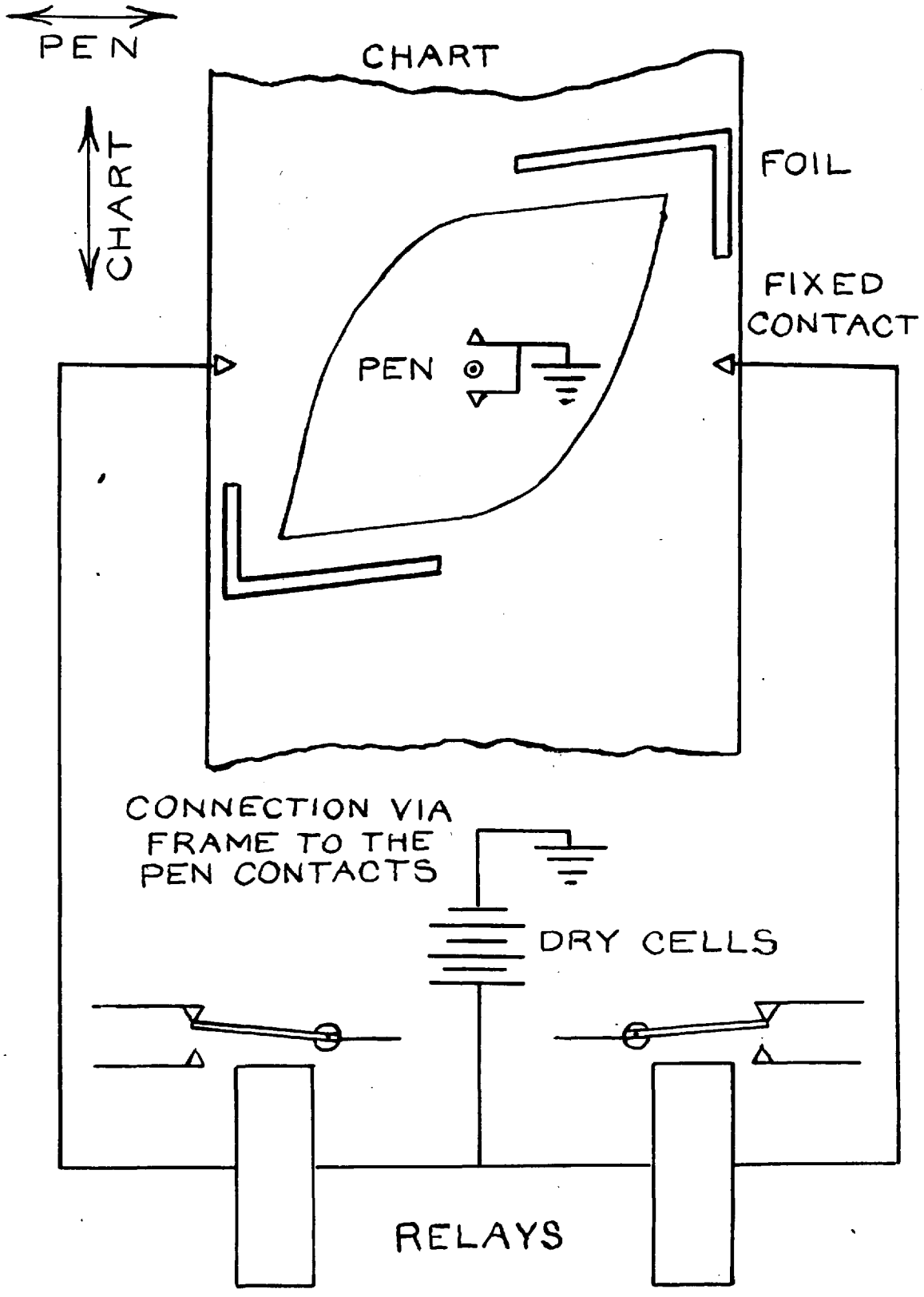

Fig. 10. Diagramatic representation of strain cycling control system.

Fig. 11.

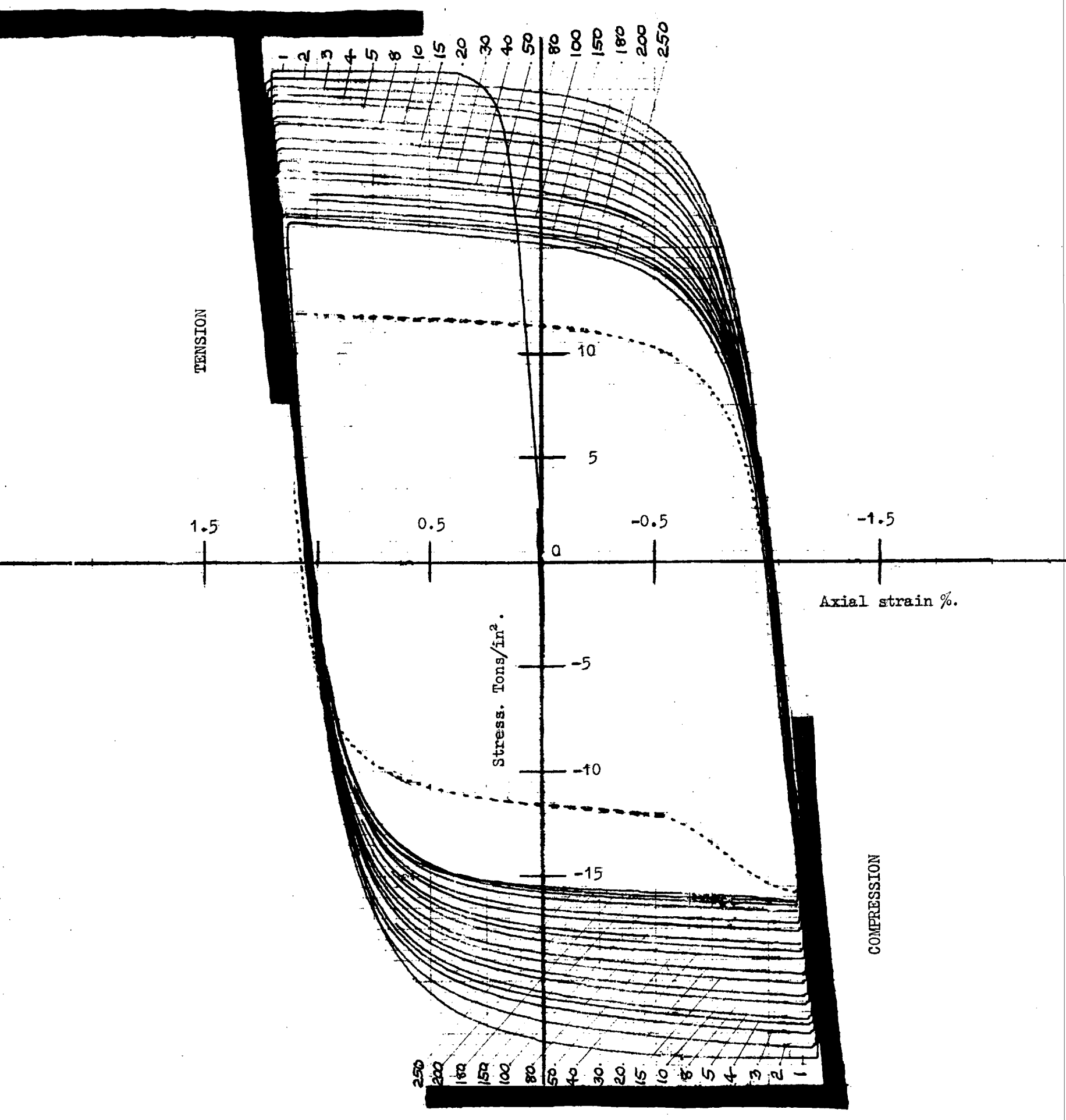

Fig. 11. Stress-strain curves for cold worked copper cycled at ±1% axial plastic strain, showing the softening caused by cycles of plastic deformation.

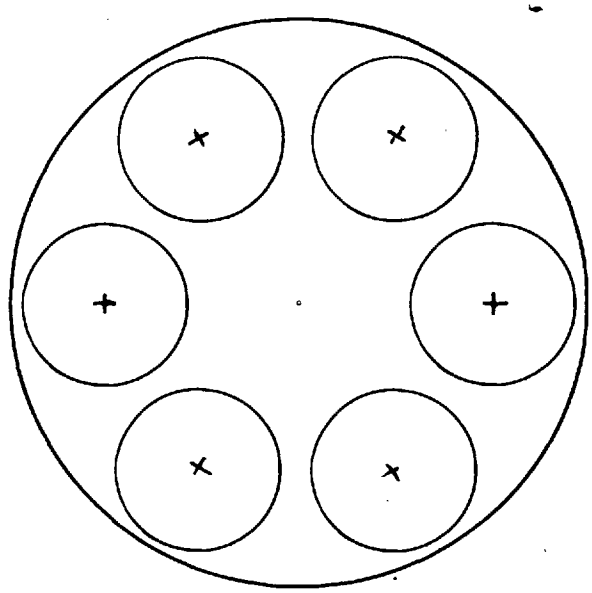

Fig. 12. Location of annealed copper specimens in 3 in. diameter bar.

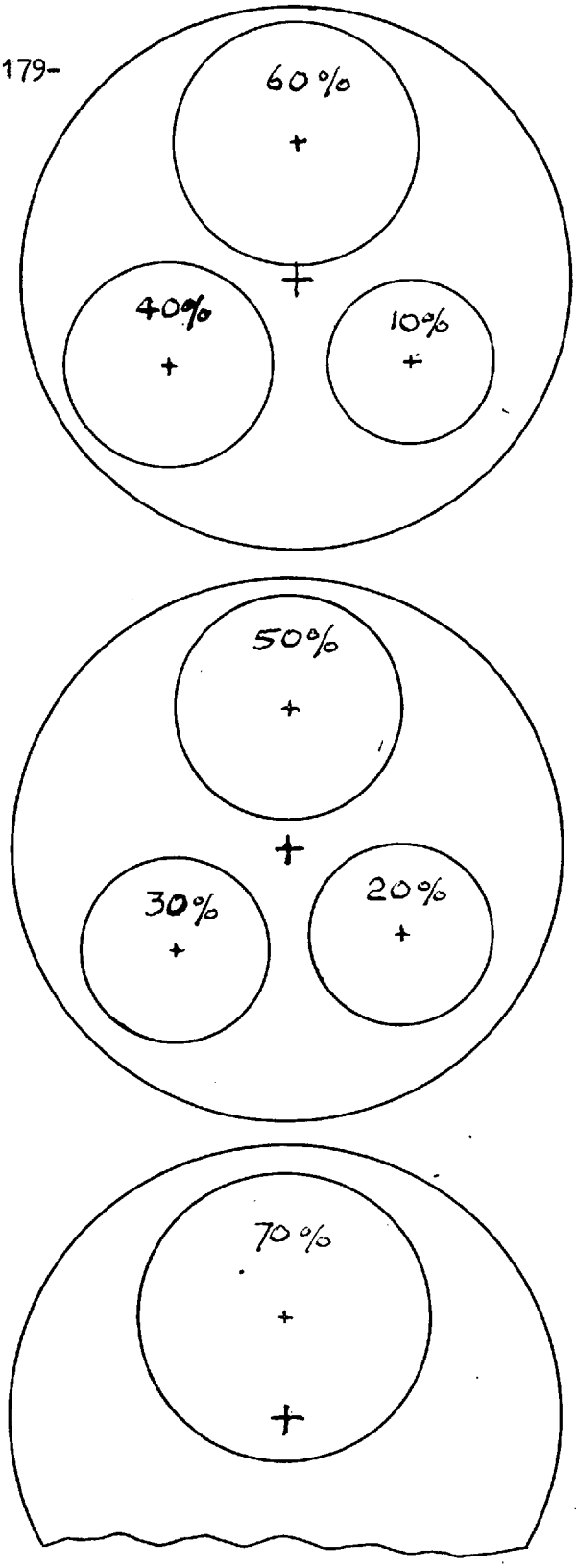

Fig. 13. Location of bars for cold drawing in the 3 in. diameter bar.

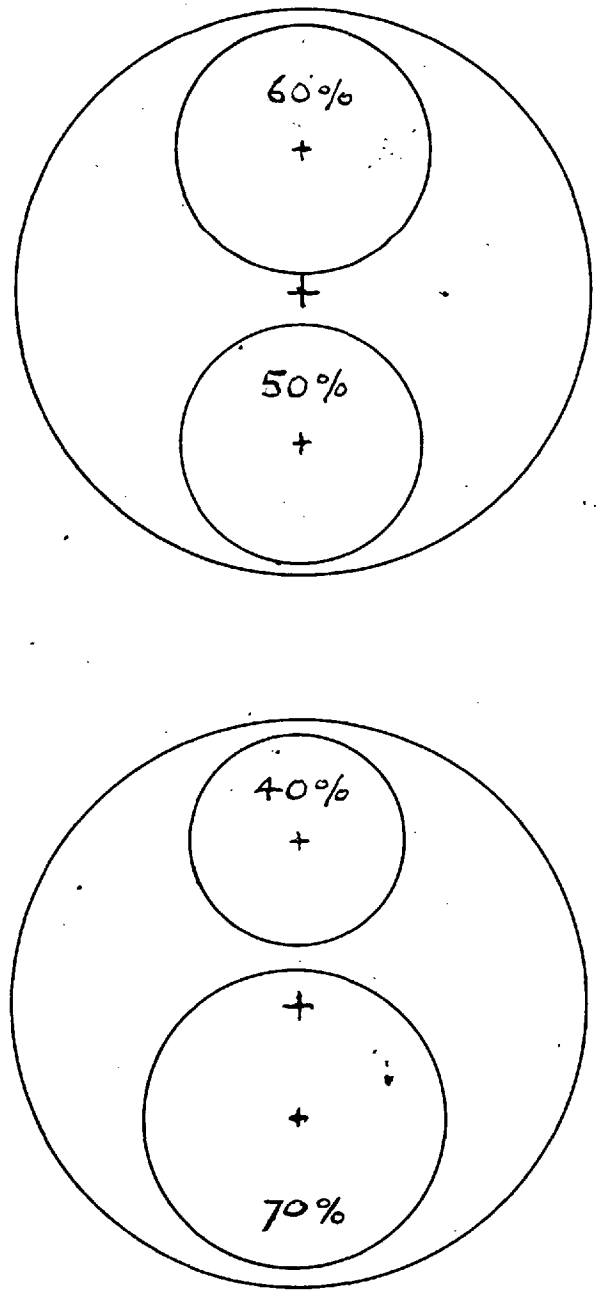

Fig. 14. Location of bars for swaging in the 3 in. diameter bar.

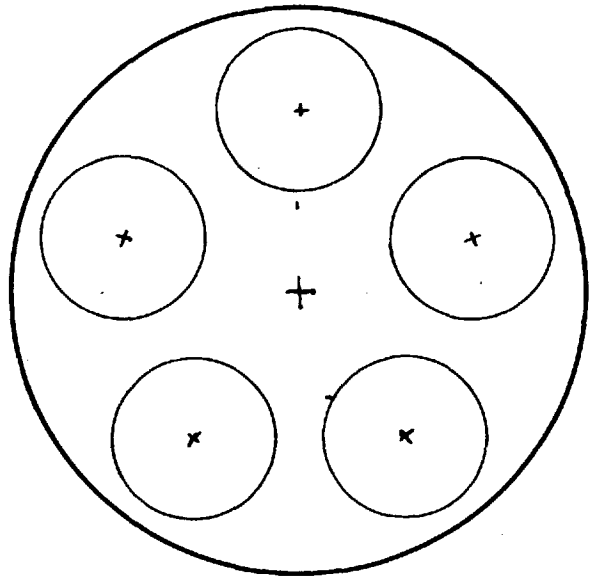

Fig. 15 Location of aluminium specimens in 2.312 in. diameter bar.

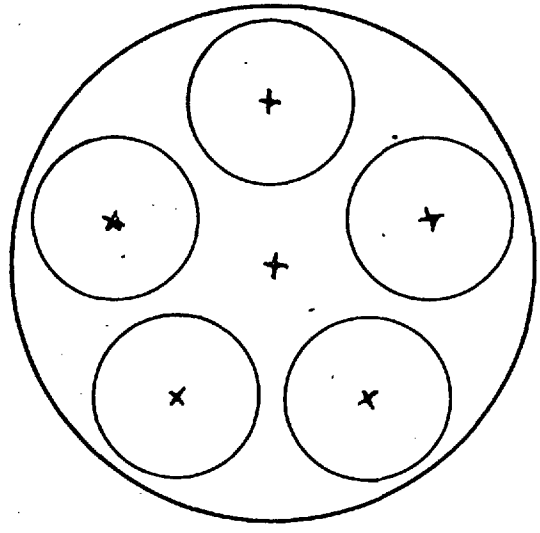

Fig. 16. Location of stainless steel specimens in 2 3/4 in. diameter bar.

Fig. 17:

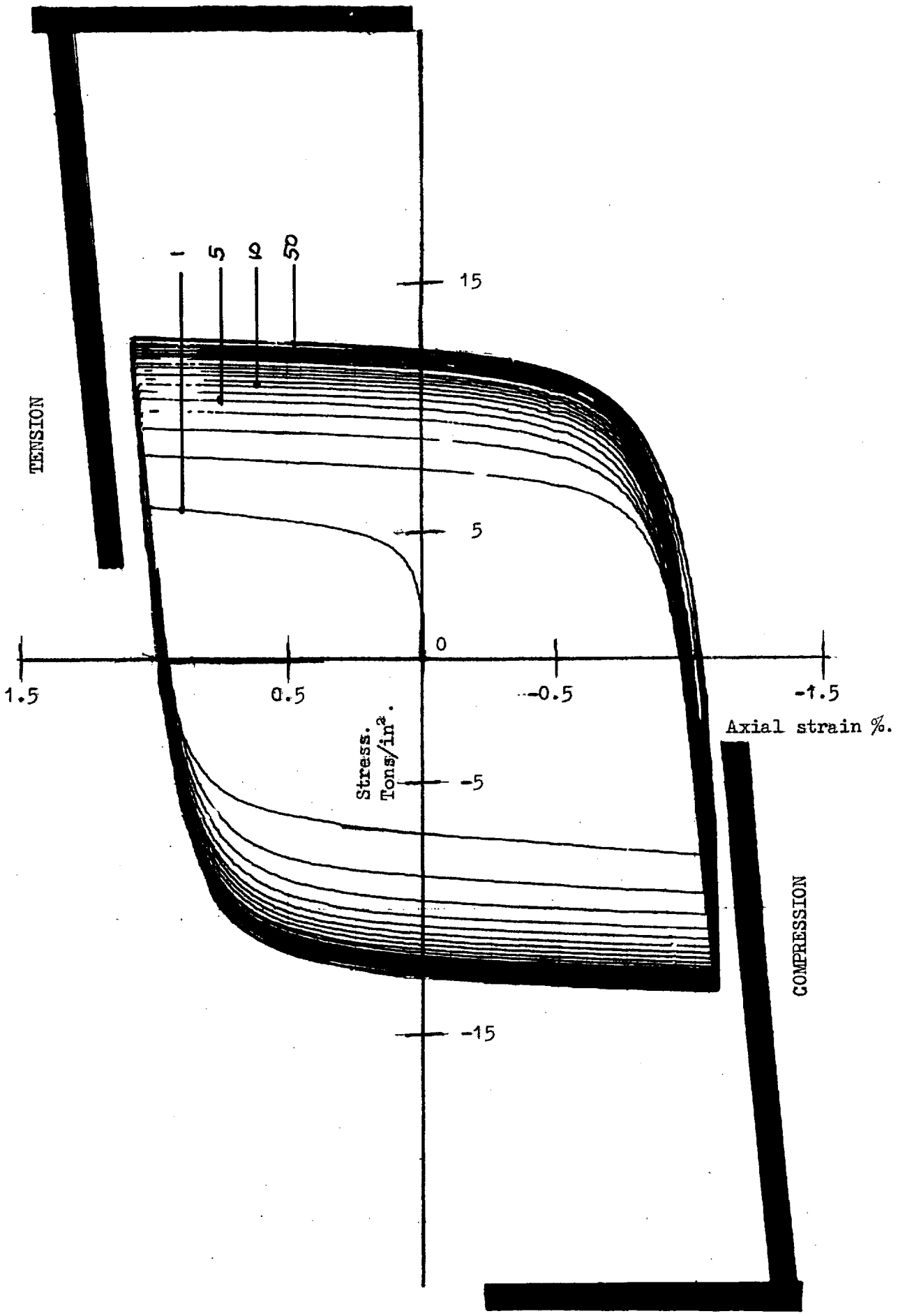

Fig. 17. Stress-strain curves for annealed copper cycled at $\pm$1% axial plastic strain, showing the hardening caused by cycles of plastic deformation.

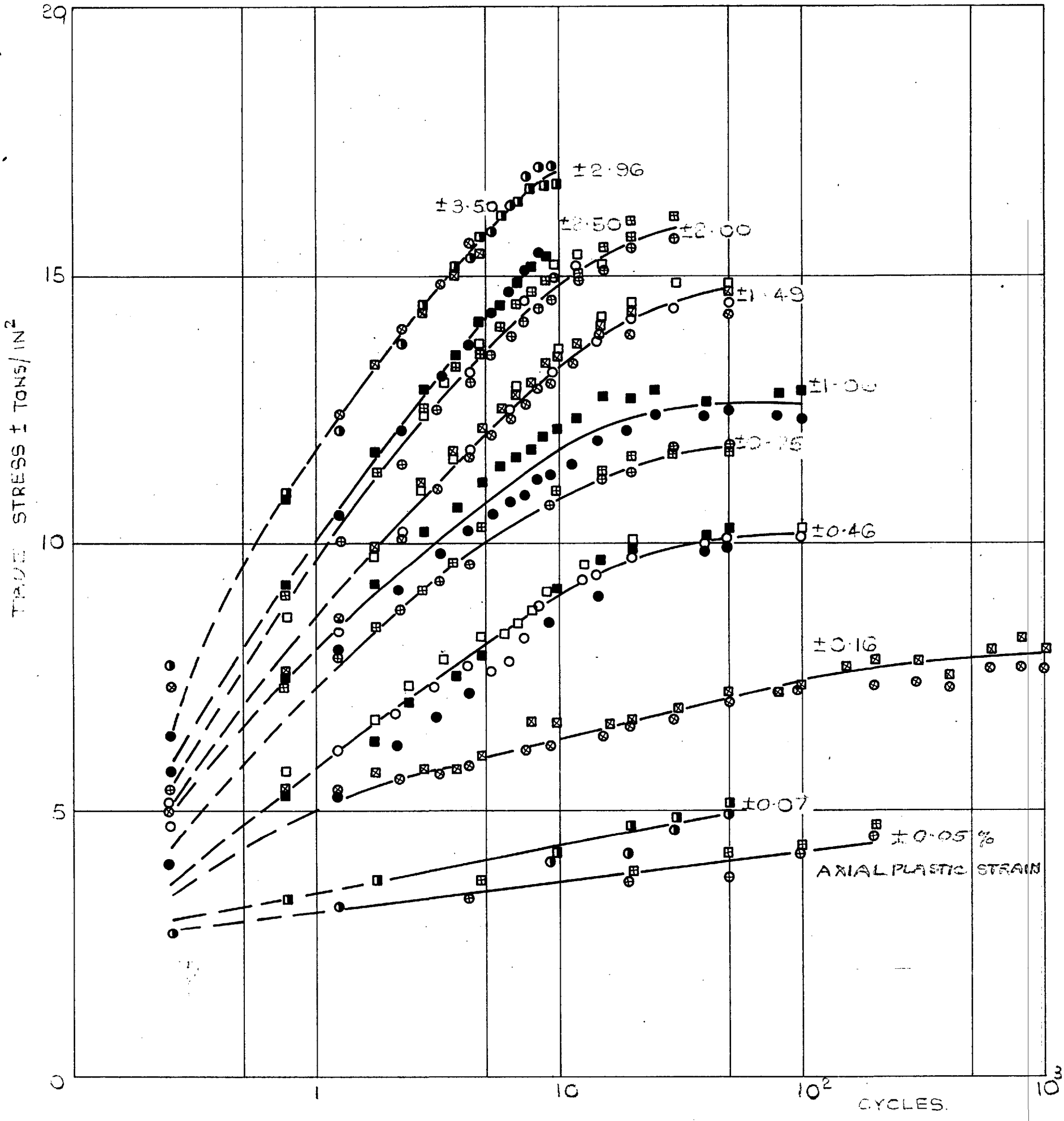

Fig. 18. Effect of plastic strain range on the cyclic hardening of annealed copper.

Fig. 18.

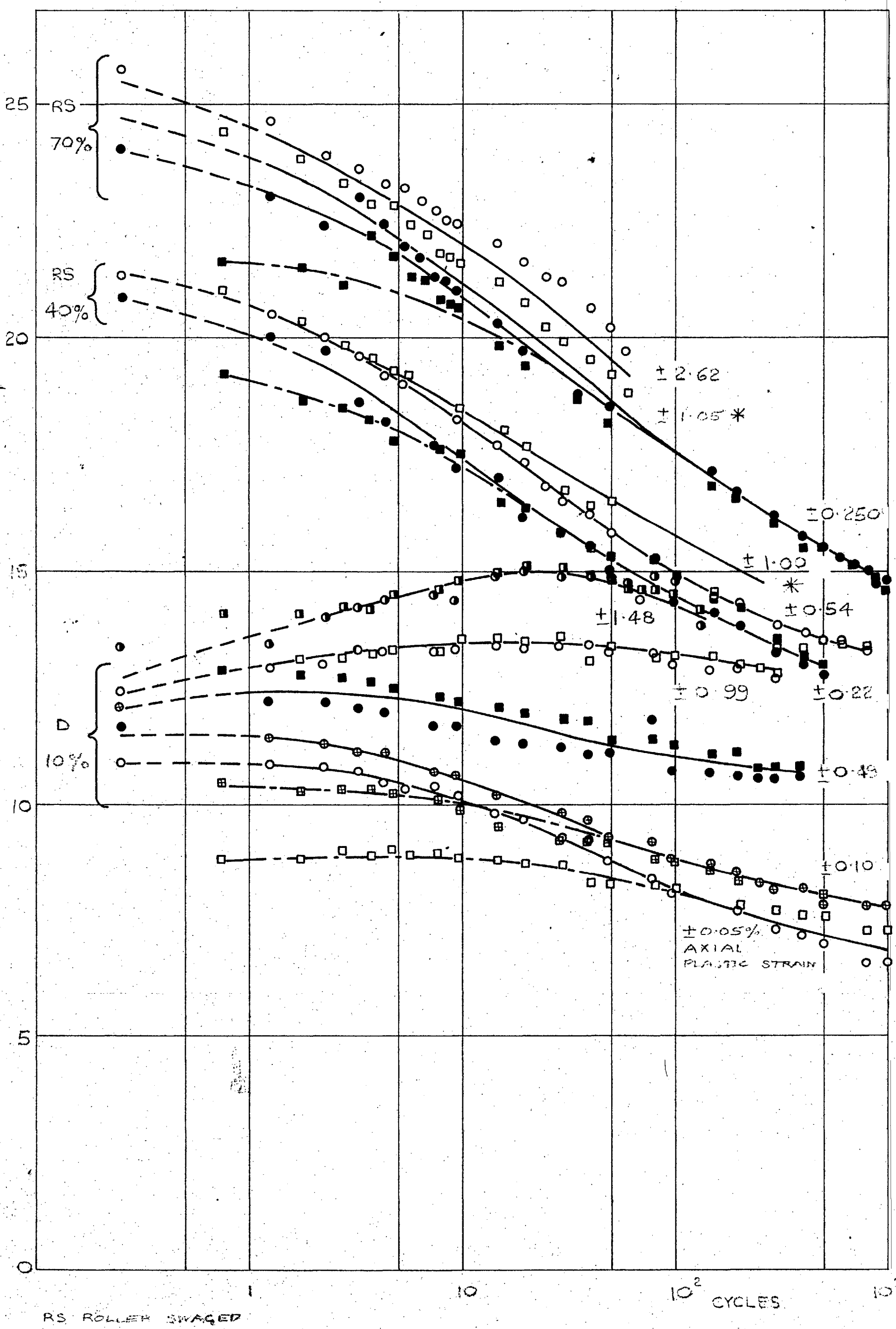

RS ROLLER SWAGED
D DRAWN

* POINTS SHOWN ON ANOTHER FIGURE.

Fig. 19. Cyclic hardening and softening of cold-worked copper.

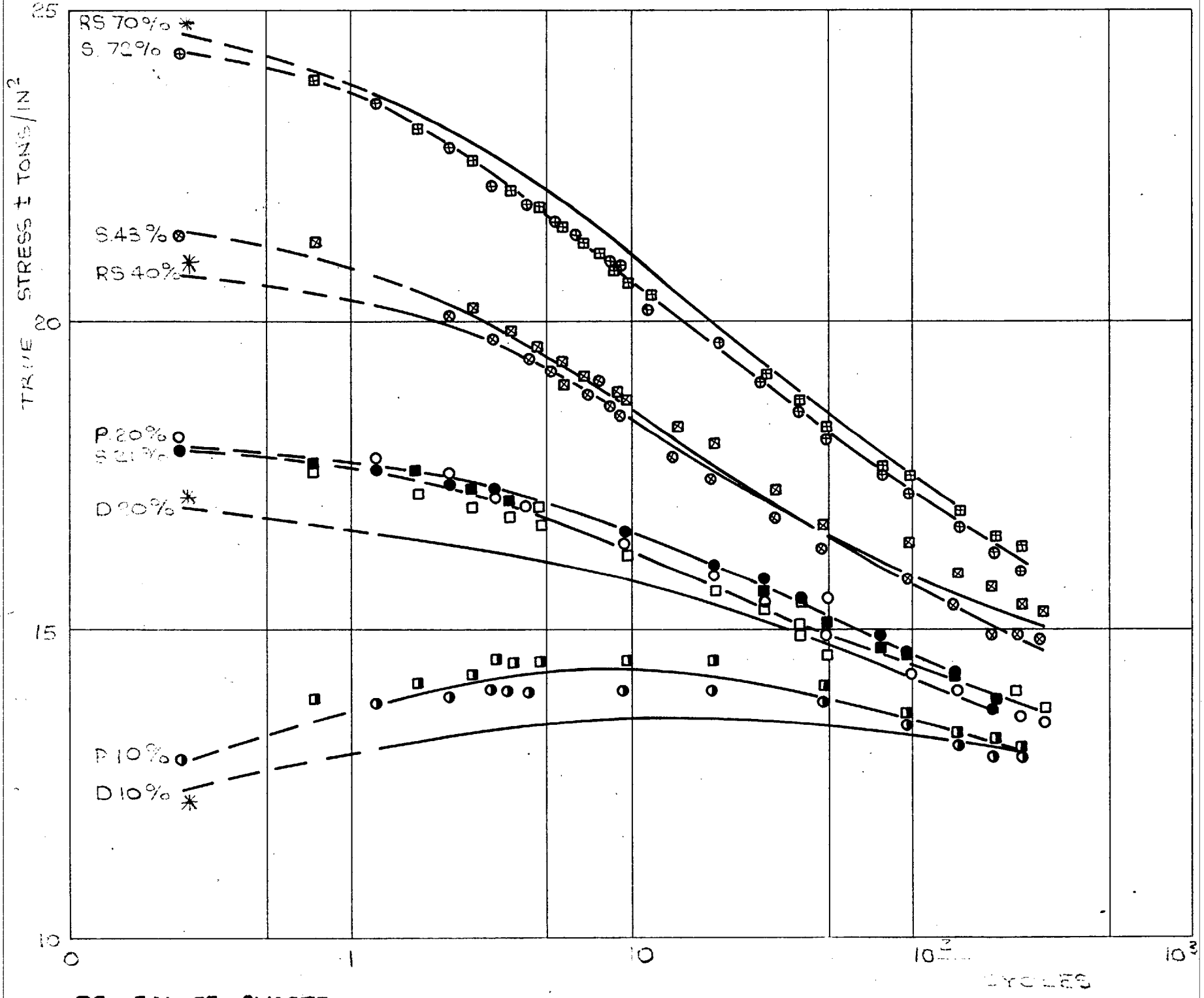

RS ROLLER SWAGED
S PRESS SWAGED
D DRAWN
P STRETCHED

* POINTS SHOWN ON ANOTHER FIGURE

Fig. 20. Effect of method of cold-working on cyclic hardening and softening of copper. ±1% axial plastic strain.

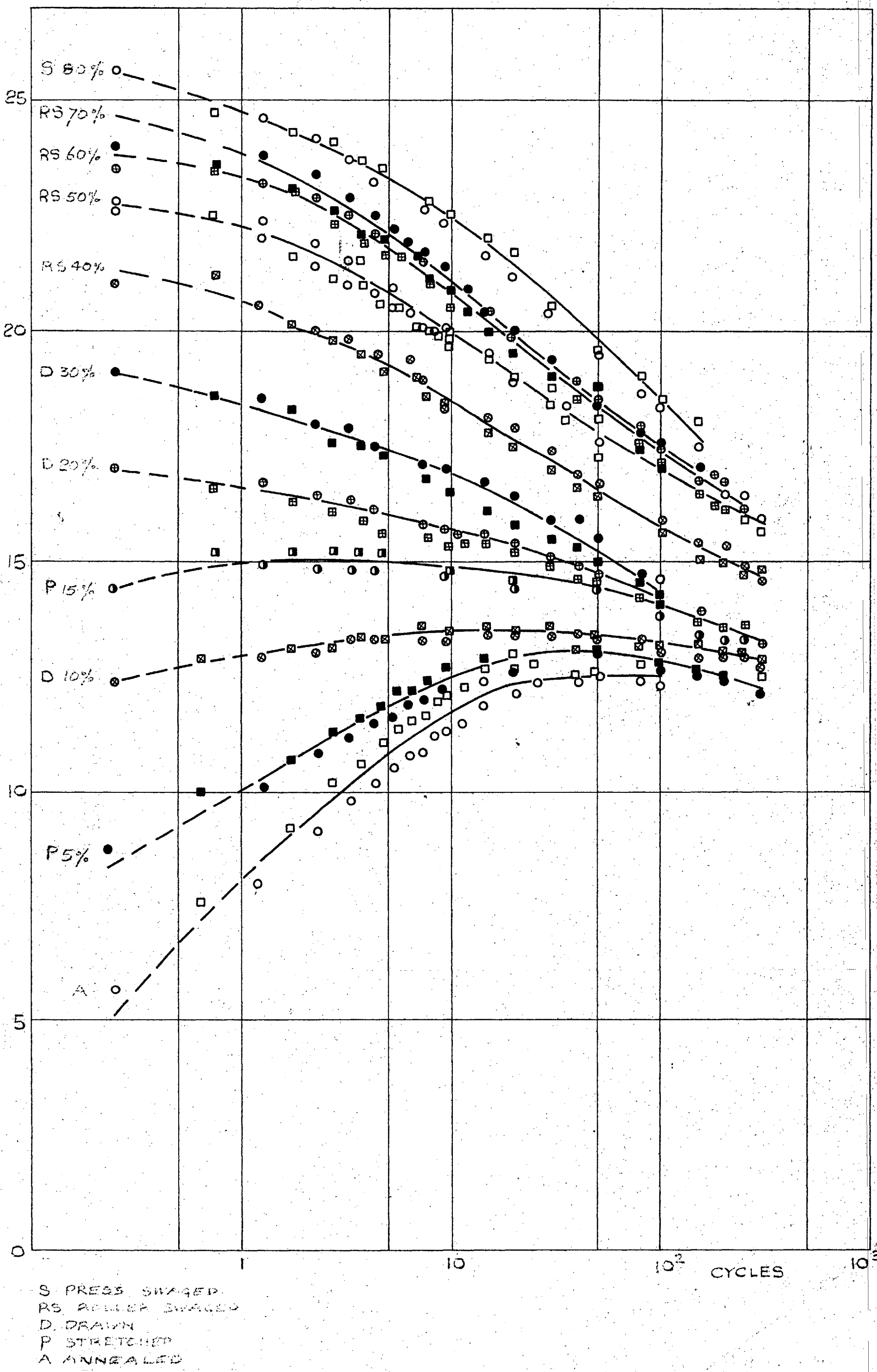

Fig. 21. Effect of degree of cold-working on cyclic hardening and softening of copper: $\pm$1% axial plastic strain.

Fig. 22.

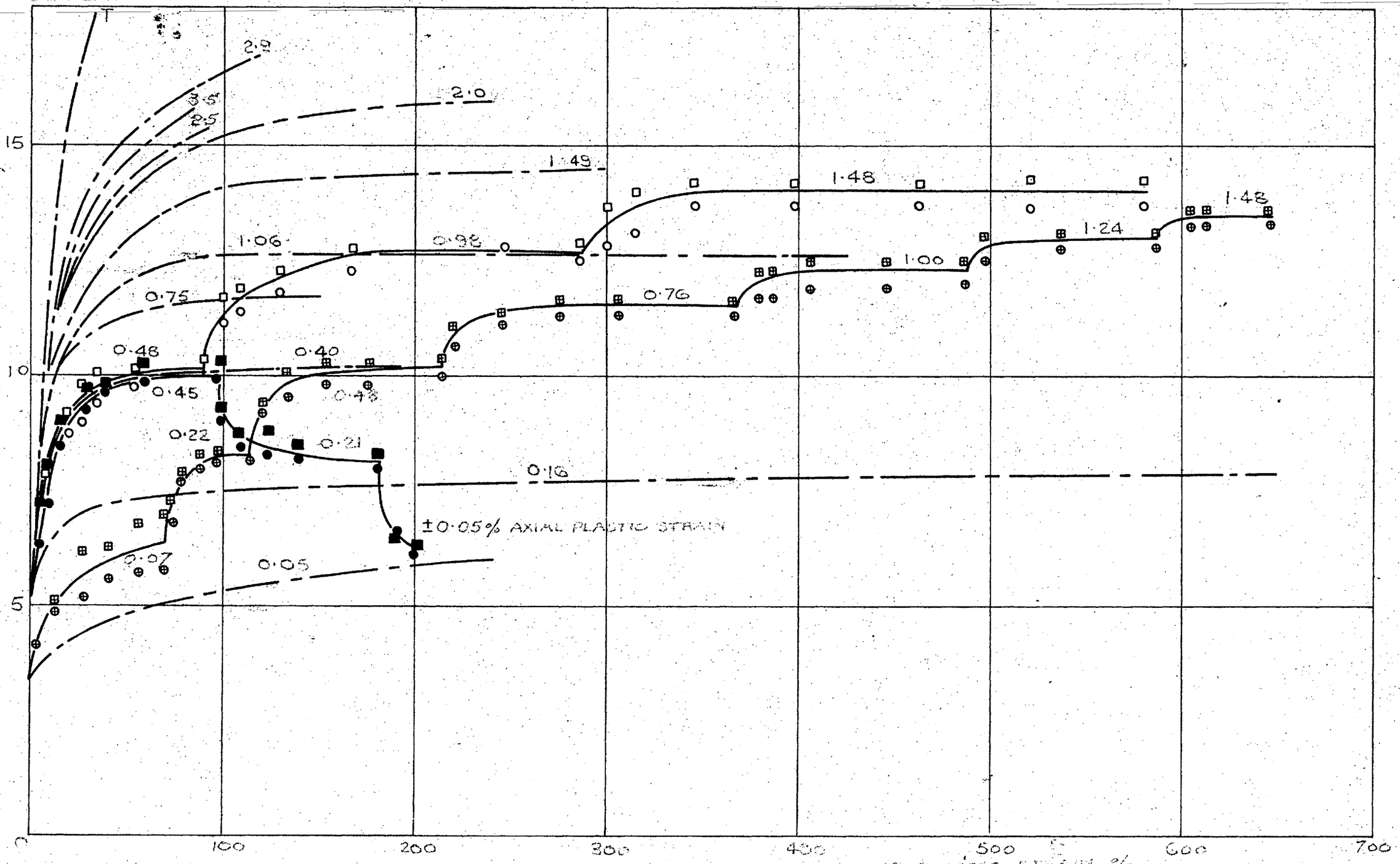

Fig. 22. Comparison of step and constant strain amplitude behaviour of annealed copper.

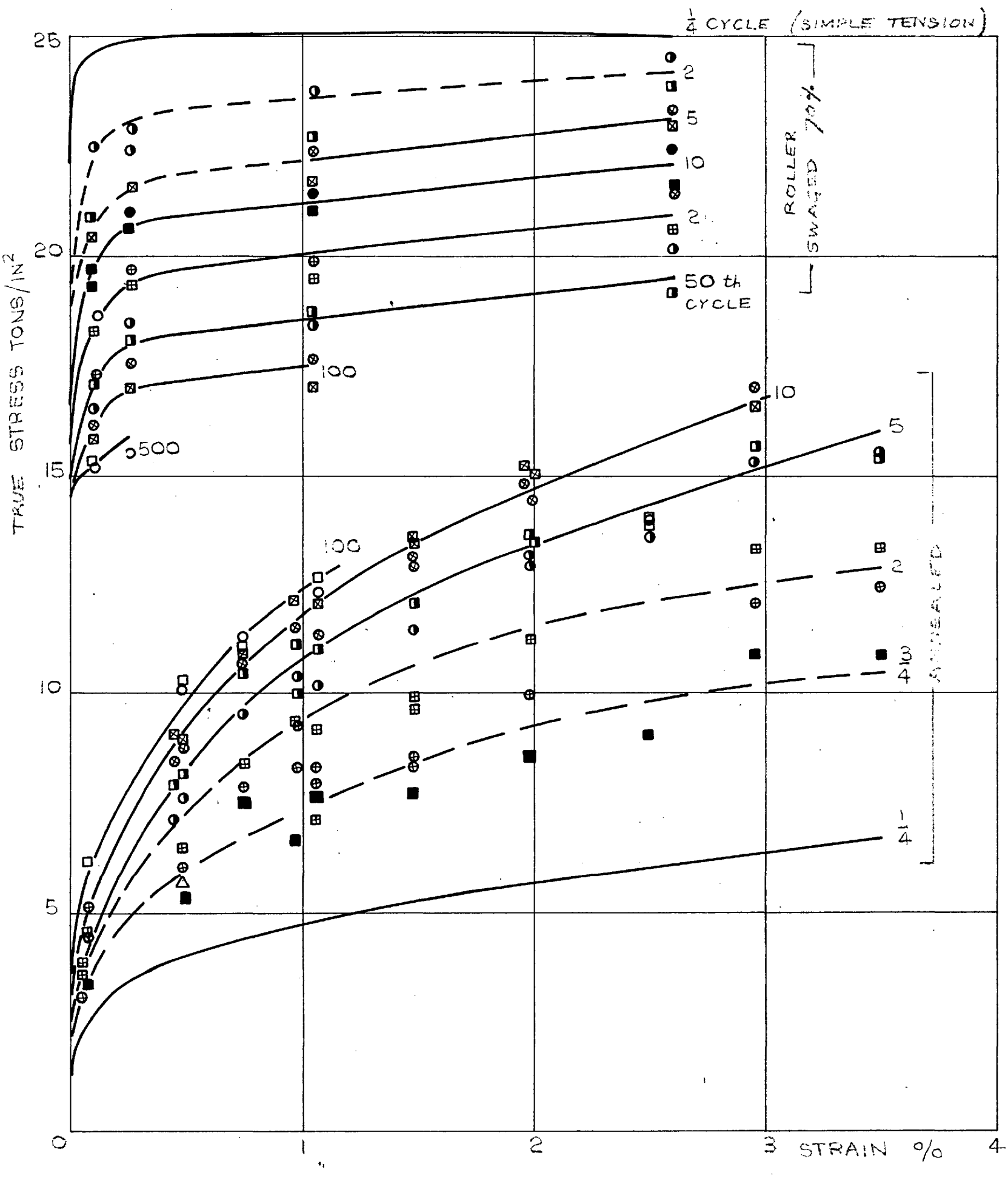

Fig. 23. Cyclic and static stress-strain curves for copper.

Fig. 24.

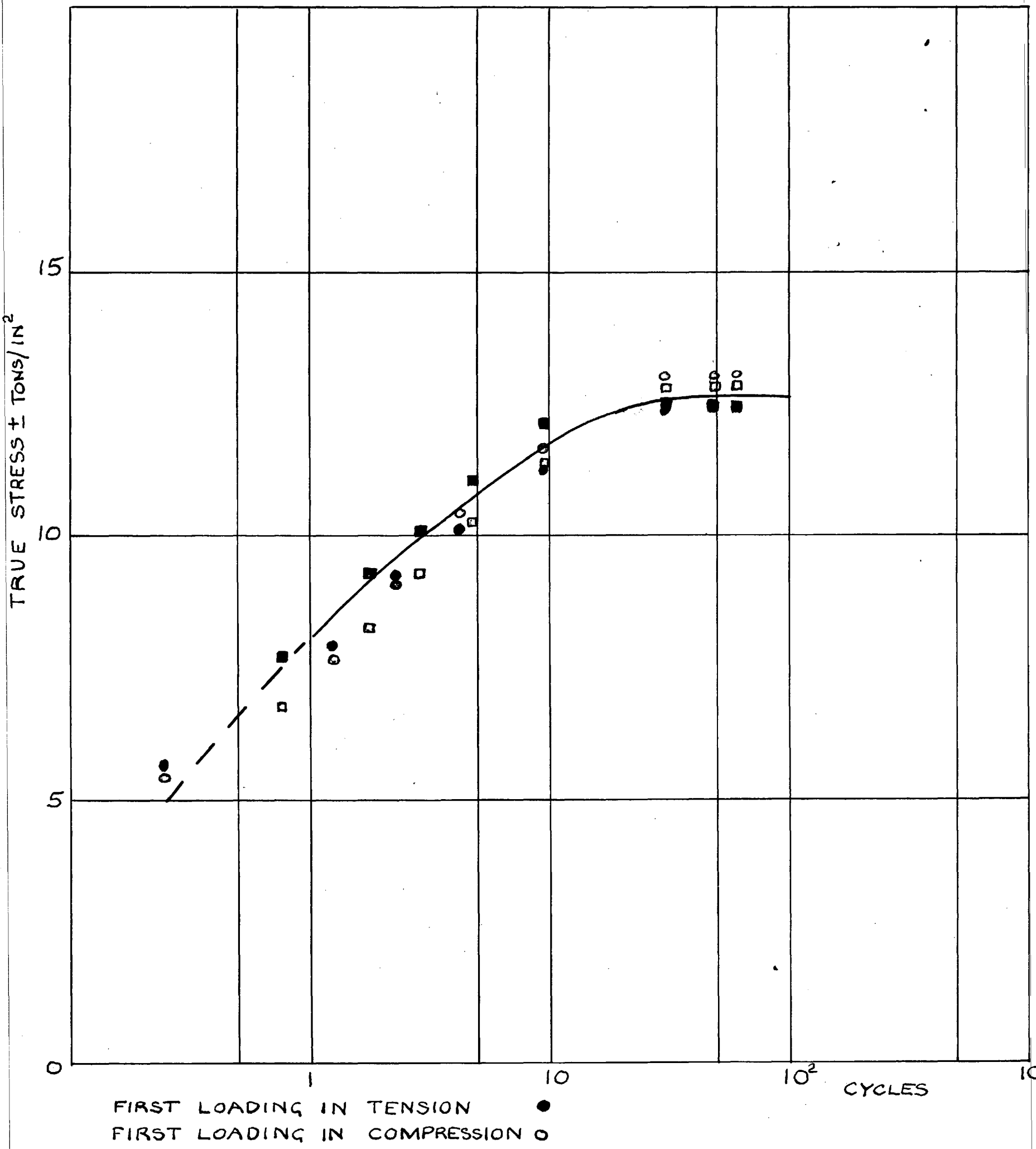

Fig. 24. Effect of direction of initial loading on cyclic hardening of annealed copper.

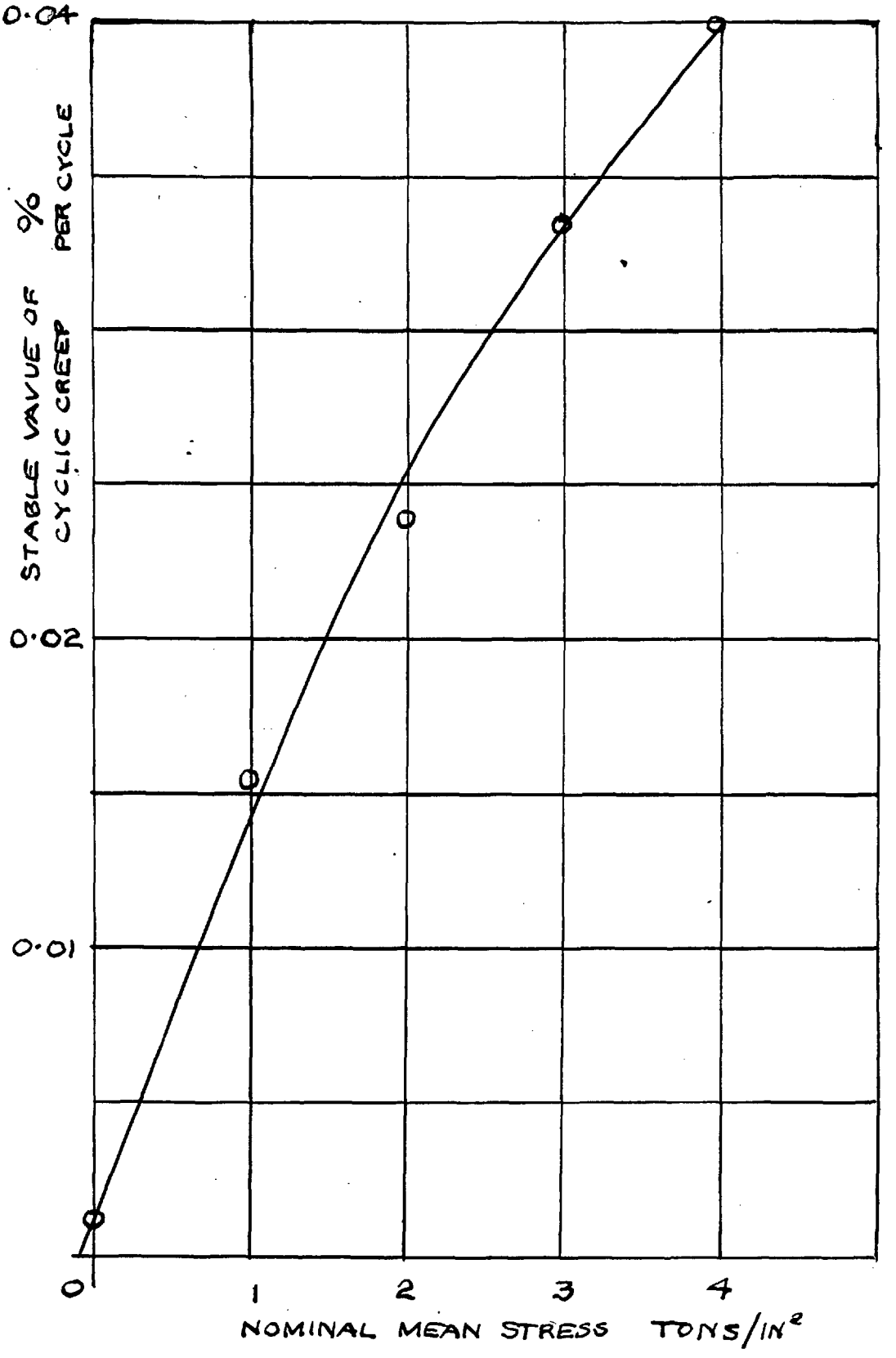

Fig. 25. Variation of creep rate with mean nominal stress; Annealed copper cycled at a stress range of 12.4 tons/in².

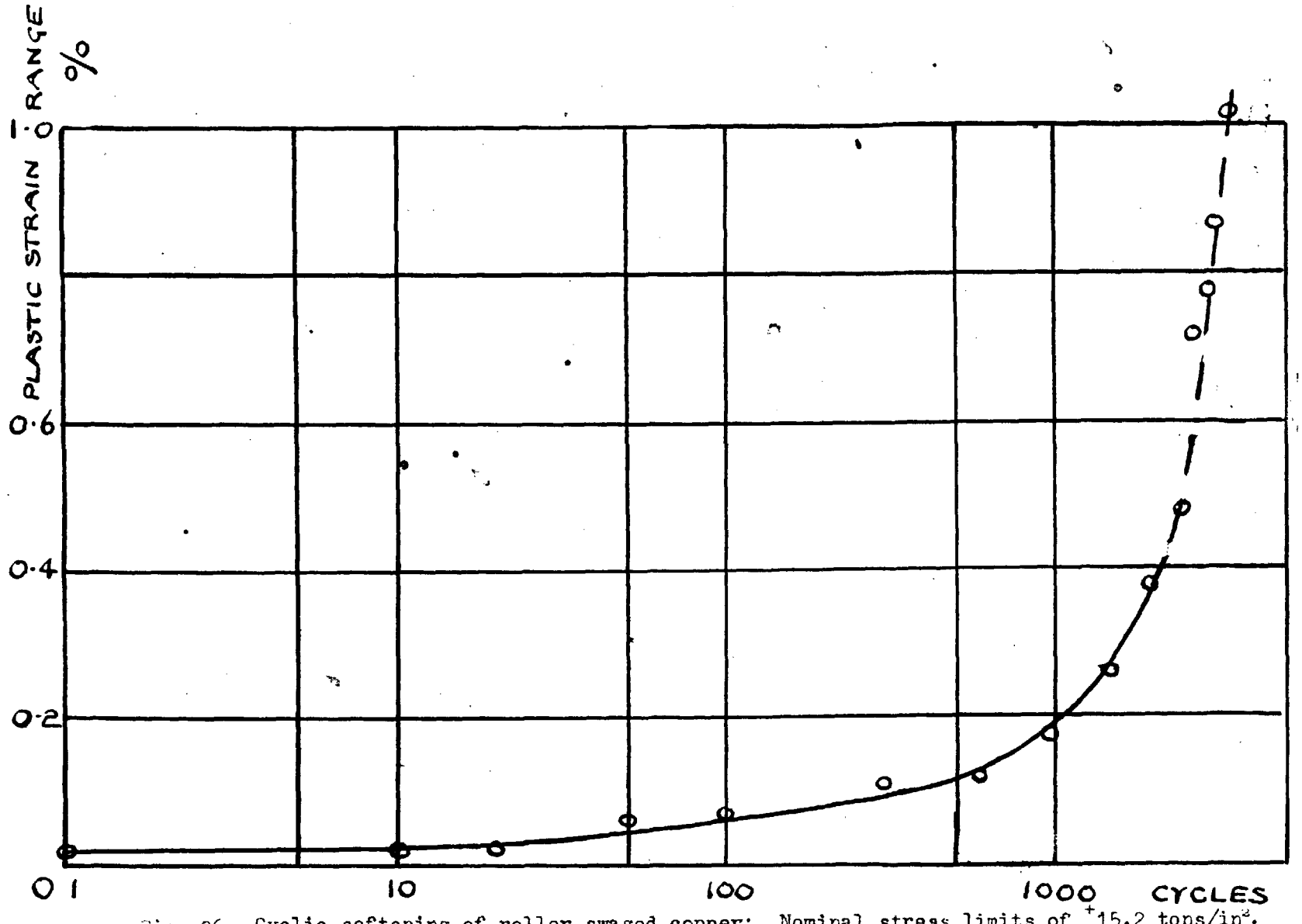

Fig. 26. Cyclic softening of roller swaged copper: Nominal stress limits of $\pm$15.2 tons/in^2.

Fig. 27.

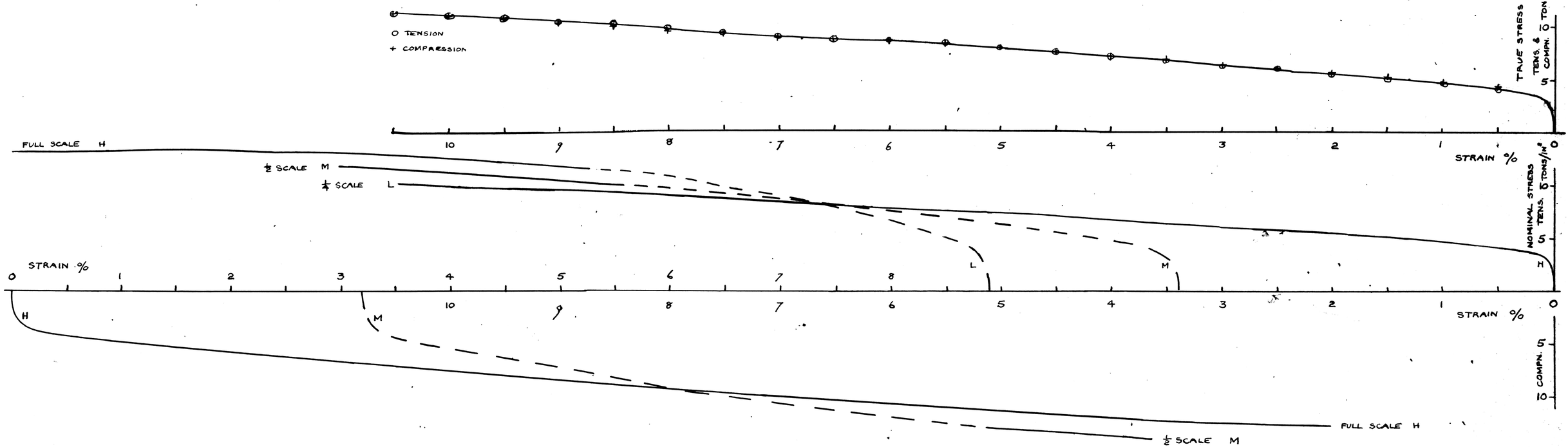

Fig. 27. Tension and compression tests for annealed copper.

Fig. 8.

Fig. 8. Calibration graph for the three strain scales.

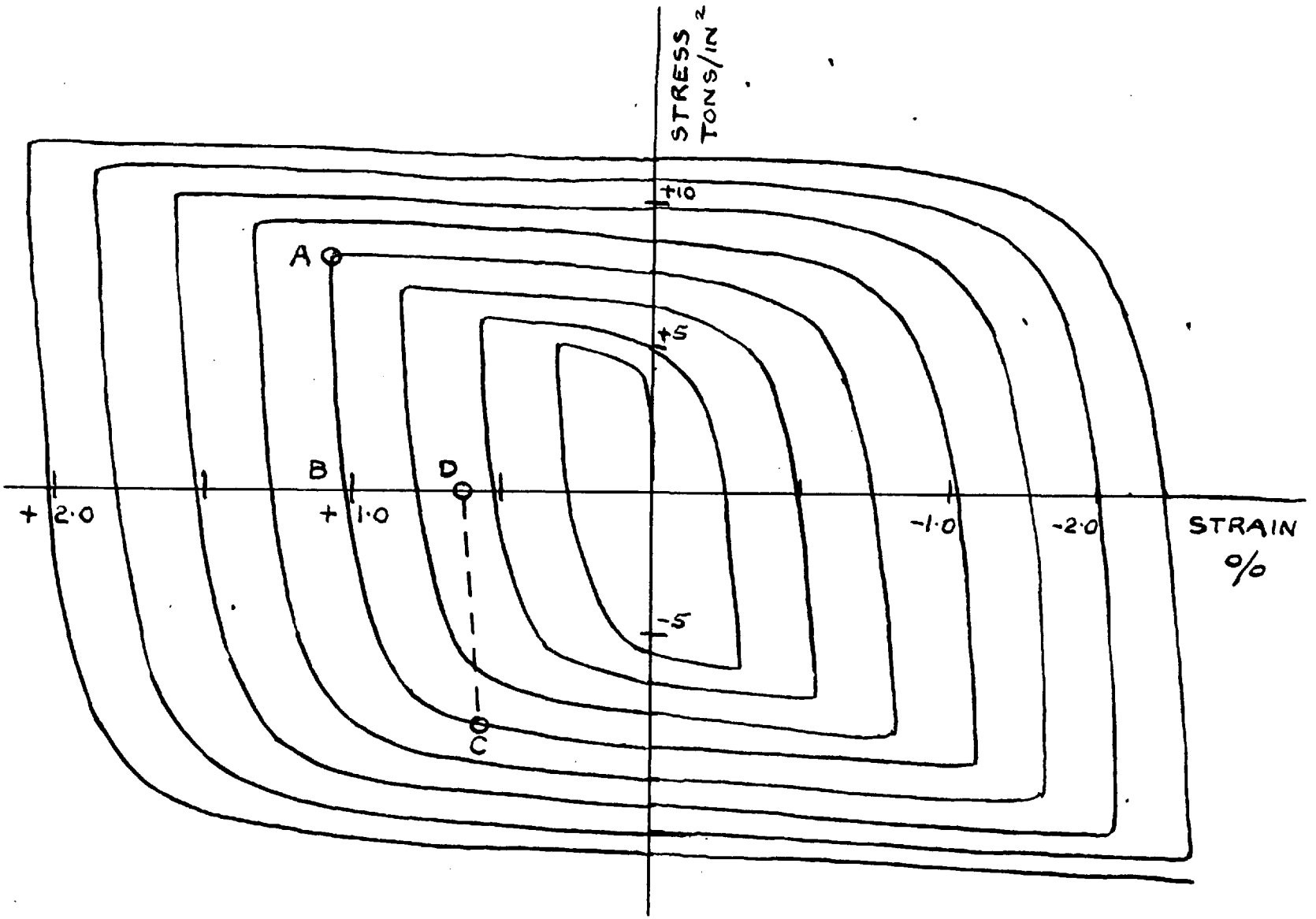

Fig. 29. Series of reverse loading tests on a specimen of annealed copper.

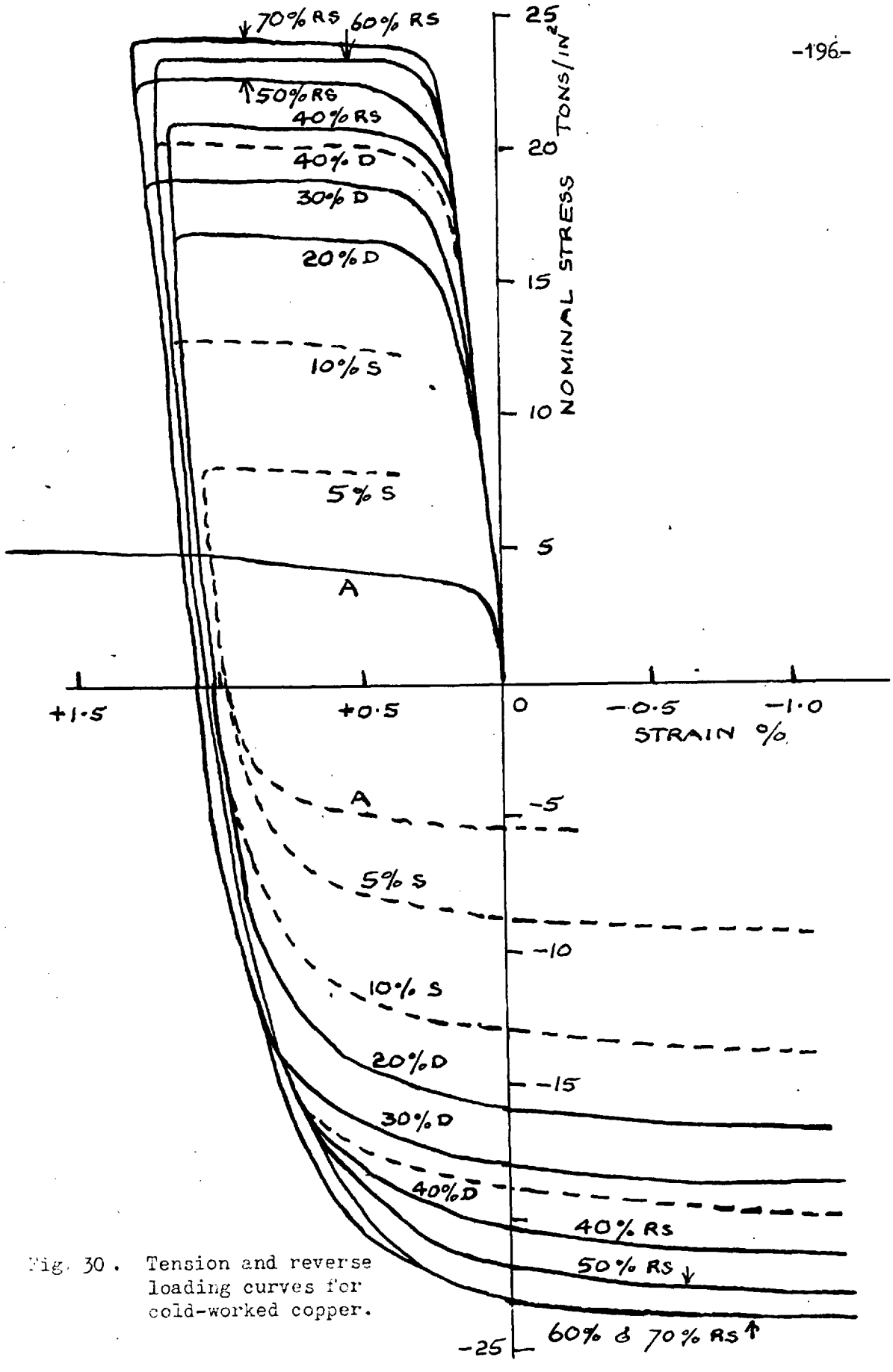

Fig. 30. Tension and reverse loading curves for cold-worked copper.

Fig. 31.

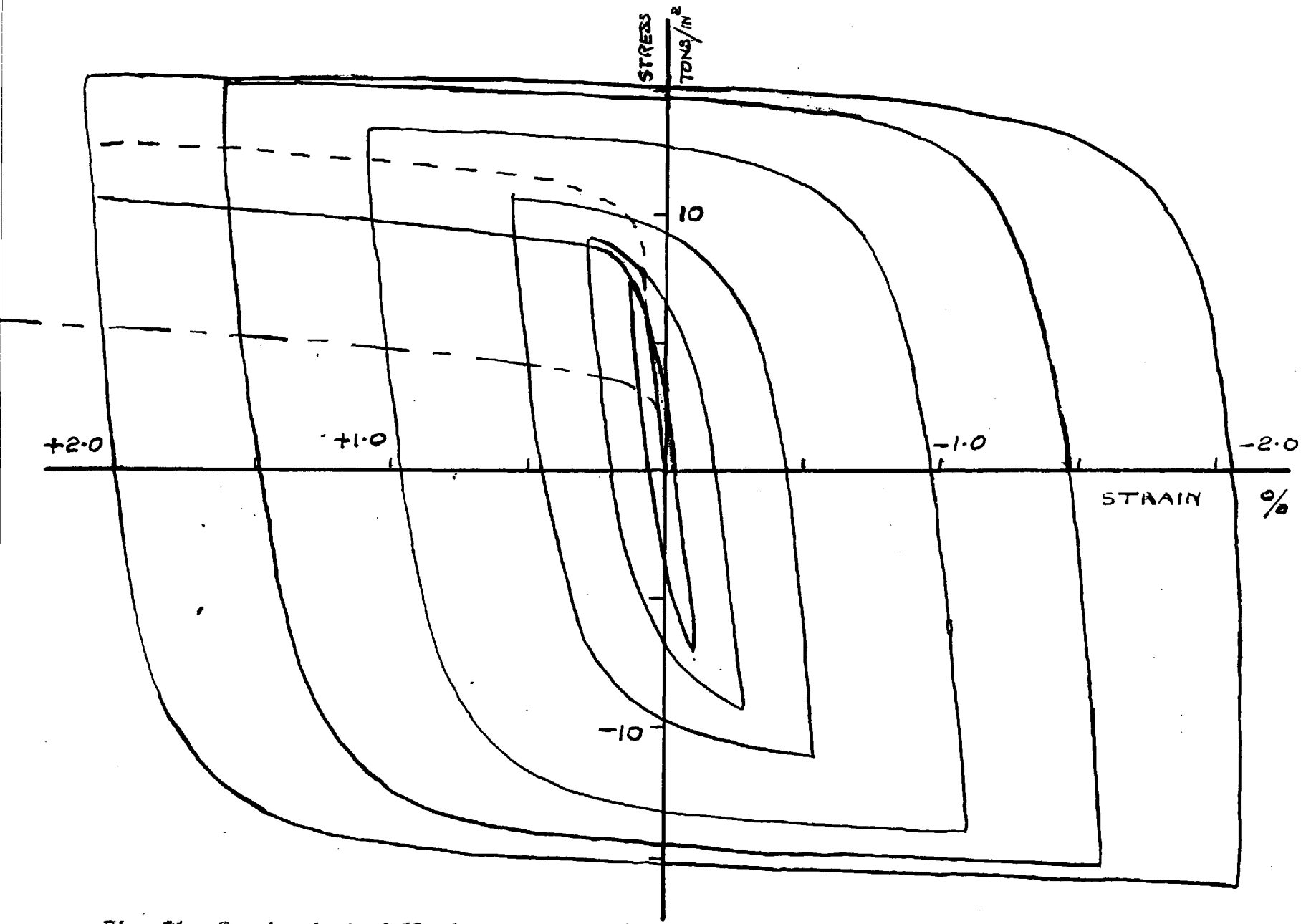

Fig. 31. Tension tests following sequences of cycling at progressively decreasing strain amplitudes.

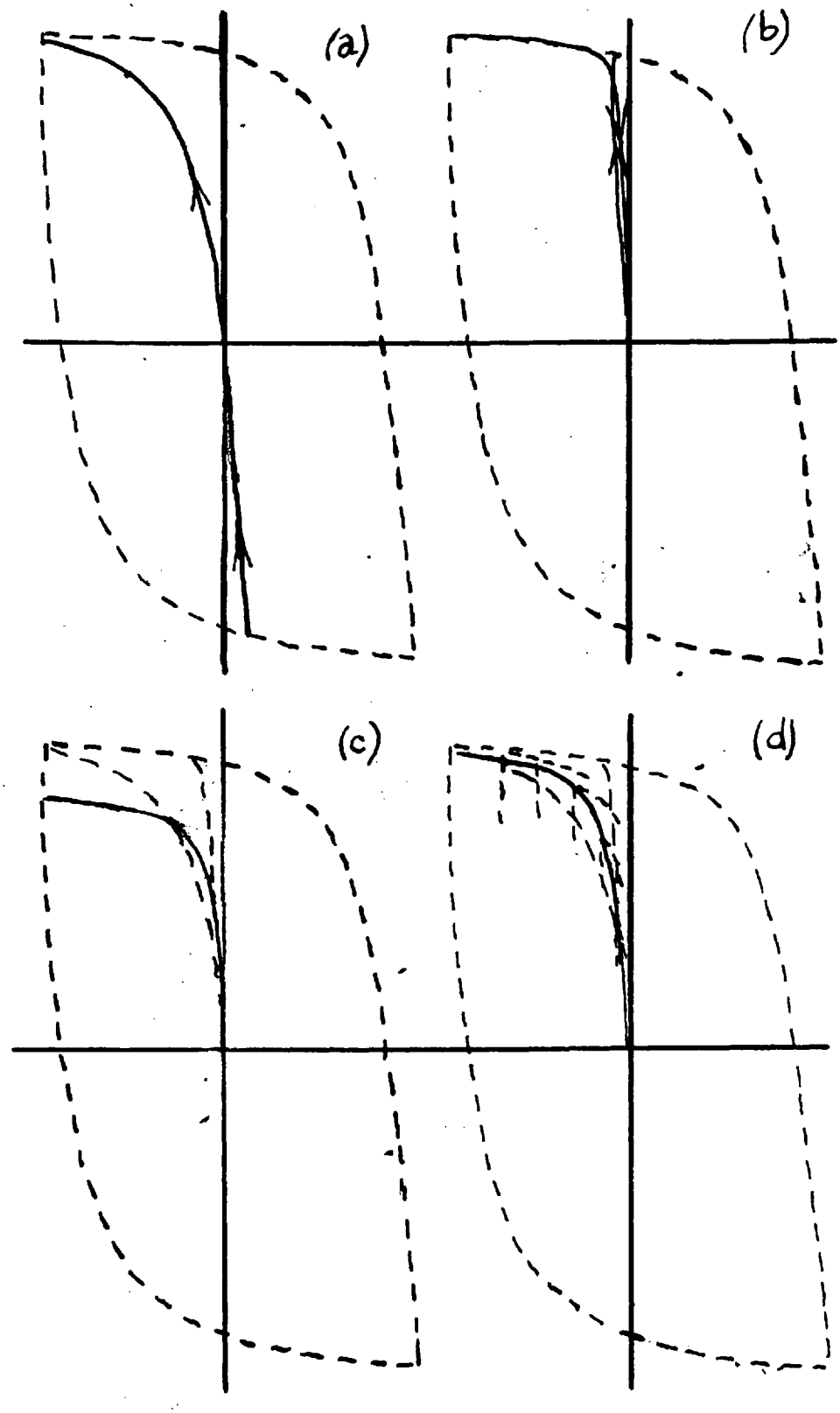

Fig. 32. Reduction of the Bauschinger effect in cycled annealed copper: Plastic strain range $\pm$0.5%.

Fig. 33.

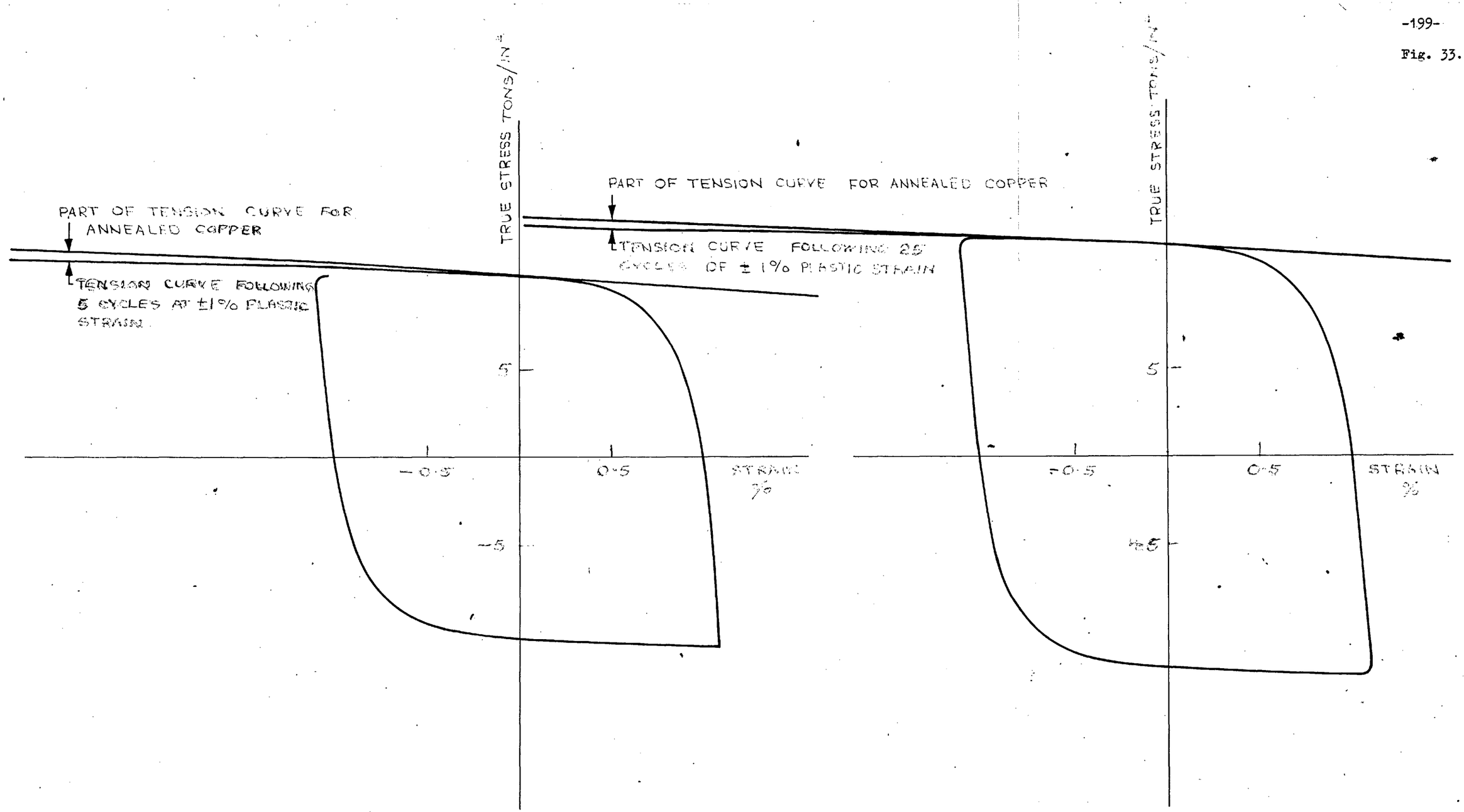

Fig. 33. Rates of hardening compared for cyclic and uni-directional deformation.

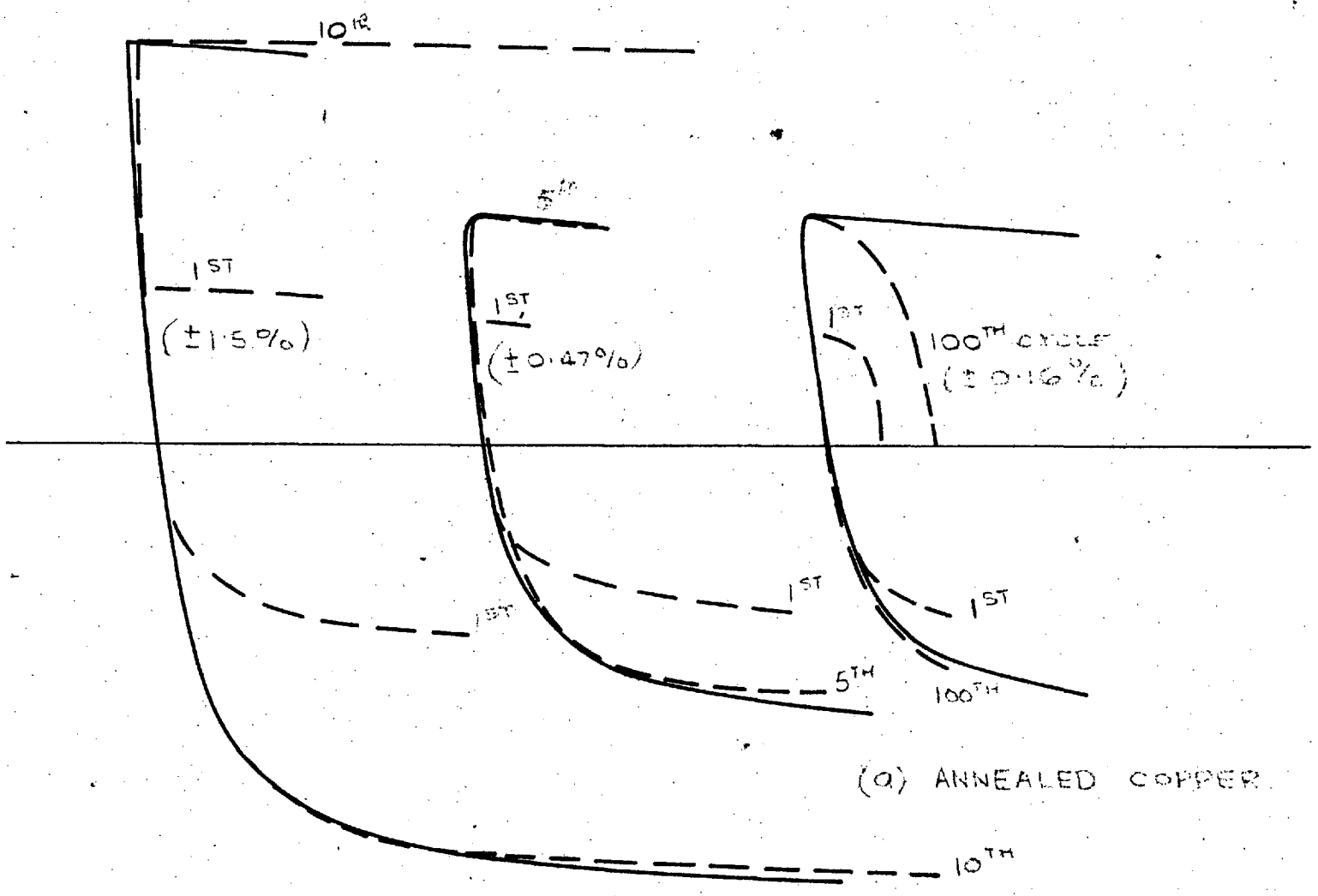

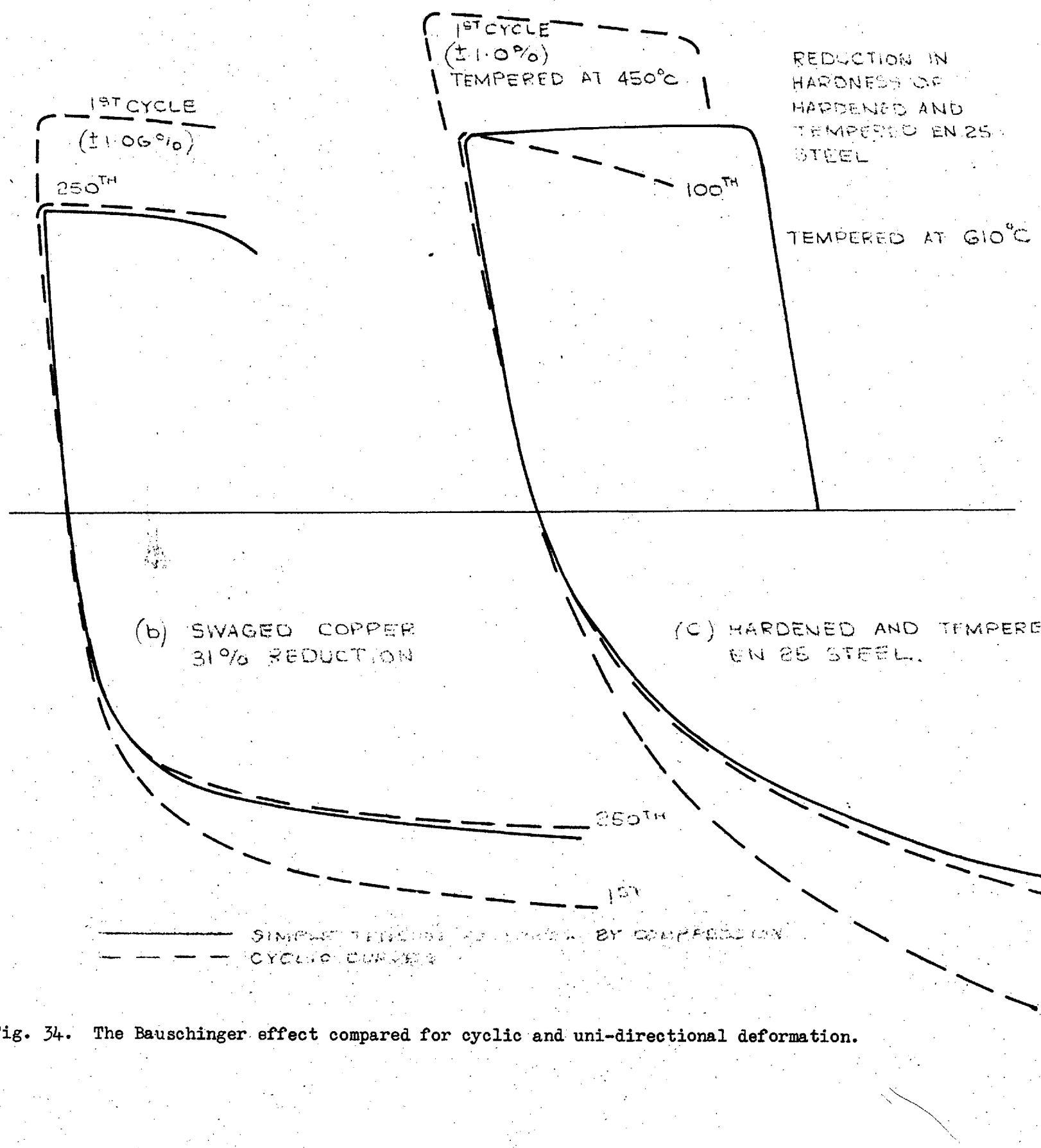

Fig. 34. The Bauschinger effect compared for cyclic and uni-directional deformation.

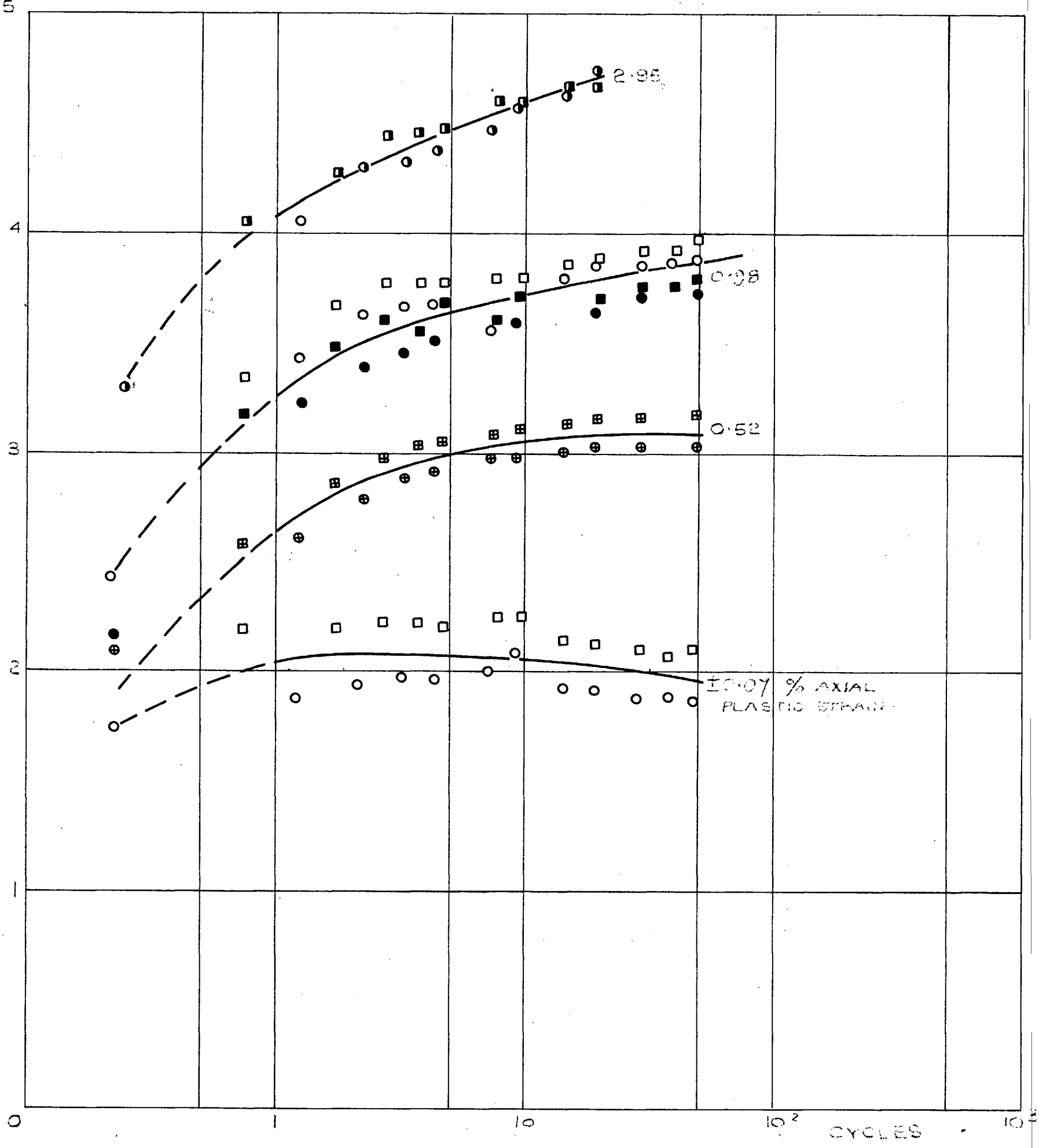

Fig. 35. Effect of plastic strain range on the cyclic hardening of annealed aluminium.

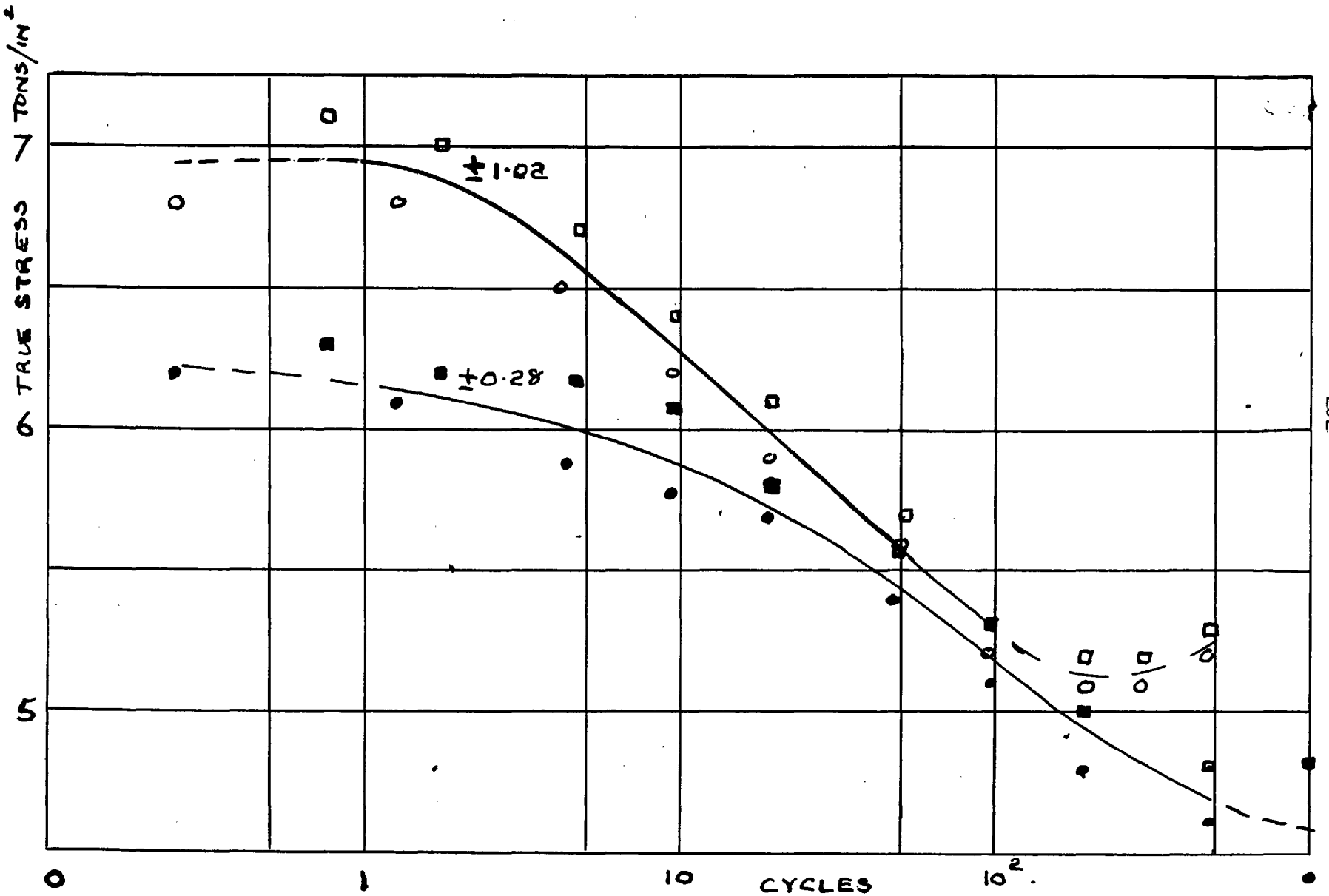

Fig. 36. Effect of plastic strain range on the cyclic softening of cold-drawn aluminium.

Fig. 37.

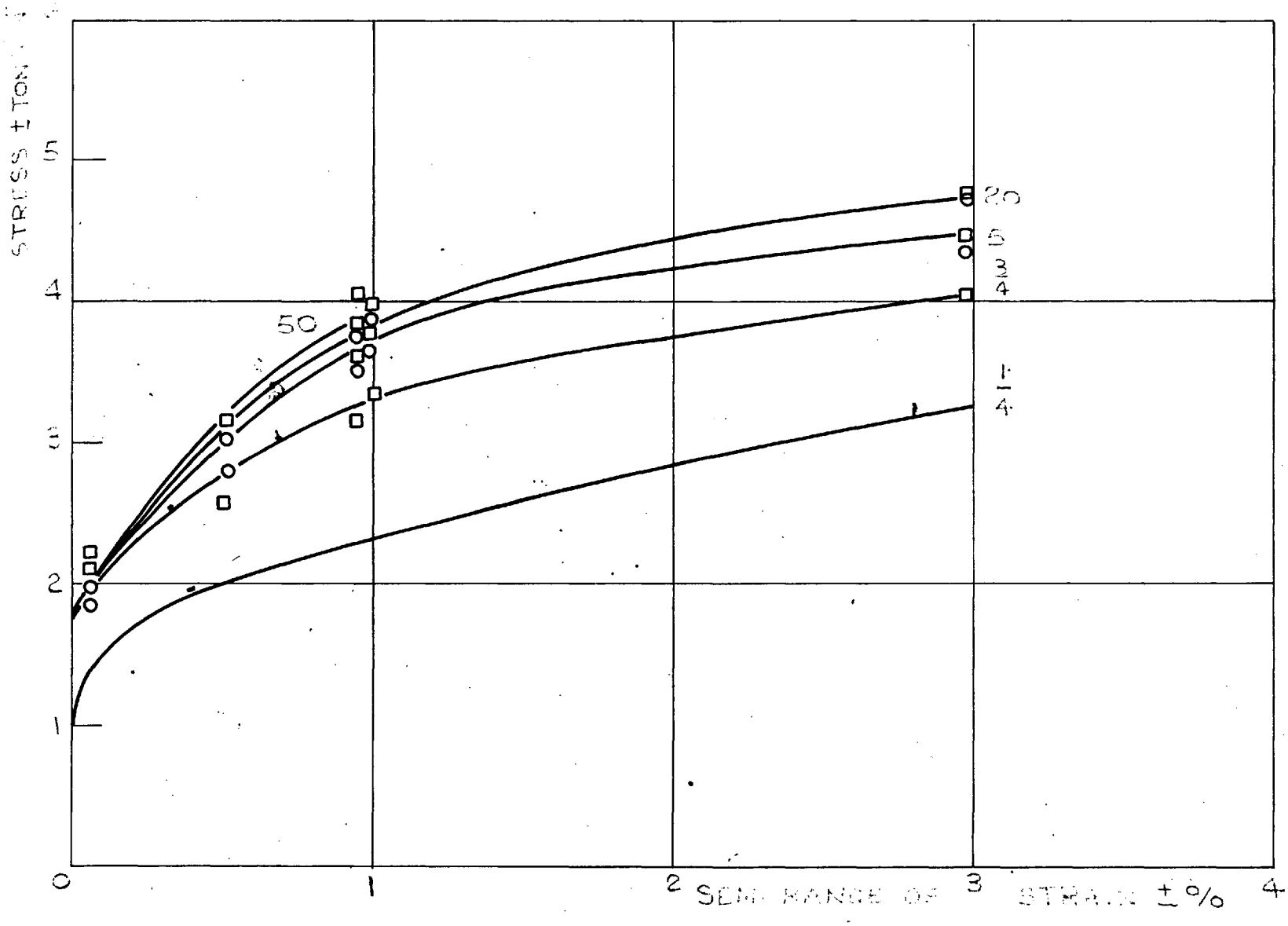

Fig. 37. Cyclic and static stress-strain curves for annealed aluminium.

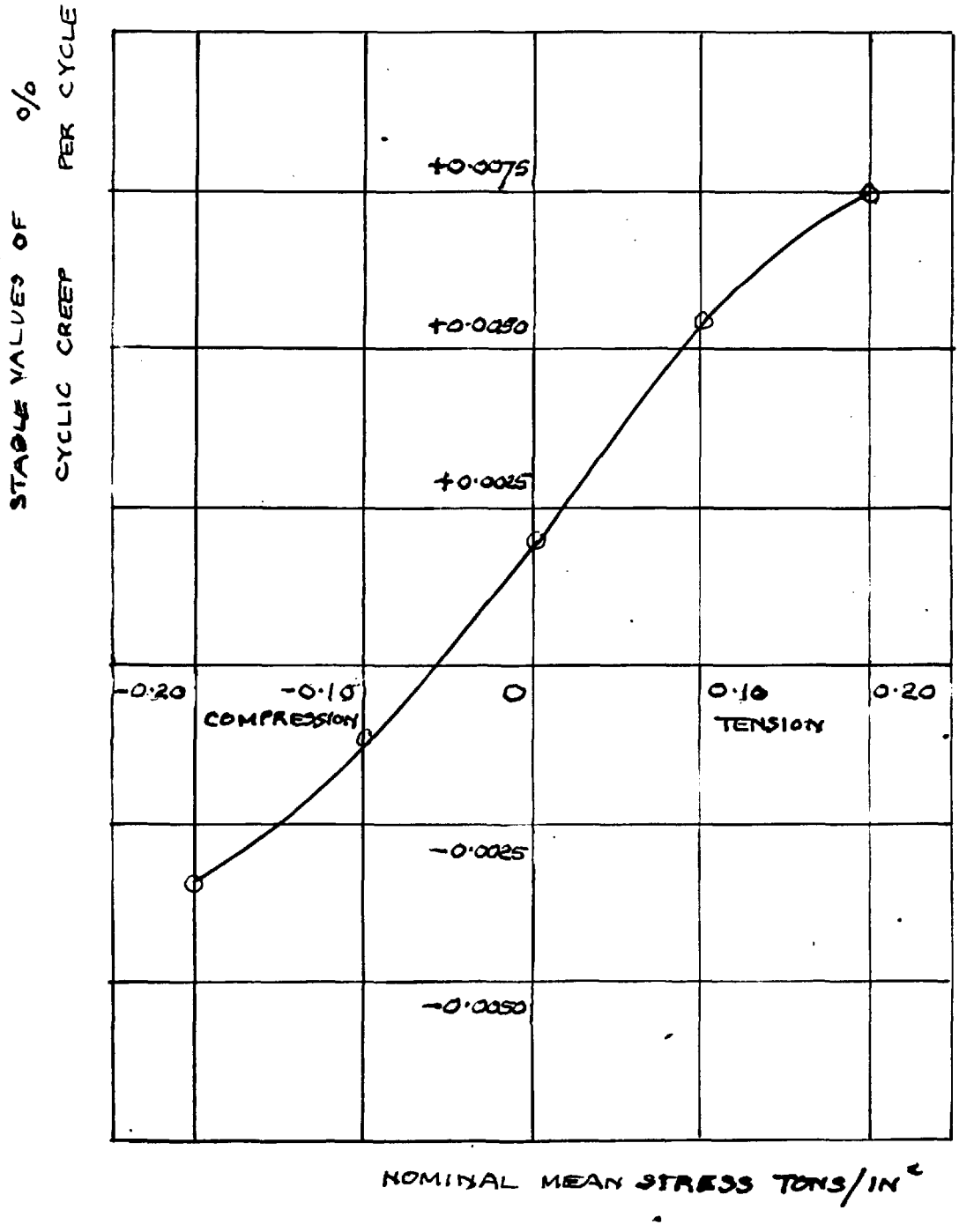

Fig. 38 Variation of creep rate with mean nominal stress: Annealed aluminium cycled at a stress range of 3.8 tons/in^2.

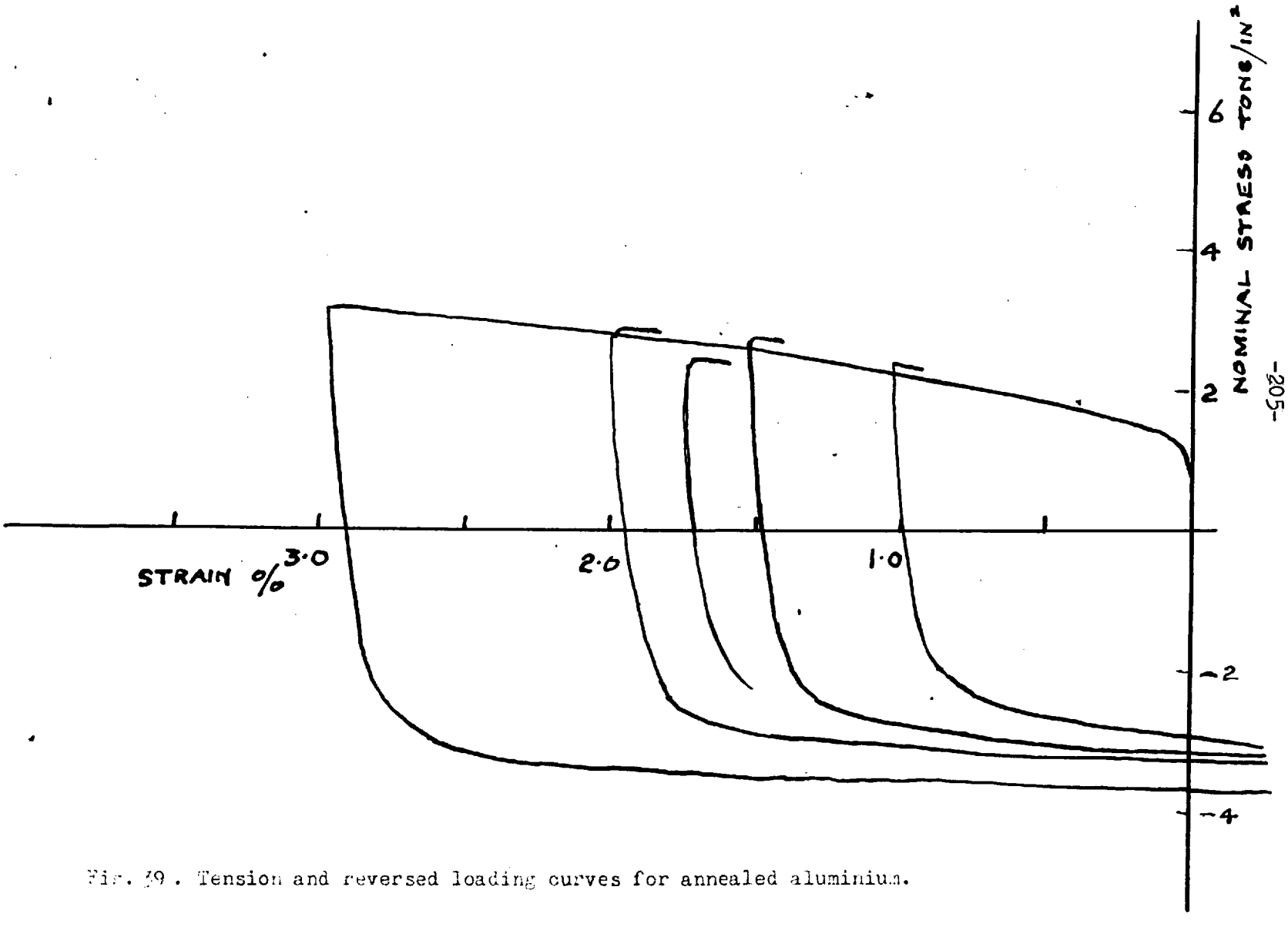

Fig. 39. Tension and reversed loading curves for annealed aluminium.

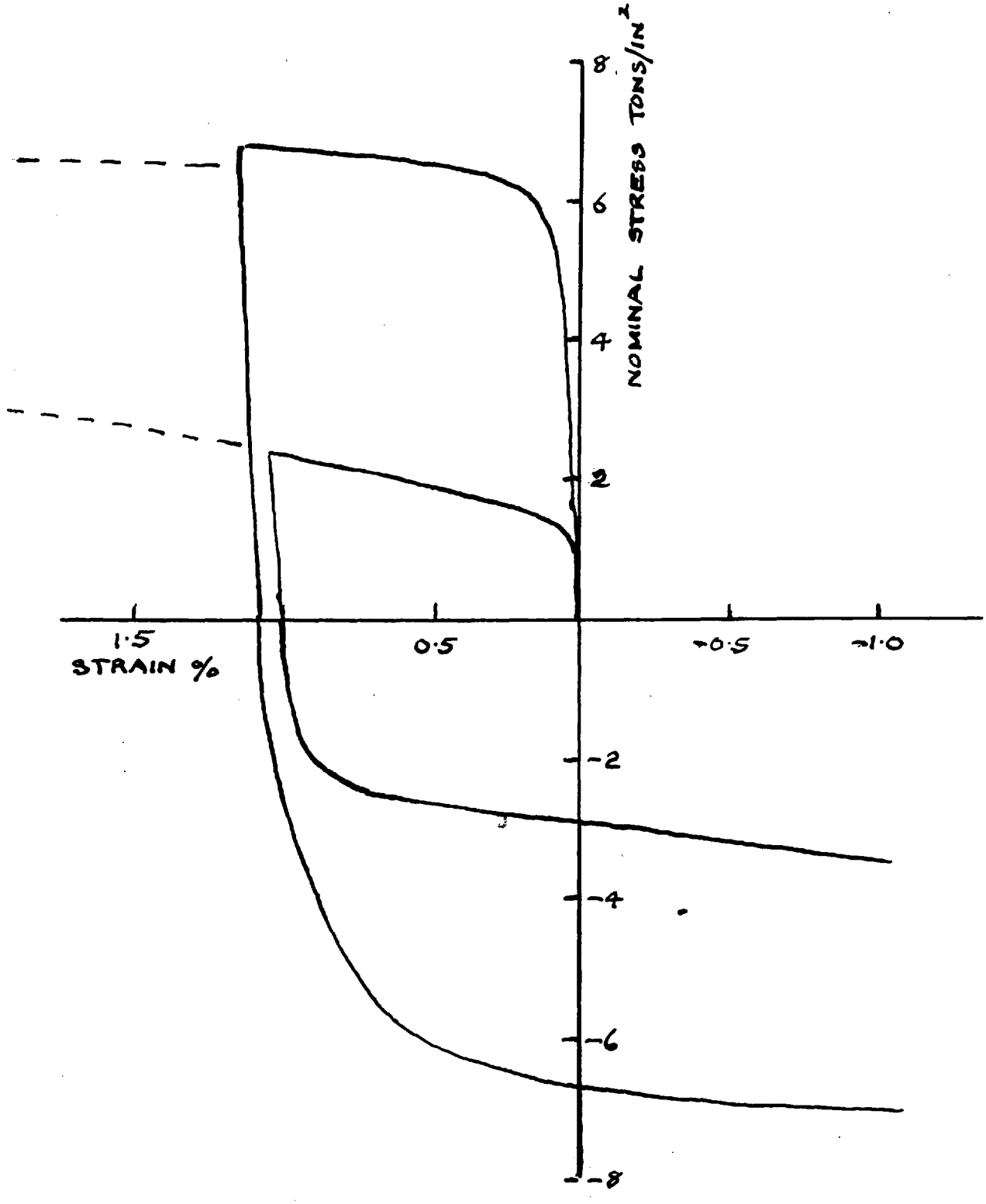

Fig. 40. Tension and reverse loading curves for cold drawn and annealed aluminium.

Fig. 41.

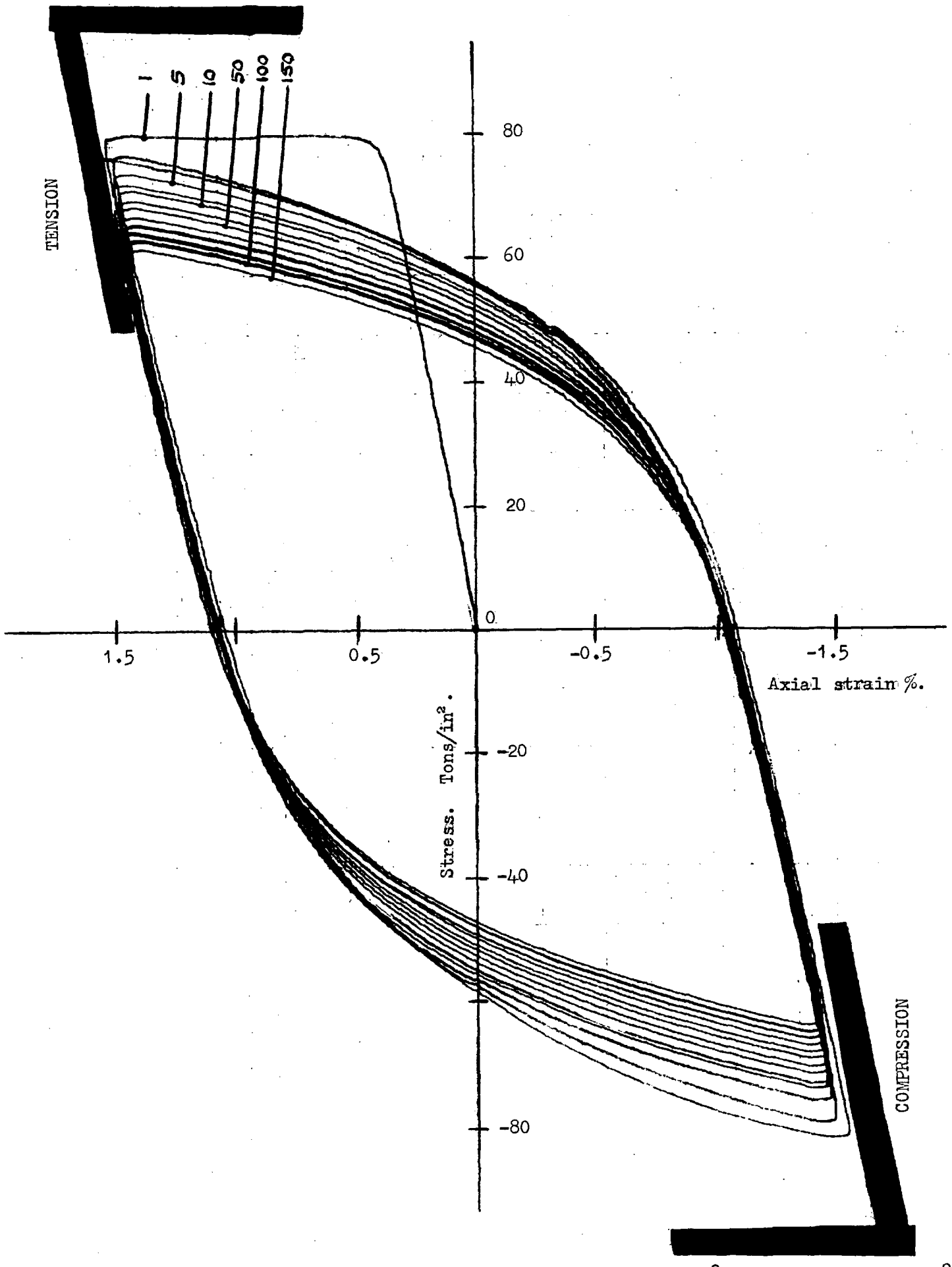

Fig. 41. Stress-strain curves for En25 steel, hardened from 840°C and tempered at 450°C, cycled at ±1% axial plastic strain.

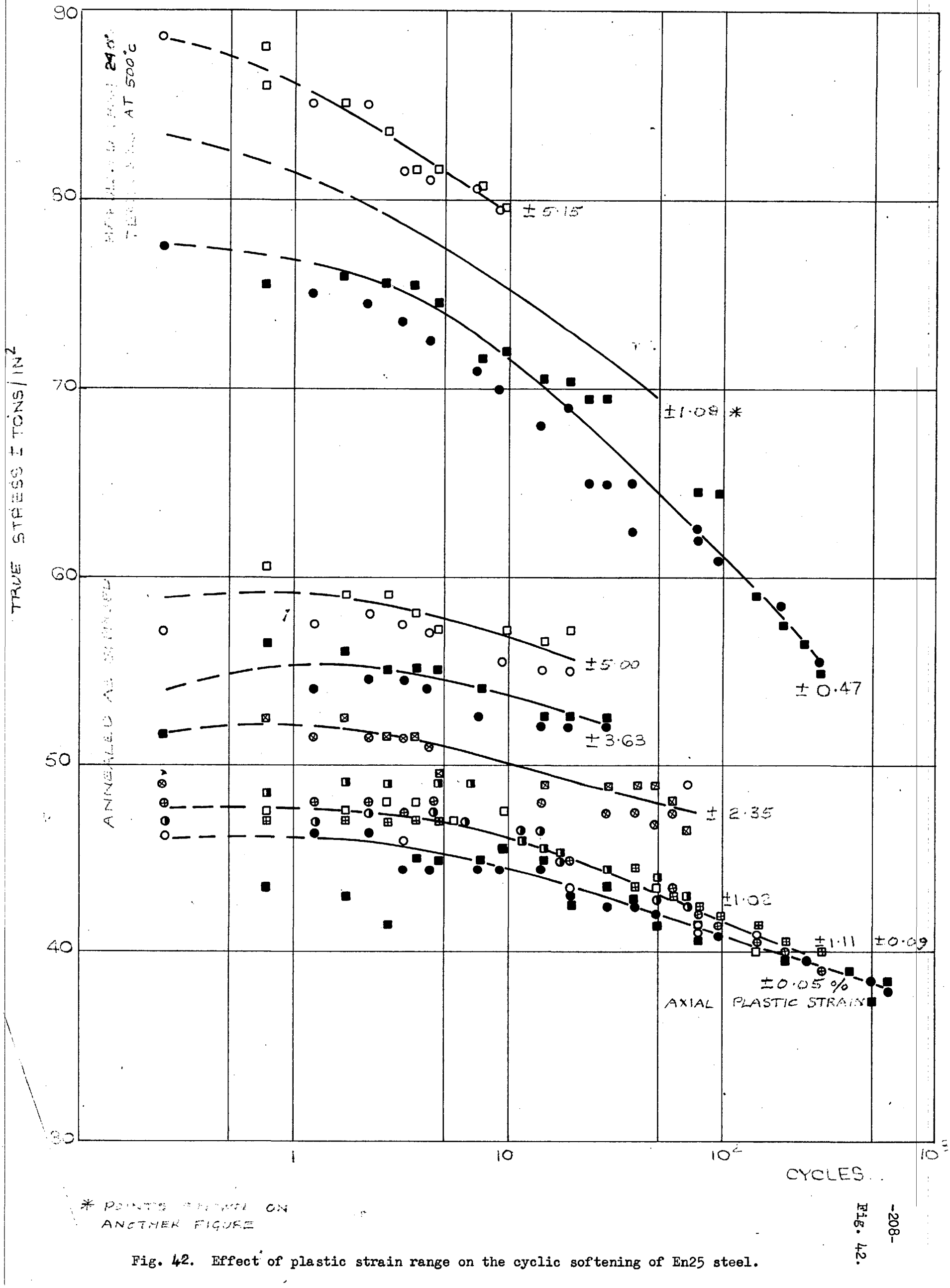

Fig. 42. Effect of plastic strain range on the cyclic softening of En25 steel.

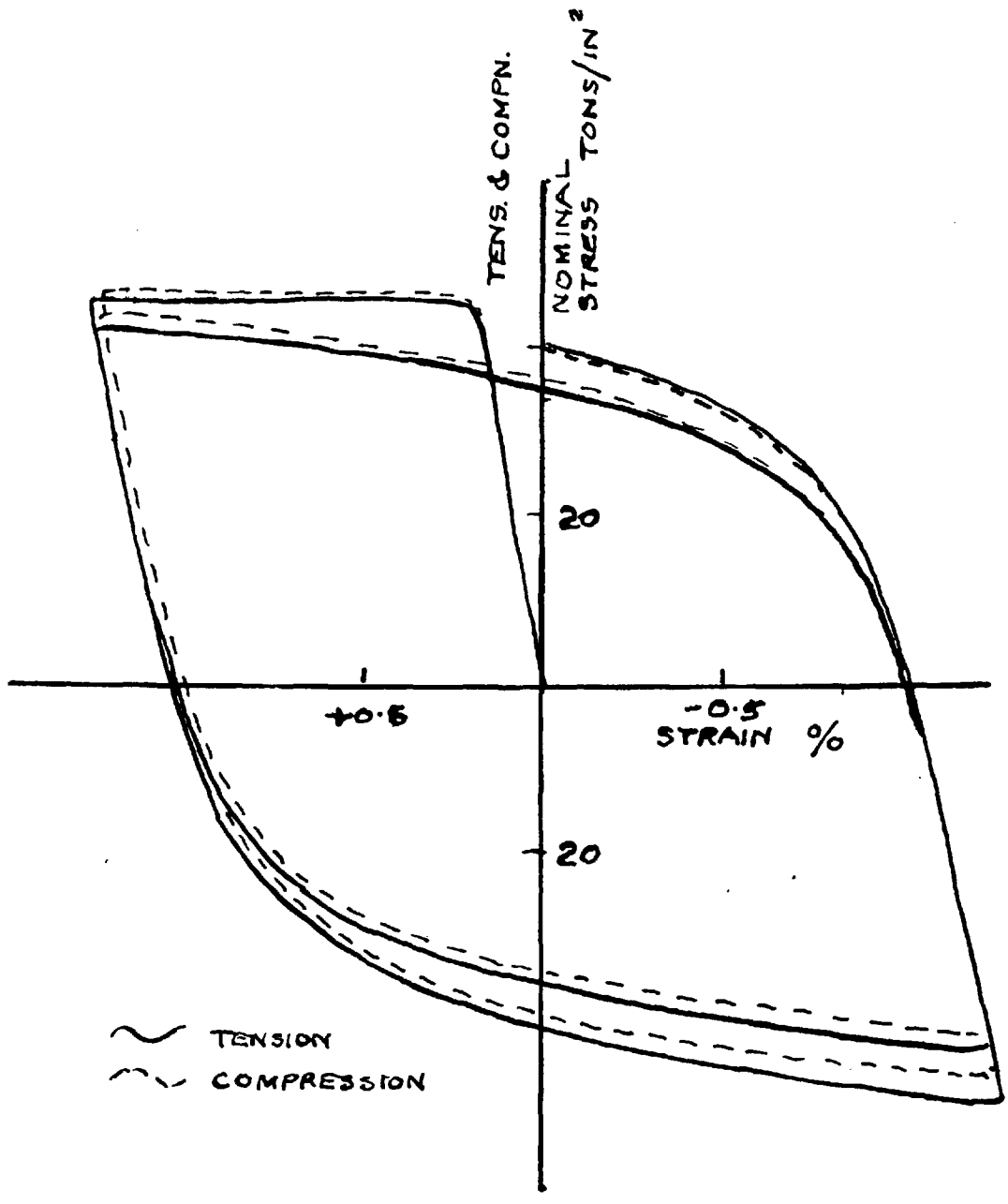

Fig. 43. Cyclic stress-strain loops compared for effect of tensile or compressive loading in the first cycle: (Latter is drawn with signs reversed): Annealed En25 steel at $\pm$1% plastic strain: 1st and 20th cycles are shown.

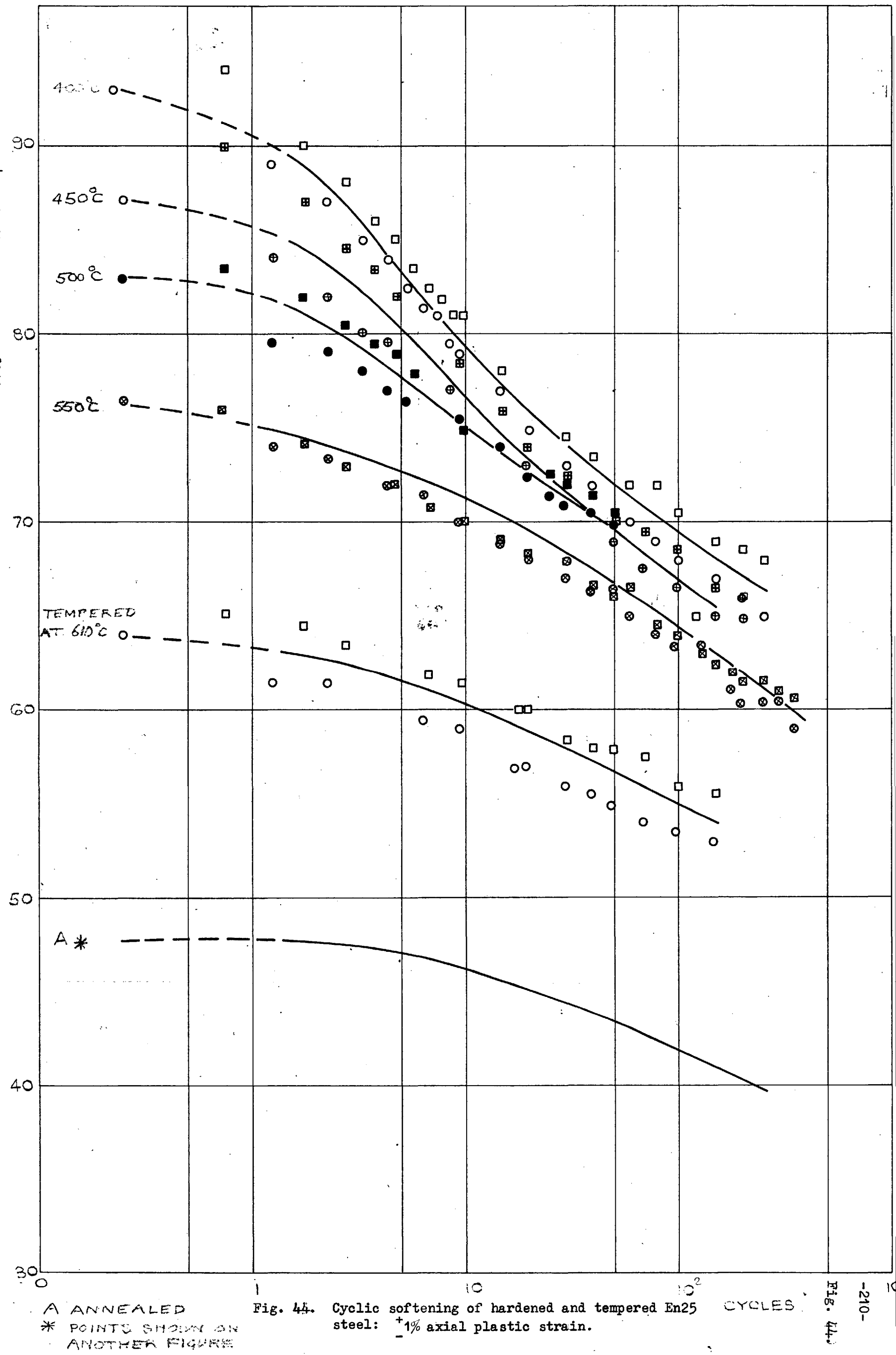

A ANNEALED
* POINTS SHOWN ON ANOTHER FIGURE

Fig. 44. Cyclic softening of hardened and tempered En25 steel: $\pm$1% axial plastic strain.

Fig. 45.

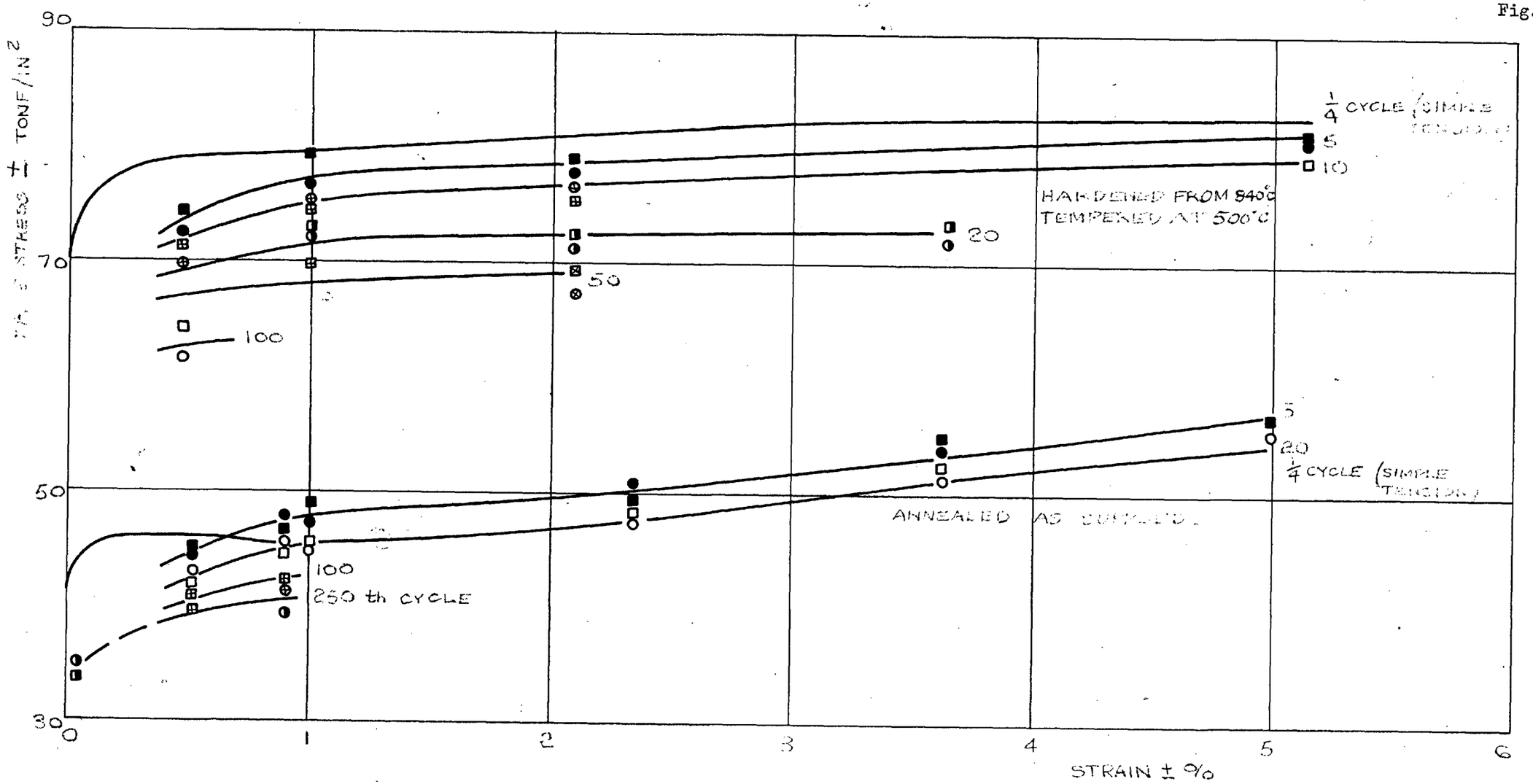

Fig. 45. Cyclic and static stress-strain curves for En25 steel.

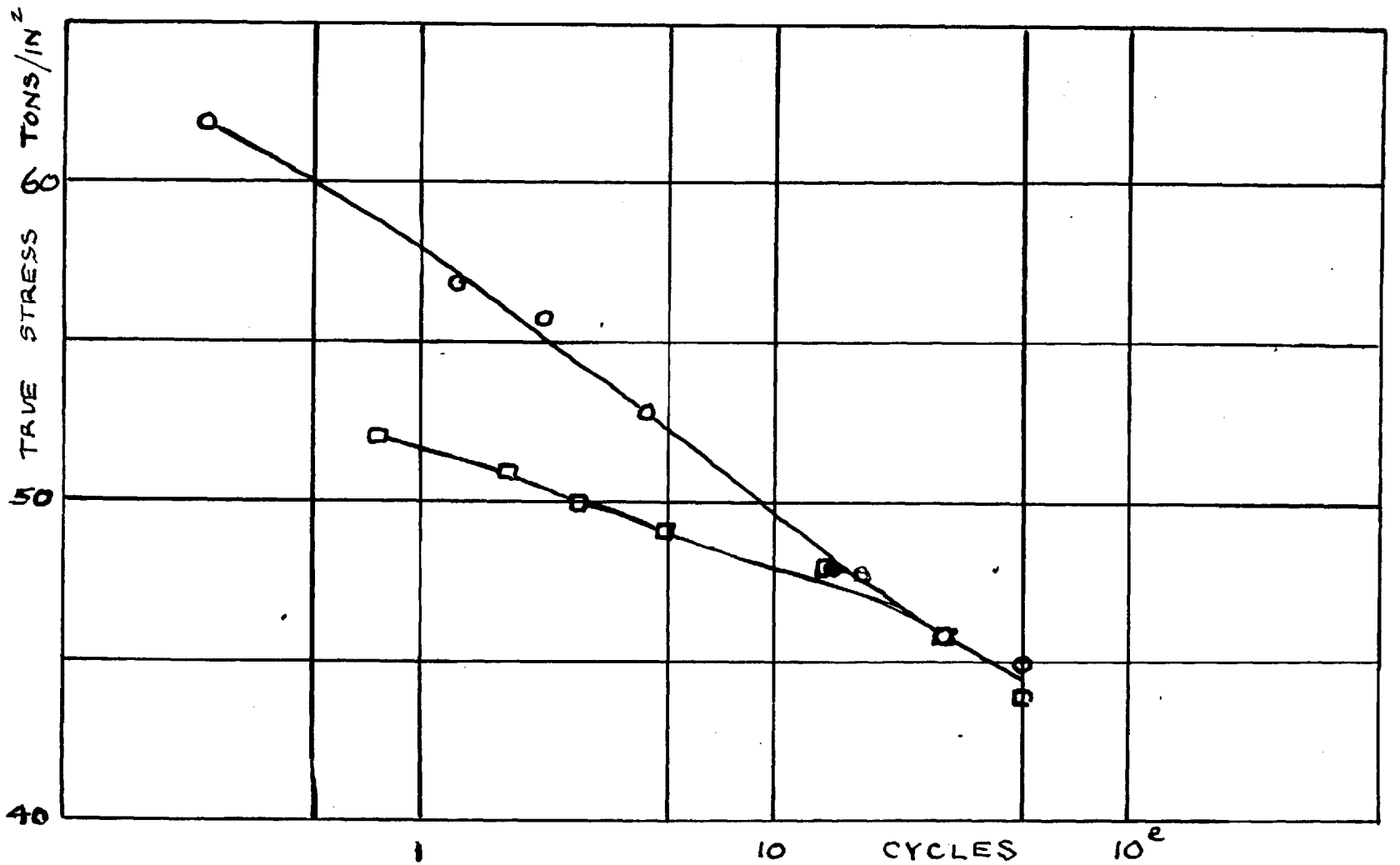

Fig. 46. The cyclic softening of cold stretched En25 steel: ±1% axial plastic strain.

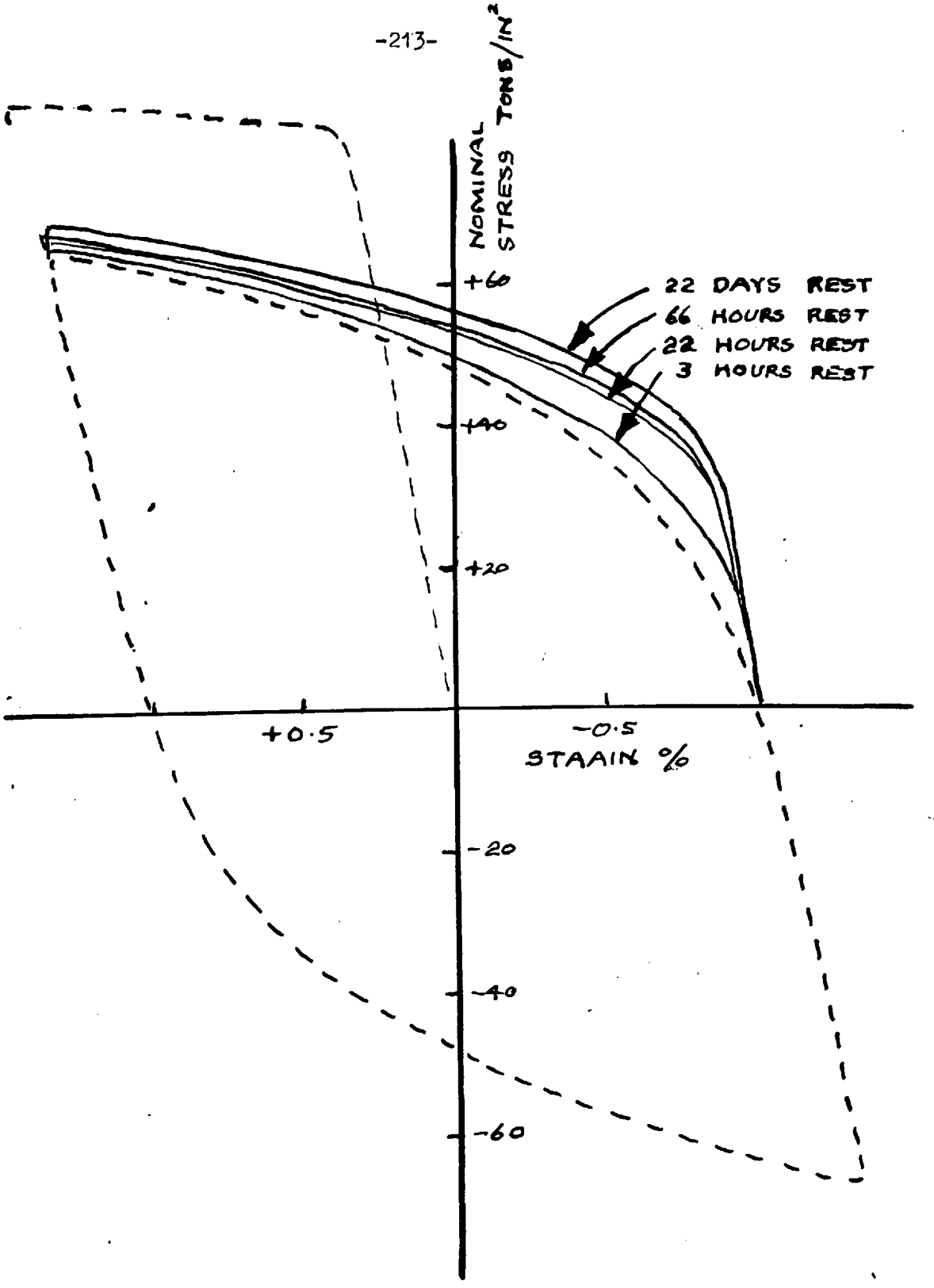

Fig. 47. Effect of rest periods between cycles on the stress-strain loop for hardened and tempered En25 steel.

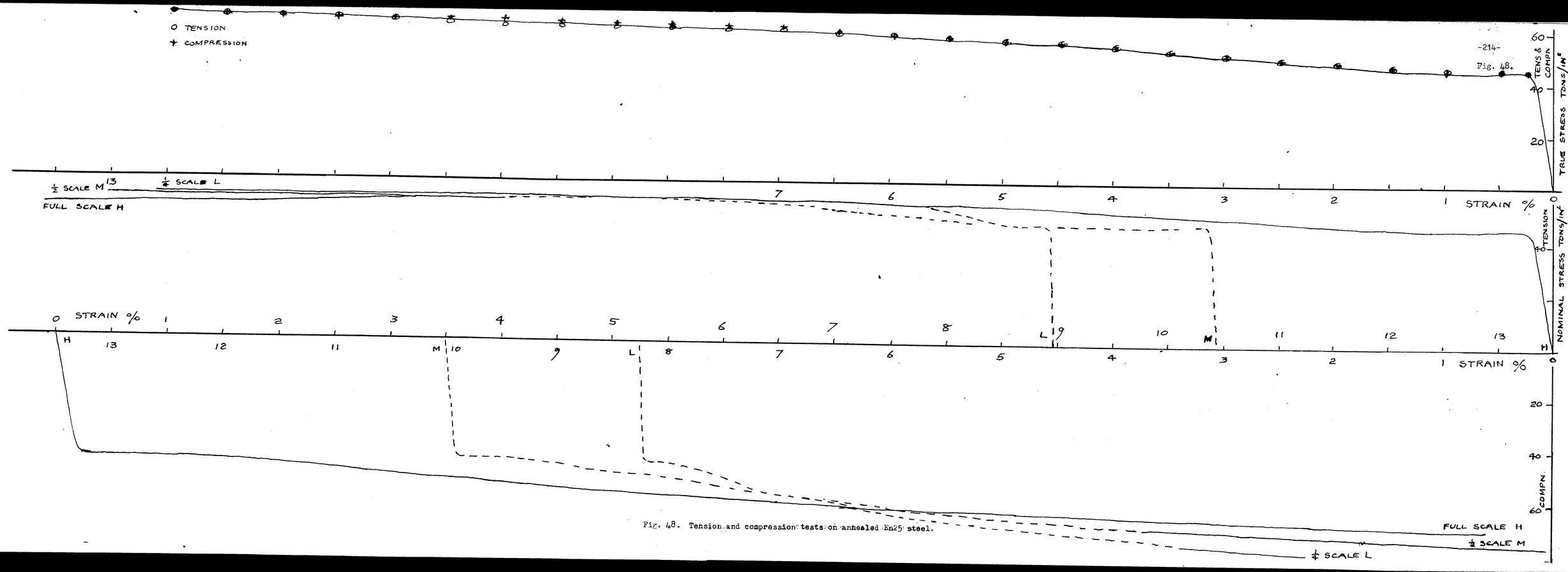

Fig. 48. Tension and compression tests on annealed En25 steel.

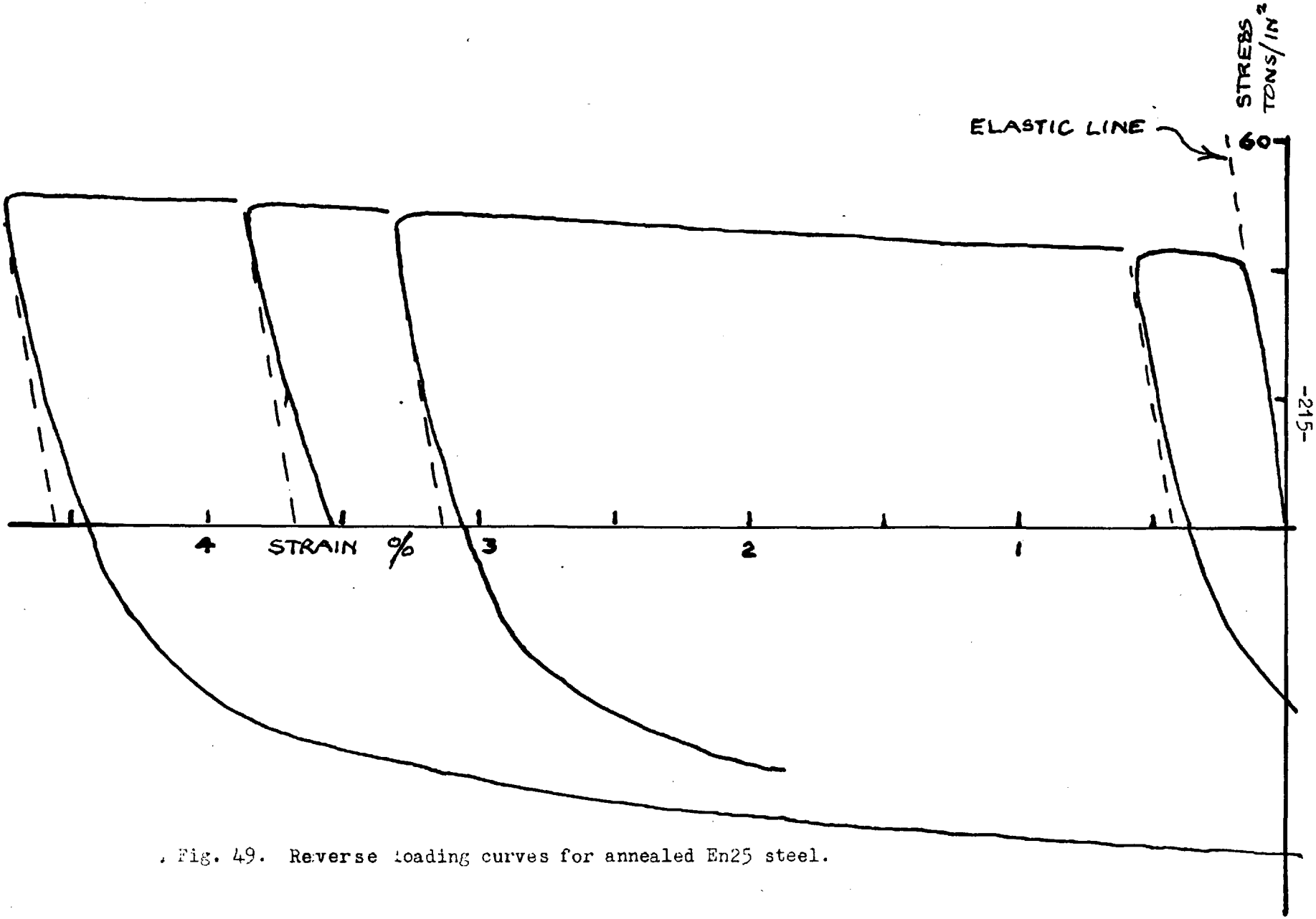

Fig. 49. Reverse loading curves for annealed En25 steel.

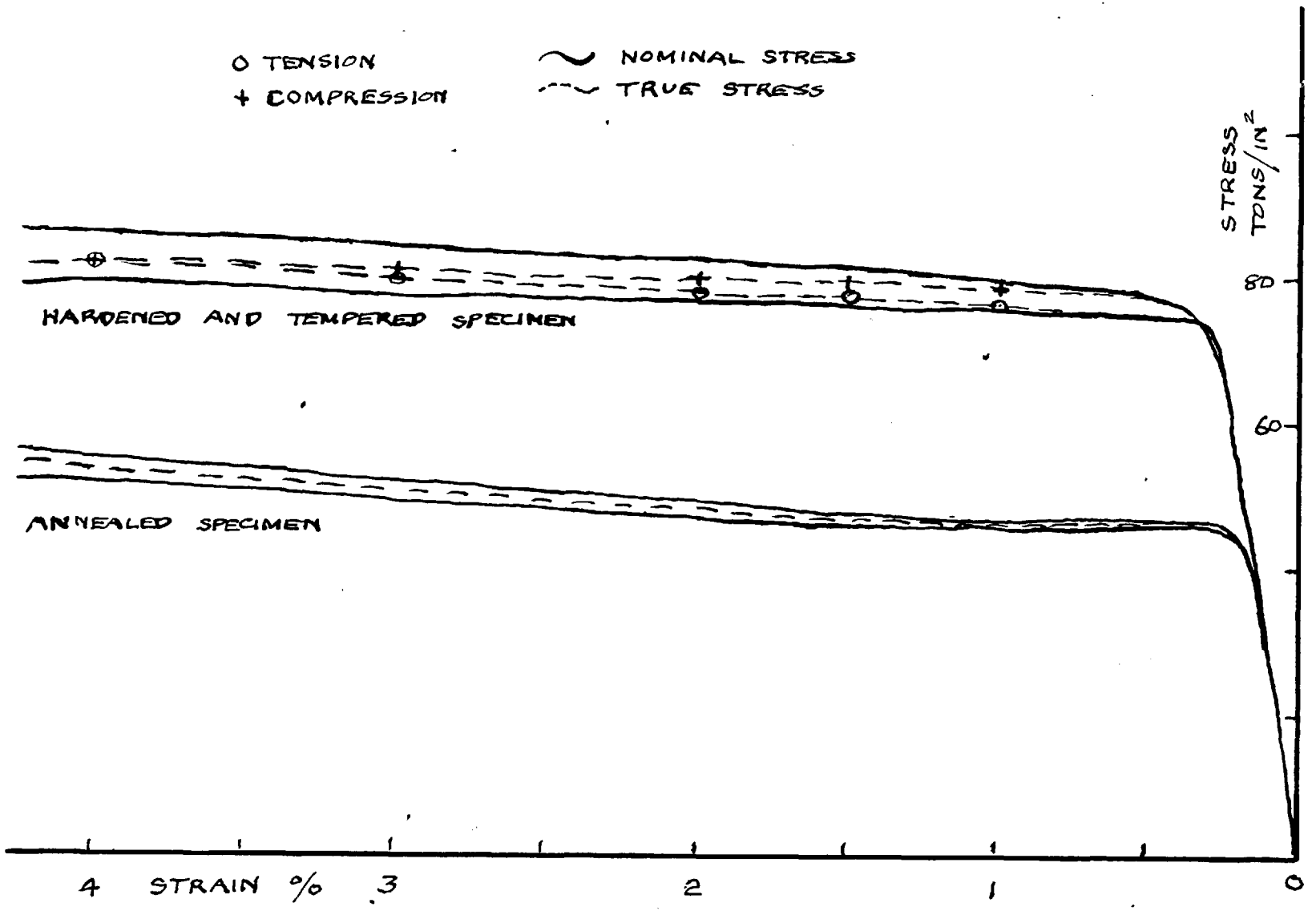

Fig. 50. Tension tests for En25 steel hardened at 840°C and tempered from 550°C.

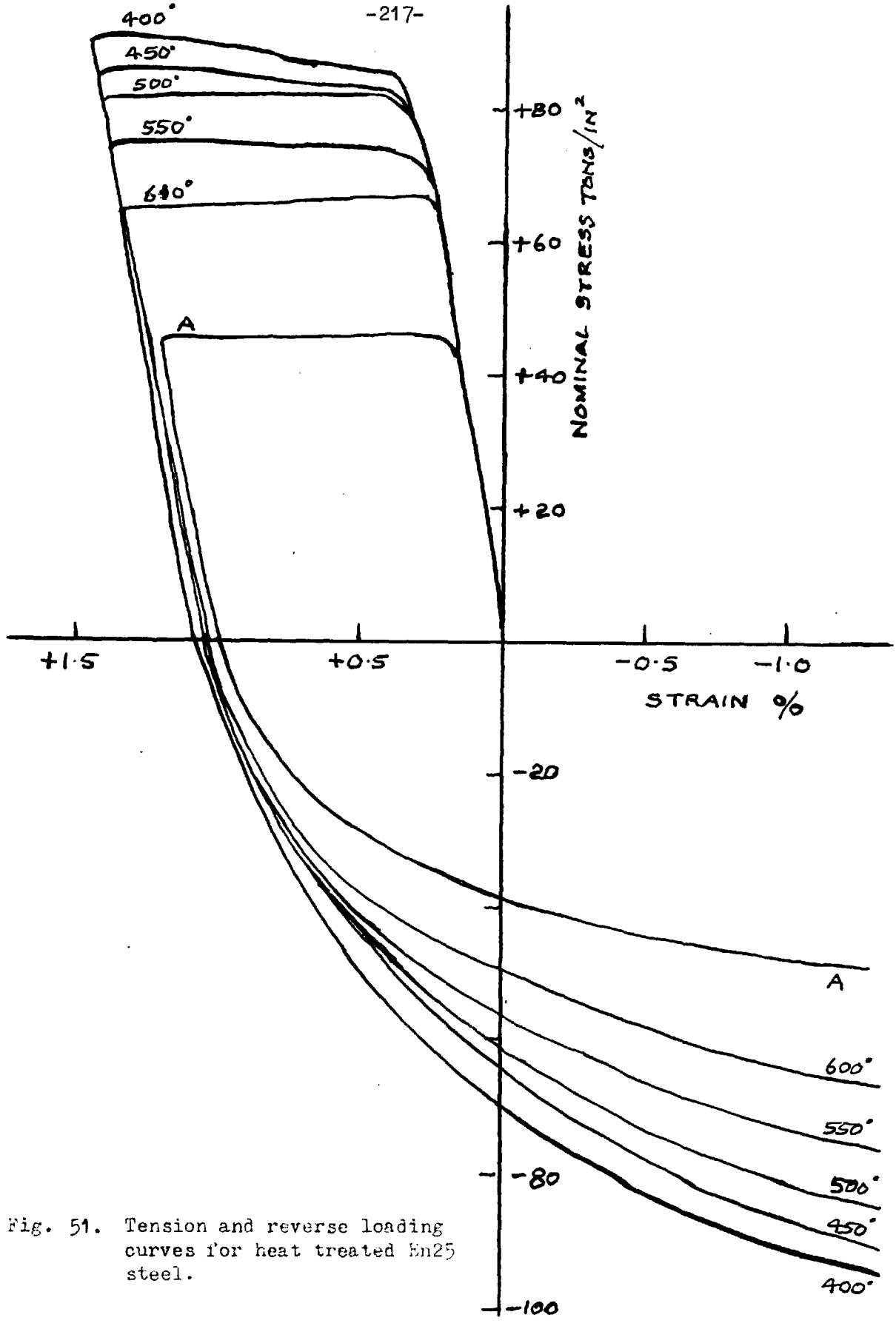

Fig. 51. Tension and reverse loading curves for heat treated En25 steel.

Fig. 52.

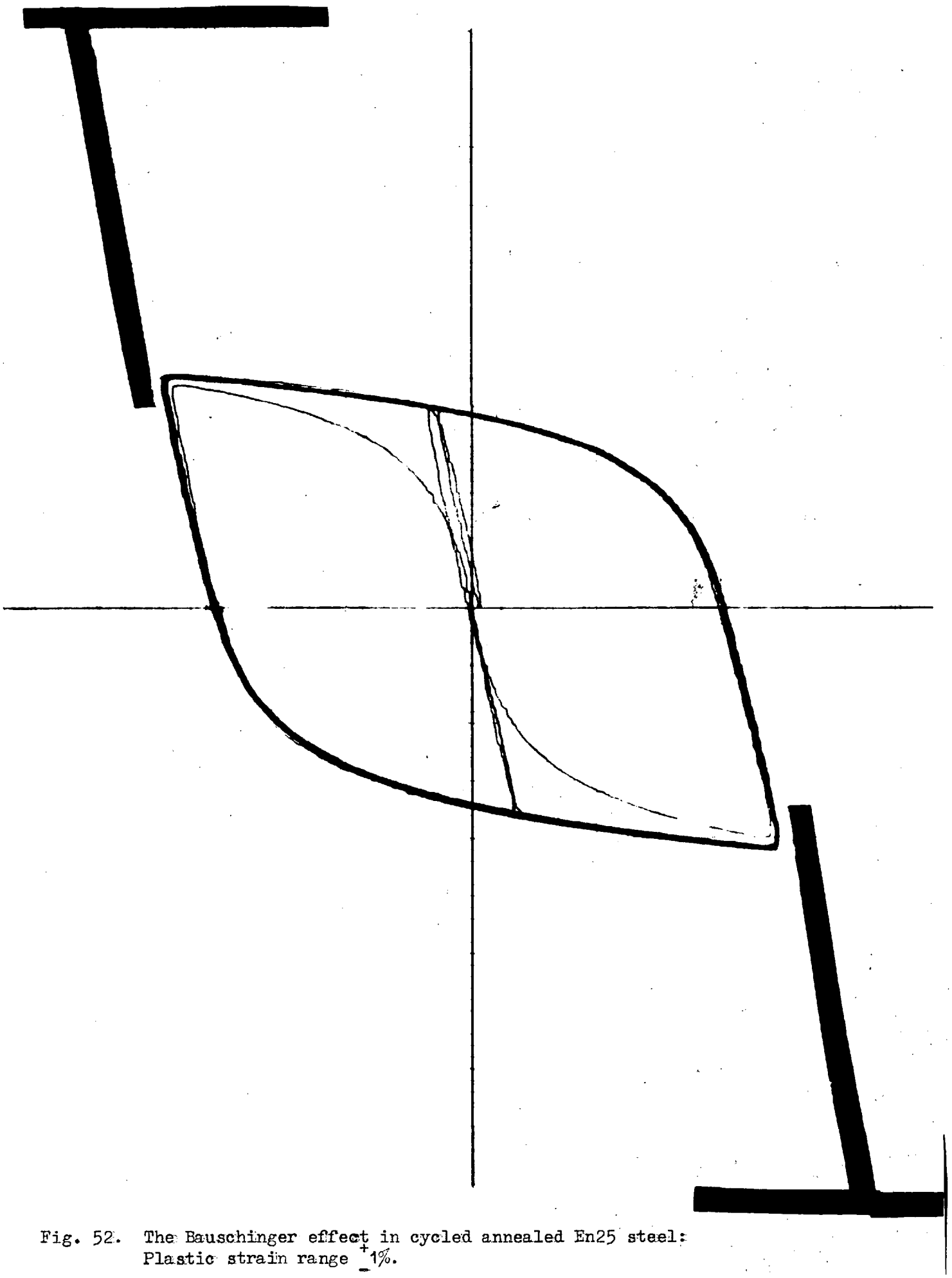

Fig. 52. The Bauschinger effect in cycled annealed En25 steel: Plastic strain range $\pm$1%.

Fig. 53.

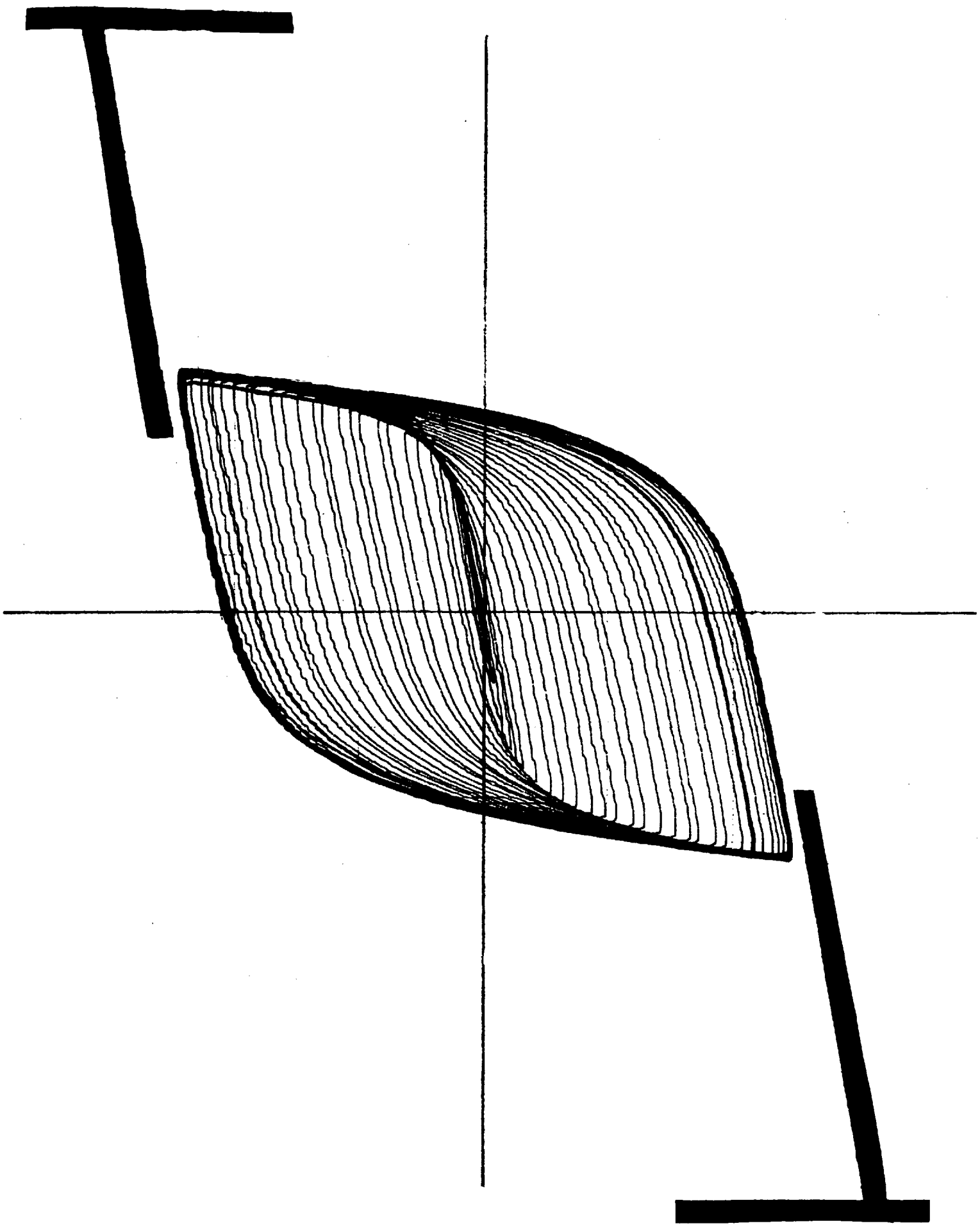

Fig. 53. Tension test following a series of cycles of progressively decreasing strain amplitude.

Fig. 54.

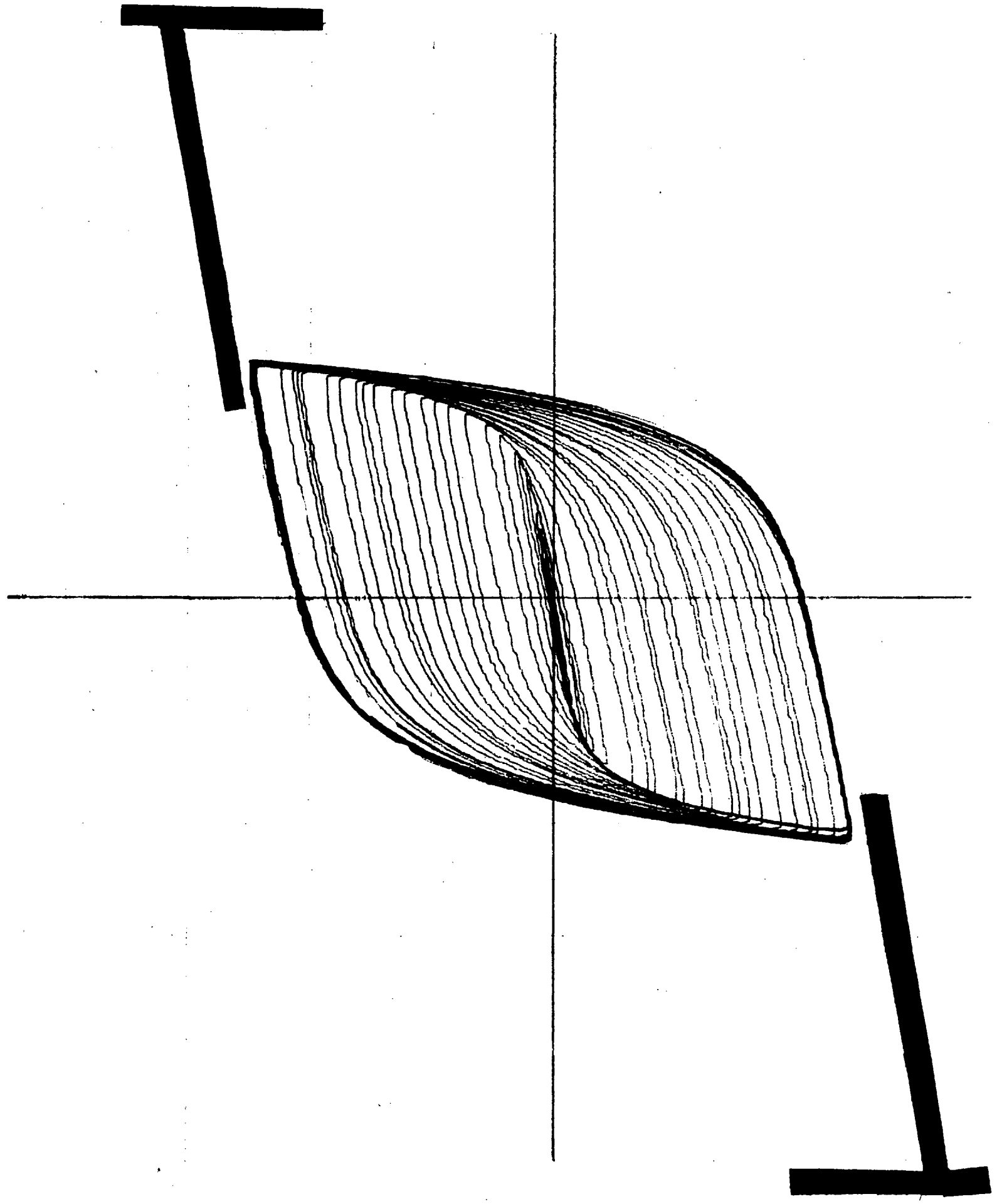

Fig. 54. Compression test following a series of cycles of progressively decreasing strain amplitude.

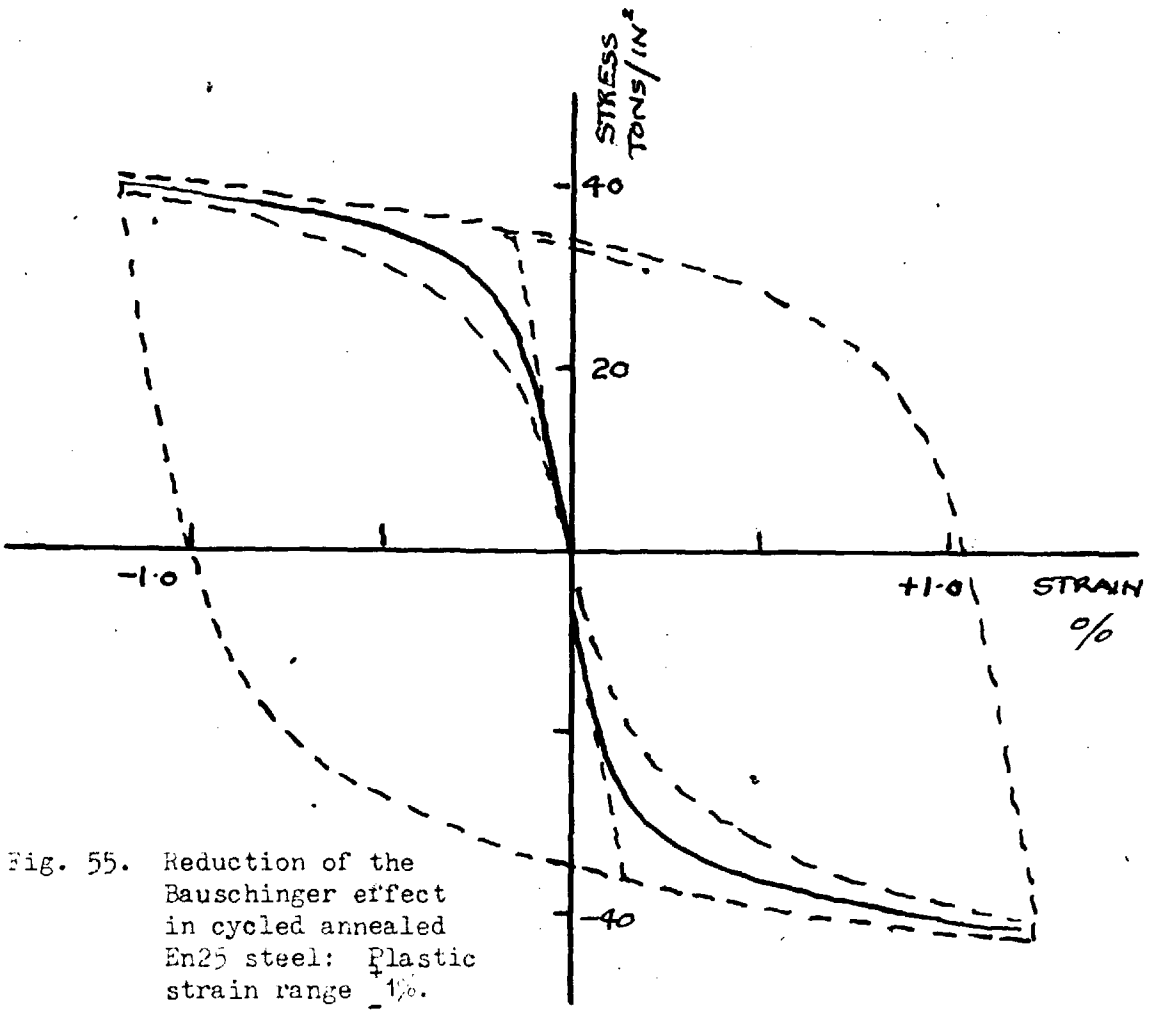

Fig. 55. Reduction of the Bauschinger effect in cycled annealed En25 steel: Plastic strain range $\pm$1%.

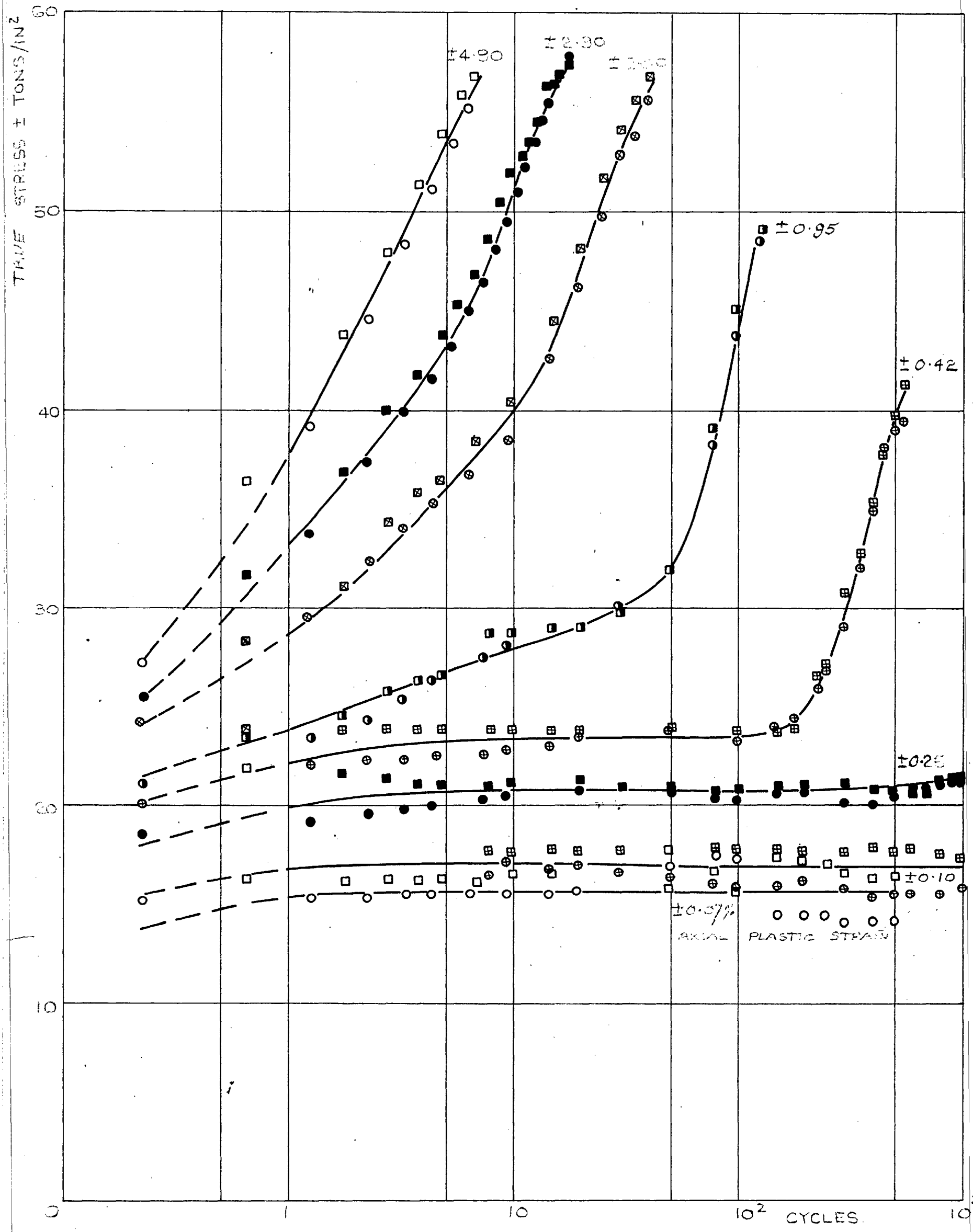

Fig. 56. The effect of plastic strain range on the cyclic hardening of austenitic stainless steel.

Fig. 57.

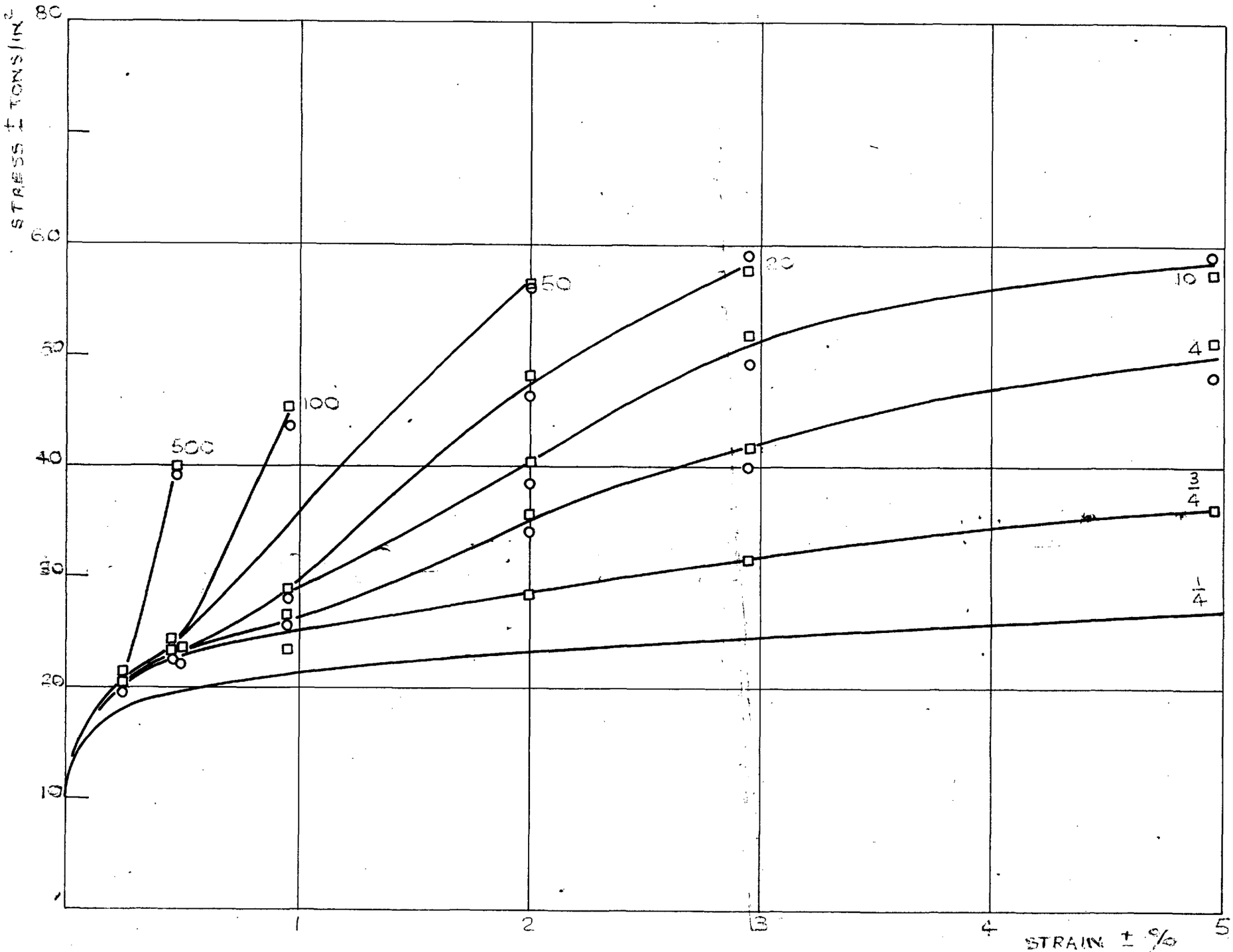

Fig. 57. Cyclic and static stress-strain curves for austenitic stainless steel.

Fig. 58.

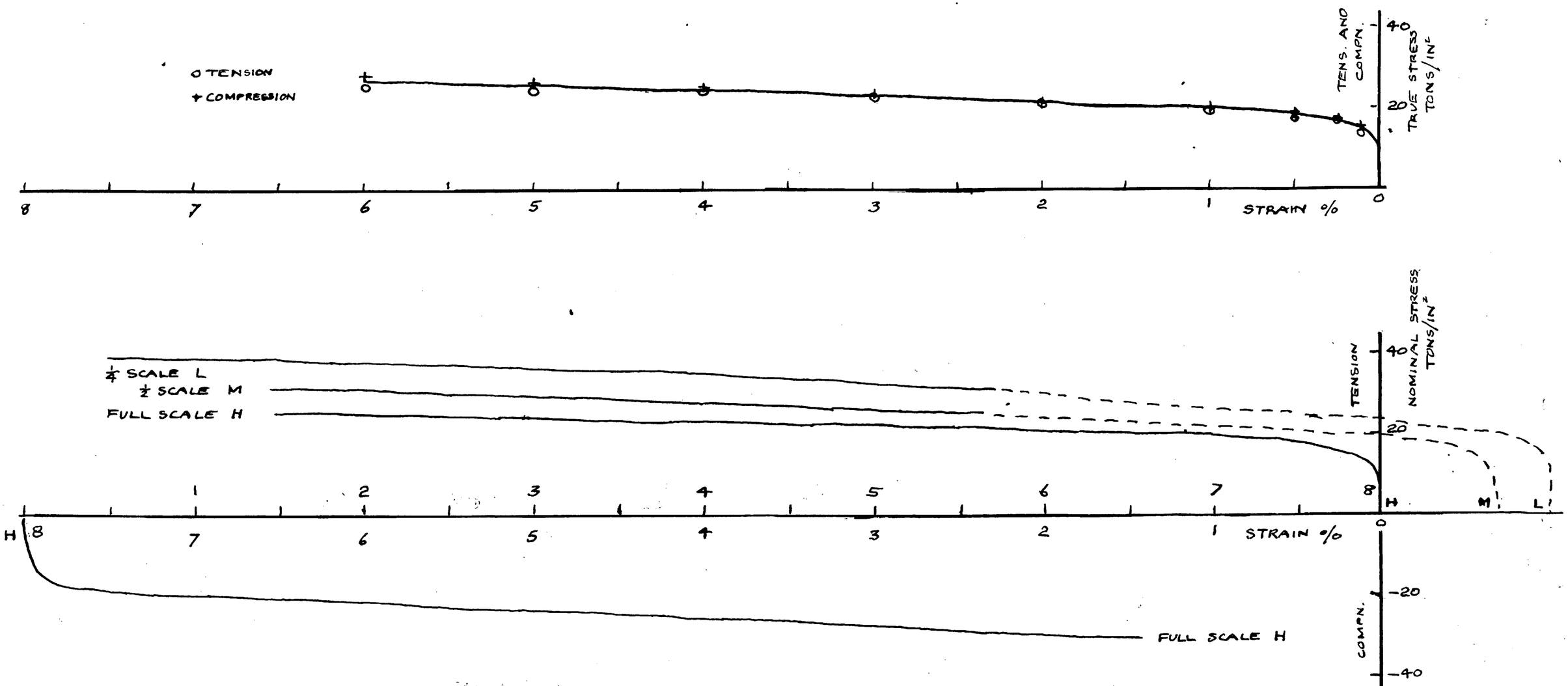

Fig. 58: Tension and compression tests on austenitic stainless steel.

Fig. 59.

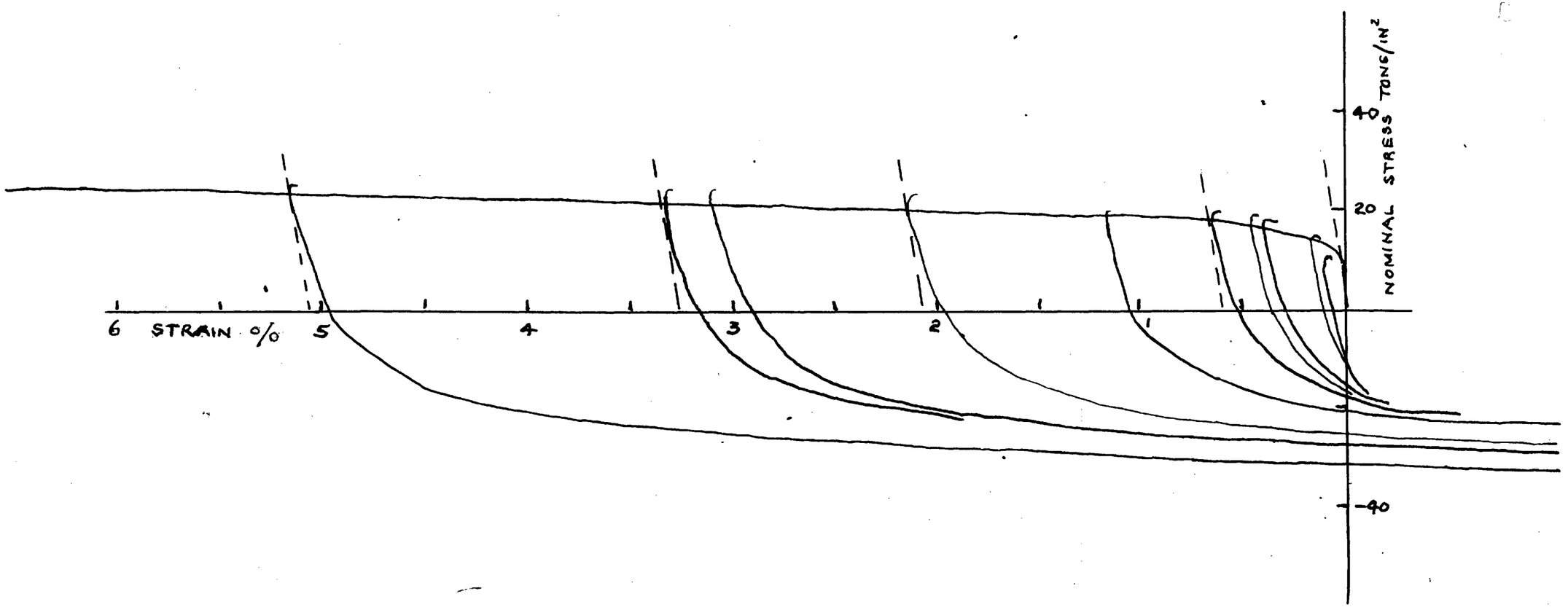

Fig. 59. Reverse loading curves for austenitic stainless steel.

Fig. 60.

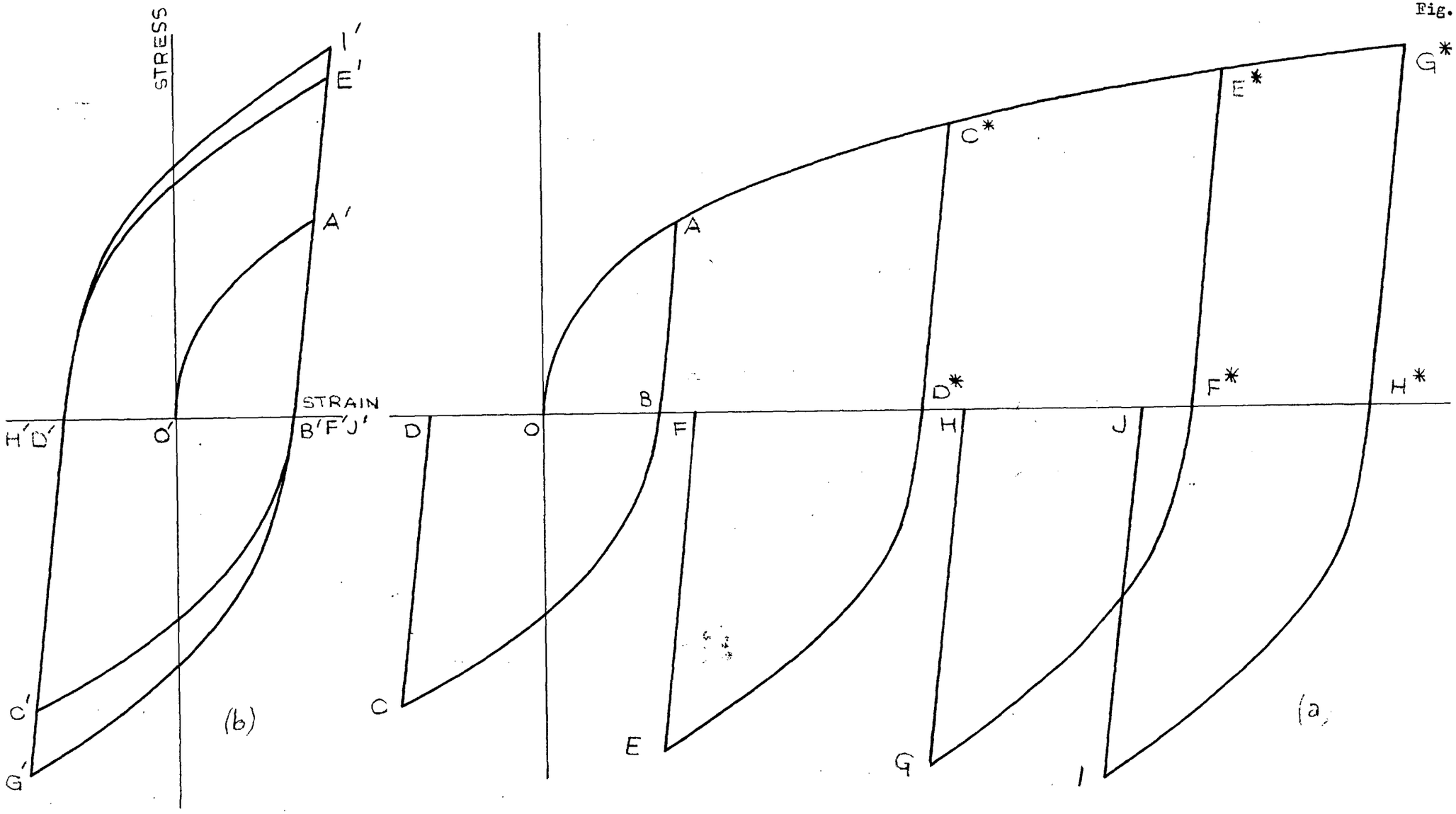

Fig, 60. Diagramatic illustration of the use of simple reverse loading curves to derive cyclic hardening stress-strain loops.

Fig. 61.

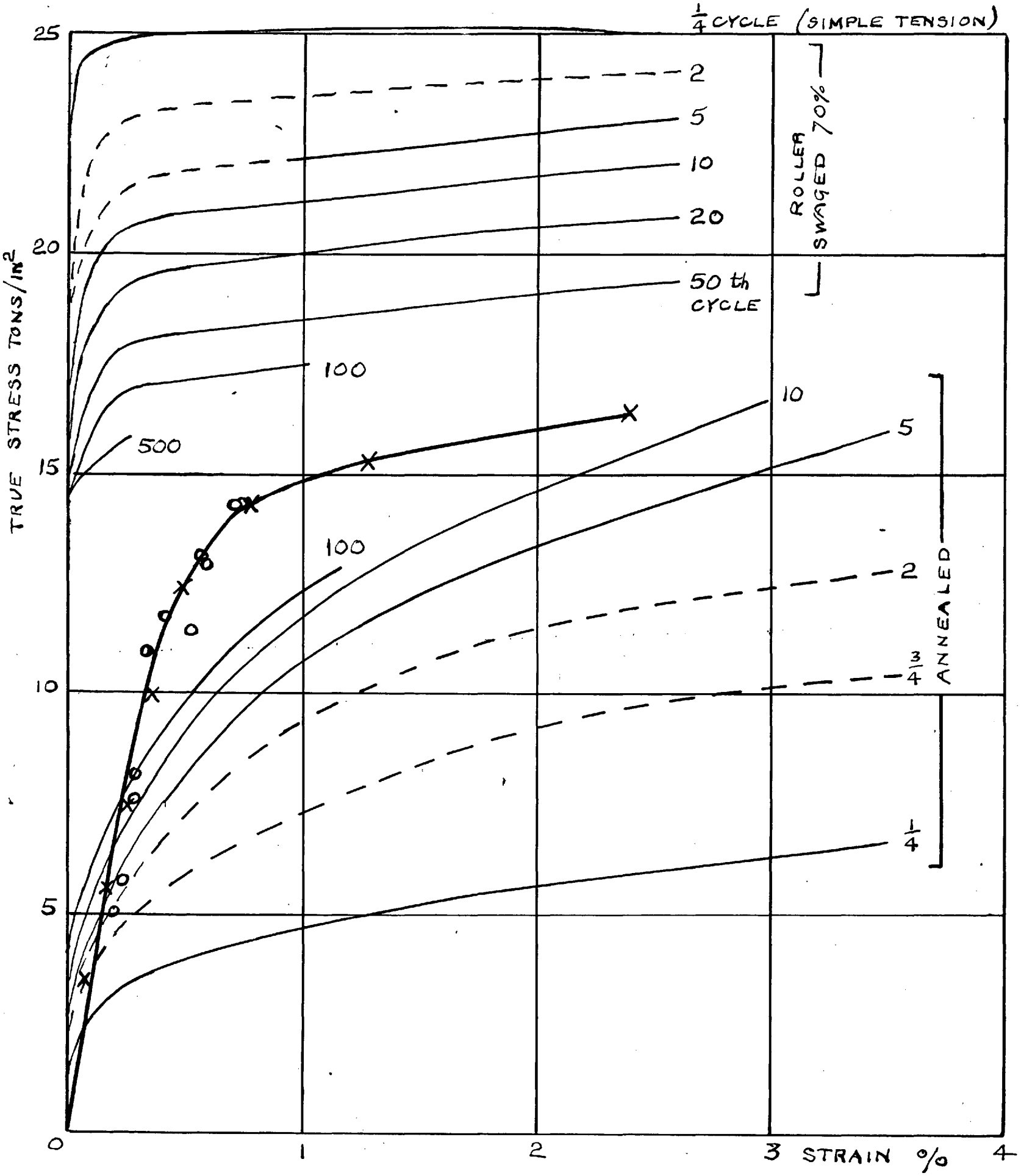

○ INDIVIDUAL SPECIMENS SUBJECTED TO A SINGLE REVERSAL OF STRESS.

X SINGLE SPECIMEN SUBJECTED TO A SERIES OF REVERSALS OF STRESS AT PROGRESSIVE INCREASES OF AMPLITUDE.

Fig. 61. The settled cyclic stress-strain curve predicted from simple reverse loading tests.

Point A is selected so that after removal of the (tensile) load the material shall have equal values of the elastic limit in tension and compression. Tests commence at point B.

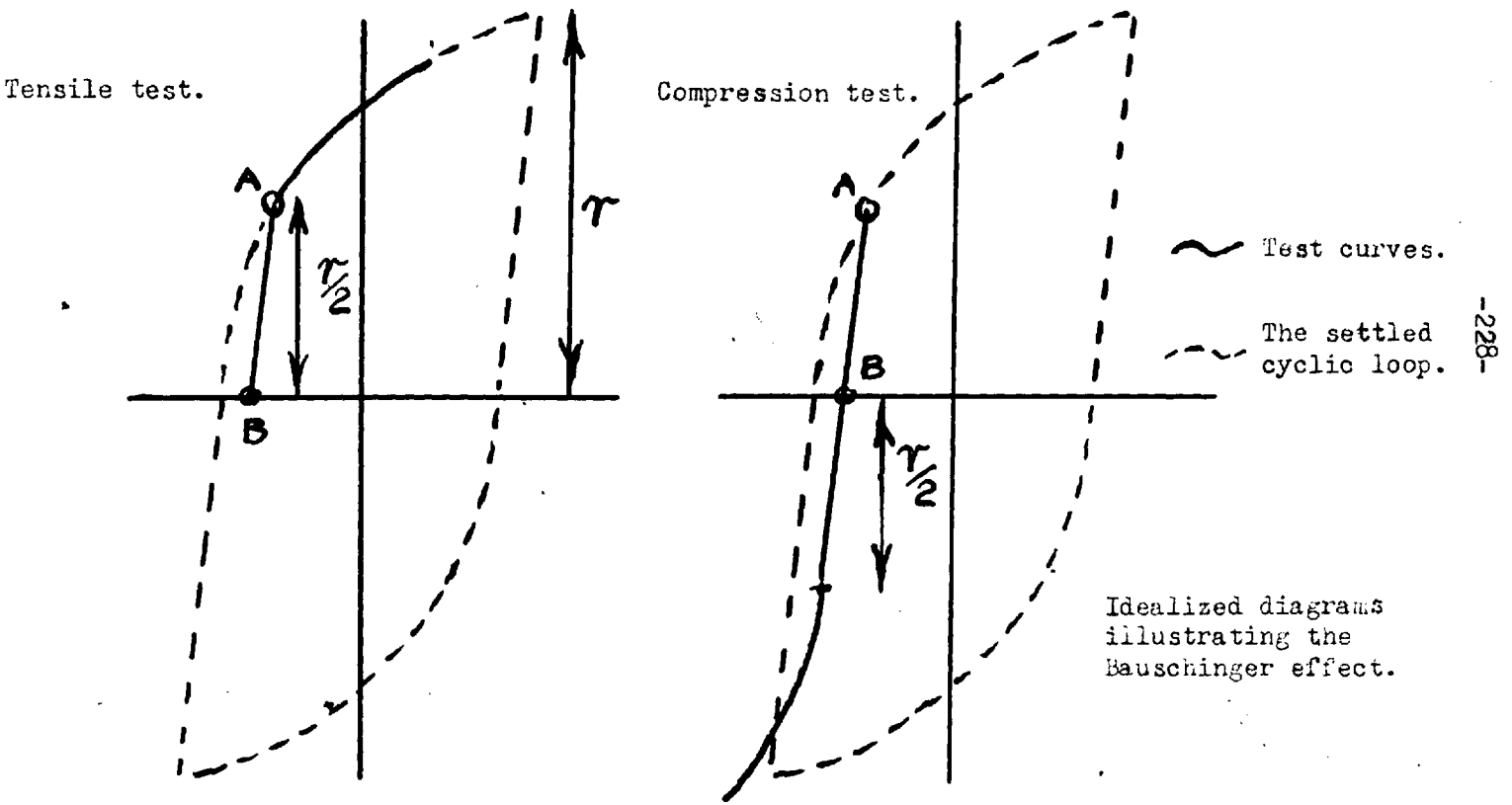

Fig. 62. Demonstration that the Bauschinger effect cannot be eliminated by interrupting the settled cyclic loop at a selected point.

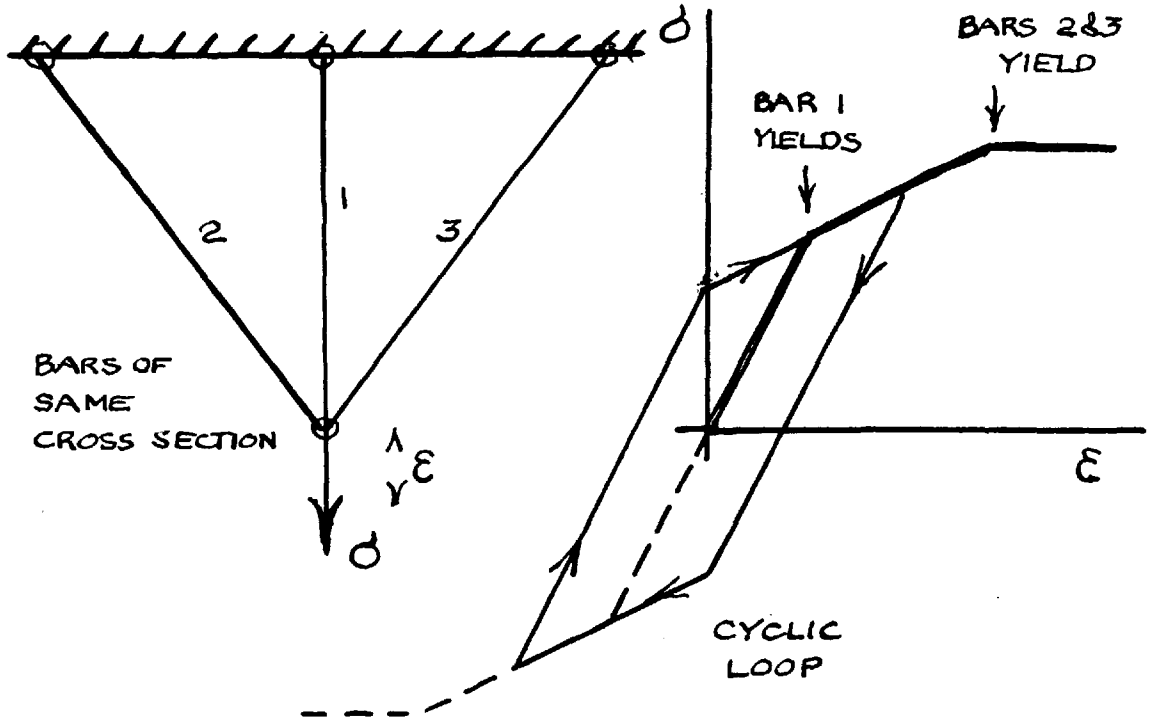

Fig. 63. Pin-jointed bar analogue model of cyclic behaviour.

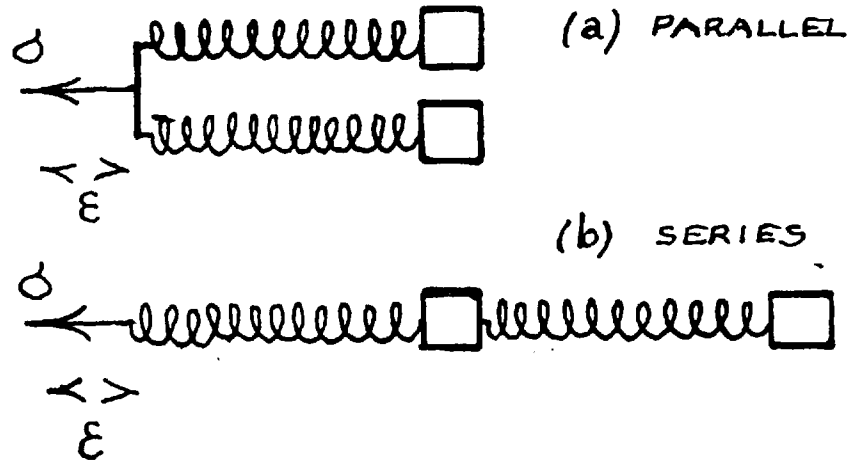

Fig. 64. Spring-block analogue model of cyclic behaviour.

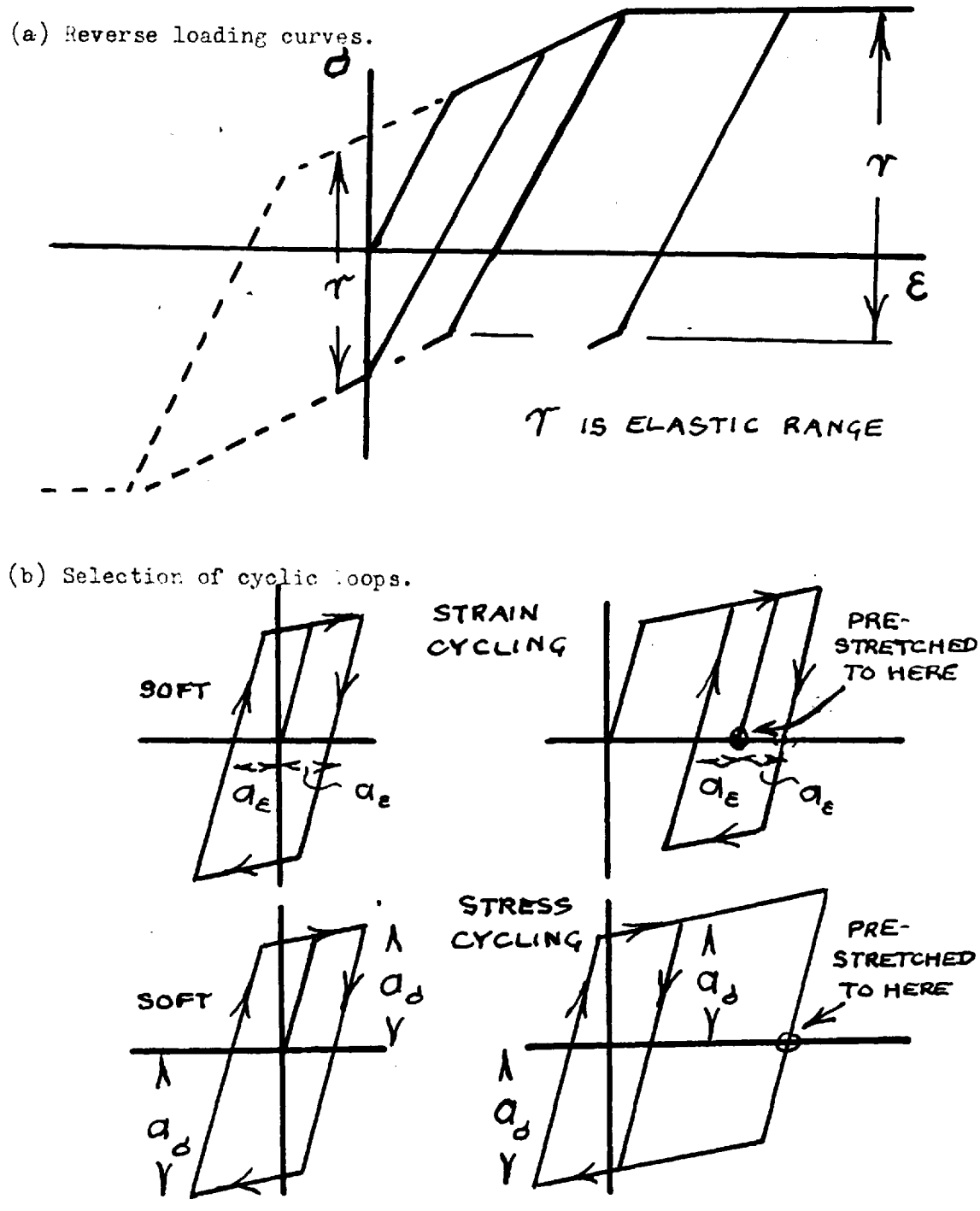

Fig. 65. Typical stress-strain diagrams for a spring-block model.

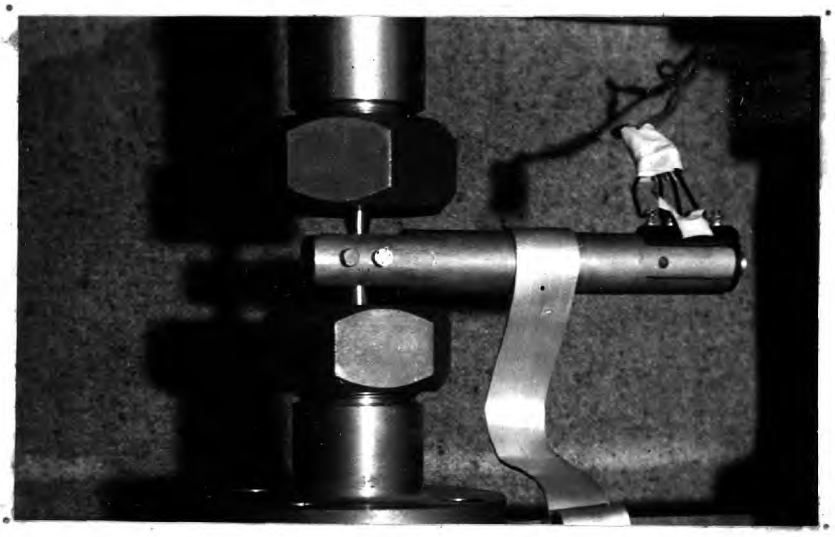

Fig. 66. The extensometer in position on the specimen.

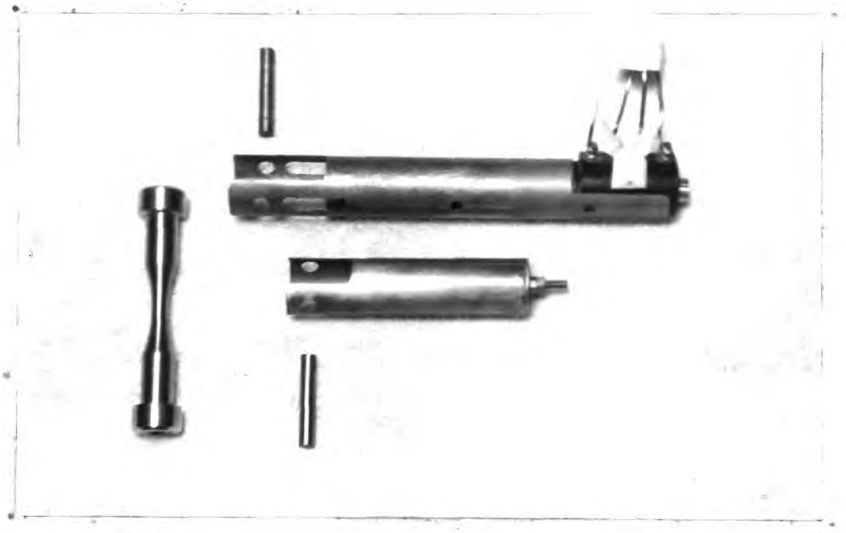

Fig. 67. The specimen and the dismantled extensometer.

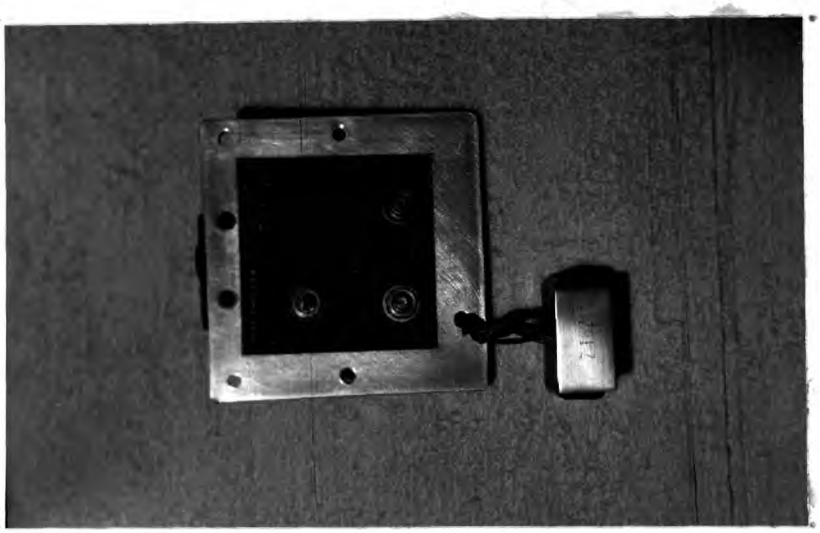

Fig. 68. Modification panel and plug ready for attachment to the chart drive circuit. (Front view.)

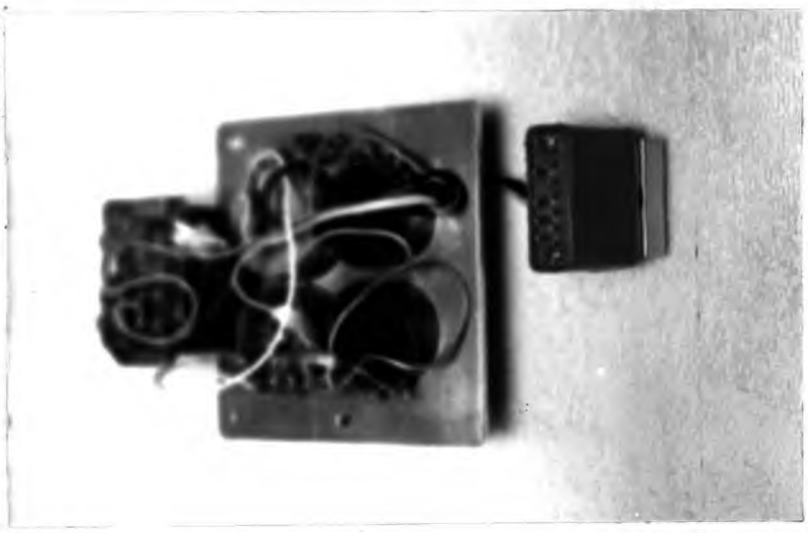

Fig. 69. Modification panel and plug ready for attachment to the chart drive circuit. (Rear view.)



Fig. 70. Modification panel in place on the chart drive amplifier.



Fig. 71. The fixed and moving contacts on the pen recorder unit.



Fig. 72. The end-fittings. (One dismantled.)



Fig. 73. The Instron testing machine.

Ph.D. 1968. P. W. J. OLDROYD.

Reprinted from

International Journal of
MECHANICAL
SCIENCES

PERGAMON PRESS
OXFORD · LONDON · NEW YORK · PARIS

Int. J. Mech. Sci. Pergamon Press Ltd. 1966. Vol. 8, pp. 77–88. Printed in Great Britain

STRESS–STRAIN BEHAVIOUR OF COPPER AND ZINC CUBES SUBJECTED TO CYCLICAL COMPRESSION

P. W. J. OLDROYD* and P. P. BENHAM†

(*Received* 3 *September* 1965)

Summary—Cubes of pure copper in annealed and cold-worked conditions were subjected to compressive loading along each of the three principal axes in turn. With successive orientation cycles of loading the measured strains for the three directions reached stable values after strain hardening or softening, and a cyclical stress–strain curve was derived.

Miniature tensile specimens cut from the cubes before and after cycling indicated that triaxial cycling retained initial isotropy and reduced previous anisotropy, while achieving a harder or softer state of the material.

Cyclical stress–strain relationships from triaxial compression tests and previous uniaxial tension–compression tests on copper showed marked differences.

The few tests conducted on cubes cut from a cast zinc ingot exhibited a similar pattern of behaviour to that for copper, except that the effects of anisotropy were more marked.

INTRODUCTION

THE effects of cyclical plastic deformation on the stress–strain properties of materials has aroused much interest[1–3] in recent years principally as a result of the many investigations in the field of low endurance fatigue. It has been found that initially soft materials strain harden, and initially hard or partly hard (caused by cold work or heat treatment) materials strain soften, when subjected to cycles of stress or strain in the plastic range for axial, bending or torsional states of deformation. Previous investigations[4,5] on pure copper have dealt with push–pull and torsional cycles, and there appeared to be a relationship between stable values of cyclical stress and strain (after hardening or softening) which was independent of strain history, and towards which the material would work irrespective of its initial condition.

In the discussion of the paper by Watts and Ford[6] on the plane strain compression test, a subsidiary test was described in which a cube of annealed copper was subjected to compression in turn along each of the three principal axes. It was found that for a strain of 2–3 per cent the flow stress increased rapidly at first with successive orientation cycles of the cube, but gradually the stress approached a stable value and no further hardening occurred. At that time the general behaviour of cyclical strain hardening and softening had not been recognized.

Although there are some obvious drawbacks to this type of test, principally that of friction and barrelling for large strains, it does provide a means for obtaining reversals of deformation, extension and compression, using only compressive stress and no tension. A comparison of cyclical stress–strain behaviour with that obtained from the previous[4] push–pull testing should

* Department of Mechanical Engineering, Imperial College, London.
† Department of Mechanical Engineering, The Queen's University of Belfast

indicate the uniqueness or otherwise of the phenomenon of cyclical hardening and softening and the dependence on type of applied stress. It was also thought that anisotropy might be removed or reduced during this test.

MATERIALS, SPECIMENS AND APPARATUS

The copper was the same as used previously,[4,5] O.F.H.C. in the form of $1\frac{1}{2}$ in. dia. bars which had been supplied cold drawn an unspecified amount (V.P.N. 95). Cubes of 1 in. side were cut from the bar so that two opposite faces were perpendicular to the axis of the bar which was designated direction A. The other two mutually perpendicular directions of the cube (diameters of the bar) were designated B and C as shown in Fig. 1(a). To obtain cubes in a soft condition, annealing was carried out at 600°C for 30 min, giving a hardness of 42·5 V.P.N.

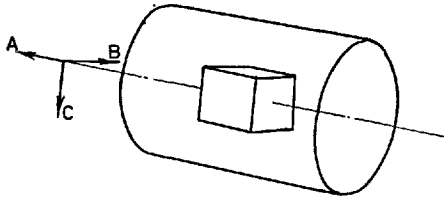

(a) Copper

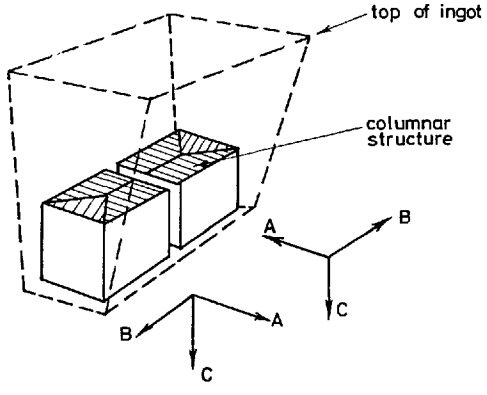

(b) Zinc

FIG. 1. Orientation of copper and zinc cubes.

The main purpose of the investigation was to study copper; however, it was suggested by a metallurgist colleague that the different structure of zinc and the crystal formation in casting might provide an interesting side-line. Consequently a small cast ingot was provided from which two cubes were cut with directions designated as in Fig. 1(b). The columnar formation of crystals was revealed by etching and the cube orientation during testing remembered by a small notch in one edge. All cube faces were lightly ground.

Compression testing was carried out on a 50 tonf universal hydraulic machine with a cube situated between the platens of a sub-press (to improve axiality of loading) which was inserted between the compression platens of the machine. Permanent deformation

of a cube was measured with a micrometer, and each time before inserting a cube into the sub-press, the faces to be loaded were smeared with a pencil lead and oil to reduce friction.

TESTING PROCEDURE

Certain practical difficulties arising in this type of test make it desirable to describe here the testing procedure adopted. The difficulties are principally due directly or indirectly to barrelling. It is well known that owing to surface friction there is not a completely uniform stress system in a compression specimen. The methods usually employed to overcome this problem cannot be utilized in the present programme and all that could be done was to keep friction as low as possible, use incremental loading when convenient and restrict deformation to fairly small plastic strains. All tests were done under the same conditions so that any error due to non-uniformity of stress was similar throughout. One source of error was in the measurement of plastic strain between faces which, owing to barrelling, were no longer plane. A second source occurs if the load is not high enough to eliminate the barrelling on a preceding pair of faces and give overall surface contact. Another difficulty was the gradual sideways collapse of some cubes (giving a parallelepiped shape) after a number of cycles, which tended to set a limit to the cyclic strain which could be investigated to about 0·06.

The sequence of cyclical operation was as follows: insert a cube centrally into the sub-press, for loading in direction A, apply the required load and hold constant for 1 min, then remove the load and measure the cube dimensions in directions A, B and C. After recoiling, the cube was inserted for loading in direction B and the above procedure repeated, and similarly for direction C, and so on.

Preliminary tests showed that cycling at constant nominal stress gave values of permanent strain which at first changed rapidly but gradually (within about 12 cycles) approached a stable value. Cycling was always continued until three successive readings were virtually the same and could be averaged to give the stable value.

When it was desired to cycle a soft cube under a fairly large load, say 10 tonf it was necessary to build up progressively to the load in the three directions, viz. 1, 2, 3; 4, 5, 6; 7, 8, 9; 10, 10, 10 tonf. If the full load was applied initially the cube form was destroyed and due to strain hardening, higher loads than that desired would have to be applied along the second and third axis to restore the cube.

The above procedure was found to give results that agreed closely with (a) large number of small changes in load which did not affect the cubic form or (b) a few large changes in load with the loading adjusted to allow for loss of cubic shape and keep stress constant.

MONOTONIC COMPRESSION TESTS

Simple monotonic compression stress–strain curves were first obtained for the range of strain to be studied on cubes of annealed and cold drawn copper for directions A, B and C and for the zinc in direction A only. These stress–strain curves are shown in Figs. 2, 3 and 6.

CYCLICAL COMPRESSION TESTS

Annealed copper: triaxial cycling

Referring to Fig. 2, curve 1 shows the stable values of strain obtained in directions A, B and C for stresses progressively increased up to 15·8 tonf/in^2. Cubes were also triaxially cycled up to this stress by the other two methods described earlier (small changes in cyclic stress and large increments of stress with adjusted loading) and agreement was very good (the points are omitted to avoid confusion.)

Curve 2 is for another cube which was brought up to 15·8 tonf/in^2 by progressive loading, then cycled down to 10 tonf/in^2 with a series of constant stresses along A, B and C and finally cycled up again (curve 3), to 15·8 tonf/in^2; only points for direction A are shown. To test the validity of the technique another cube (points not shown) was loaded immediately to 15·8 tonf/in^2, and then reground to restore the cubic form. It was then

cycled down to 10 tonf/in² and gave stable values of strain which agreed quite well with curve 2.

Annealed copper: biaxial cycling

The effect of compression alternately on two axes (B and C) only and hence incremental growth in direction A is illustrated by curve 4, Fig. 2. The stable values of strain were for progressively increasing cycles of stress.

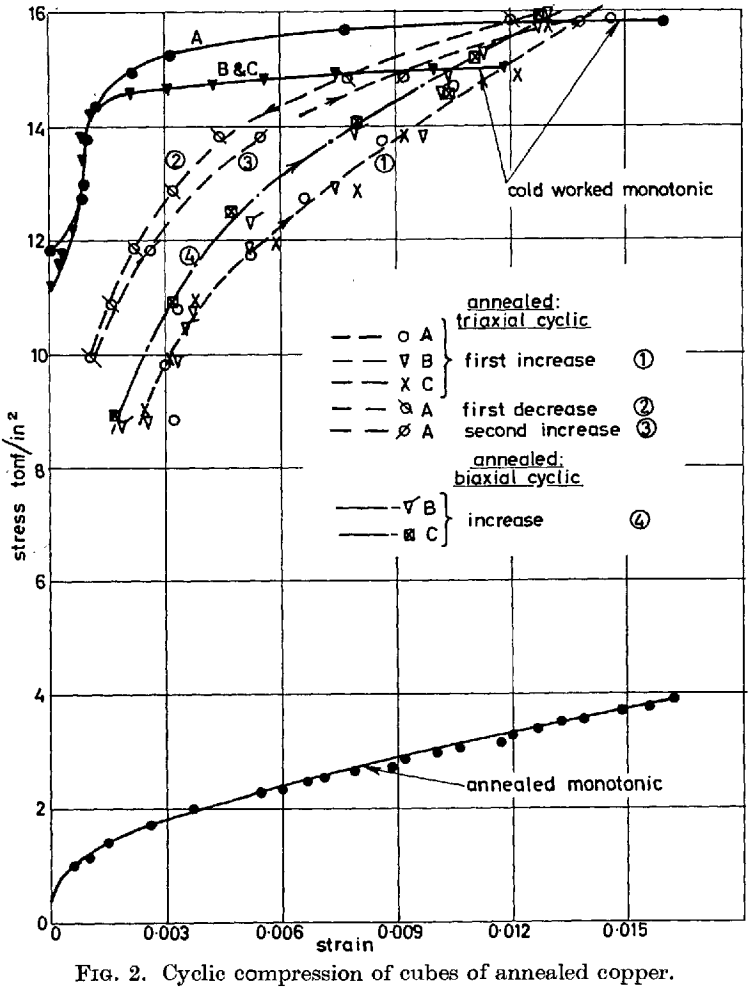

FIG. 2. Cyclic compression of cubes of annealed copper.

When the lateral loading cycles on the above specimen had caused a log strain of 0·24 in direction A, it was remachined to a cube and tested monotonically in compression along direction A. The resulting stress–strain curve is shown in Fig. 3. Also shown in this figure are some of the curves on Fig. 2 extended to larger strains.

Cold drawn copper

A cube cut from the cold drawn bar was progressively cycled triaxially up to 15·8 tonf/in² and the stable values of strain for directions A, B and C are shown in Fig. 4. Another cube was cycled at 15·8 tonf/in², then taken in a single step down to 11 tonf/in²

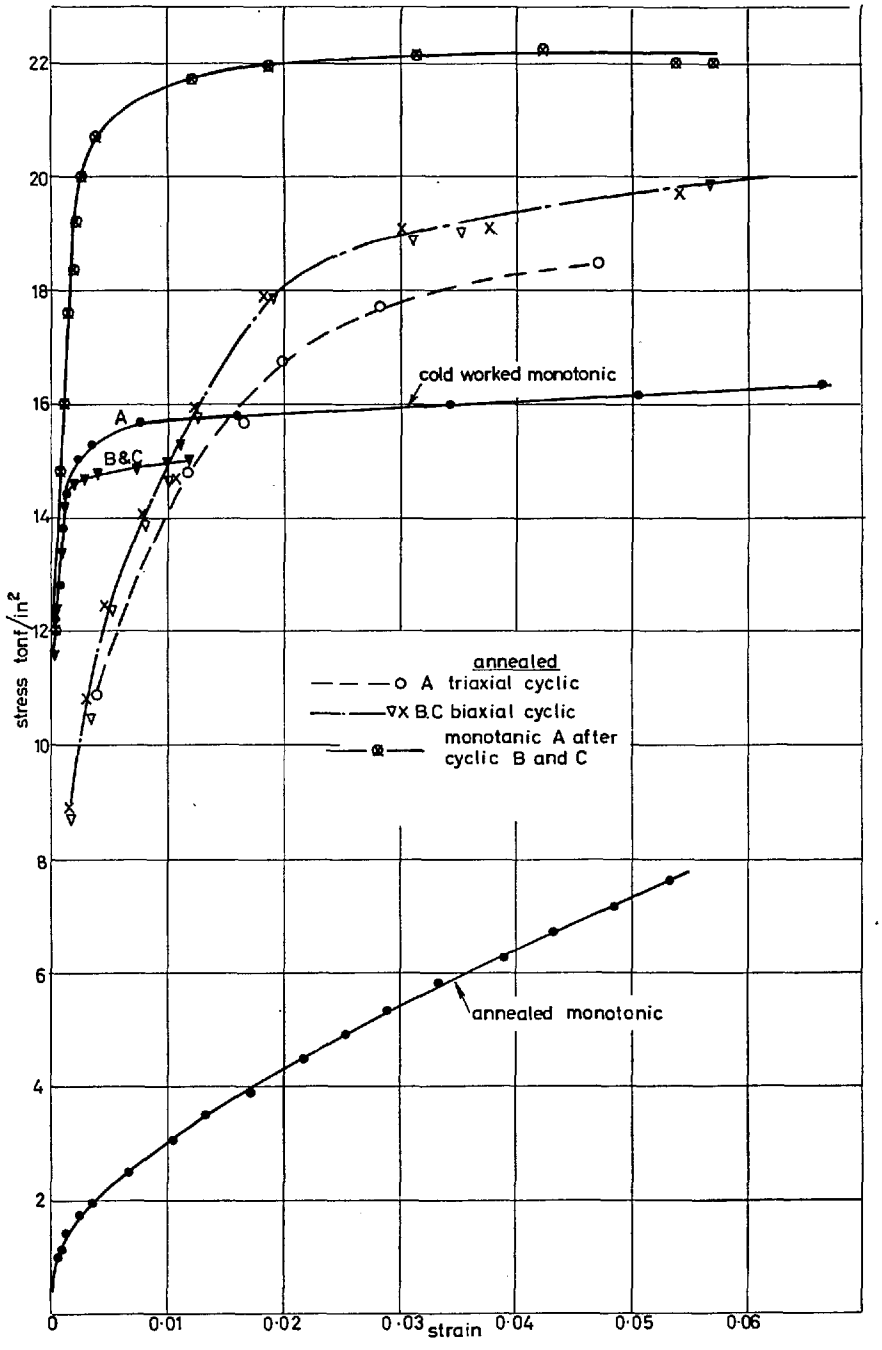

FIG. 3. Cyclic compression of cubes of annealed copper up to larger strains.

and cycled to give a stable strain, finally it was cycled progressively up to the original stress. The stress–strain behaviour during this latter operation is plotted also in Fig. 4 for comparison with the first increasing stress path.

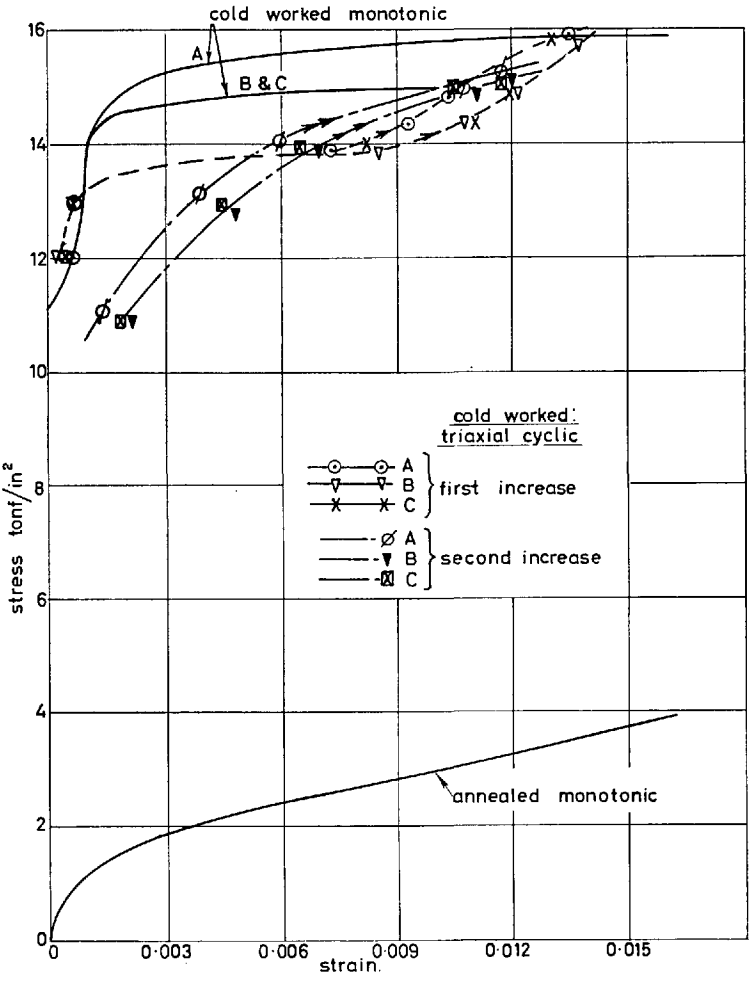

FIG. 4. Cyclic compression of cubes of cold-drawn copper.

Variation in strain during cycling from one stress to another

Annealed and cold drawn cubes were cycled triaxially at 13 tonf/in² until strain values became stable. The stress was then increased to 14 tonf/in² and the strain values obtained for directions A, B and C were plotted as in Fig. 5 until the cubes became stable. It is seen that the stable strain per cycle is closely similar for the annealed and cold worked states, although more cycles were required in the latter case before softening was completed.

MINIATURE TENSION TESTS

In order to study further the effect of compression cycling on the state of the material, miniature Hounsfield tension specimens were cut from virgin material and cycled cubes.

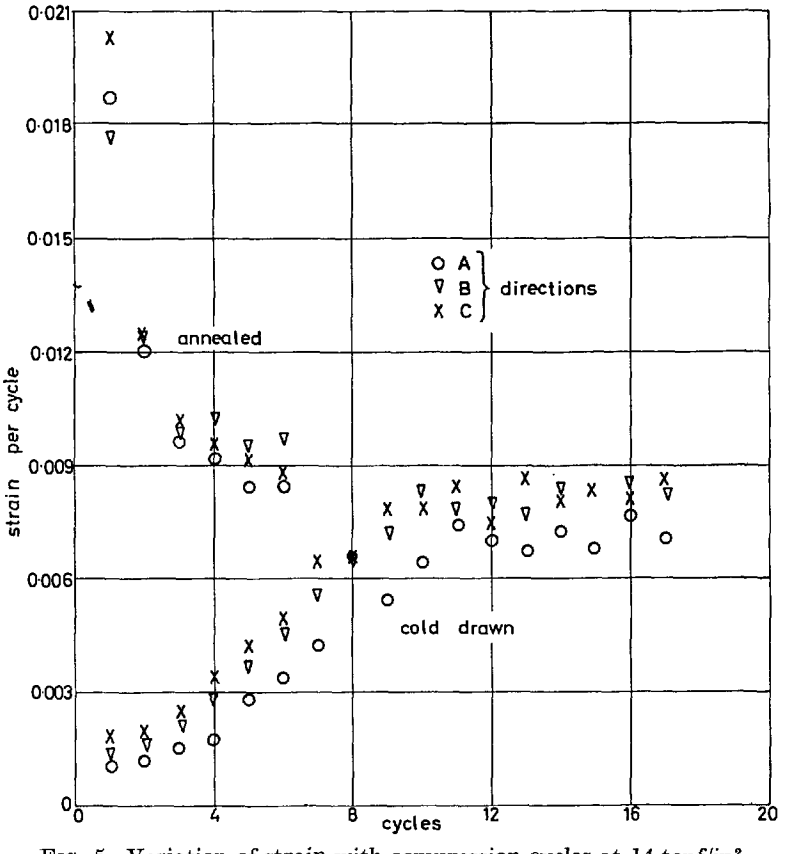

FIG. 5. Variation of strain with compression cycles at 14 tonf/in² following cycling at 13 tonf/in² for copper.

In the latter case cubes were machined to yield a pair of tension specimens for each of directions A, B and C. The results in terms of tensile strength and ductility are presented in Table 1.

TABLE 1

Condition	Cube direction	Tensile strength tonf/in²	Elongation per cent $4\sqrt{A}$	Reduction area (per cent)
Annealed, uncycled	A	13·8	58	76
	A	13·9	55	84
	B	13·5	58	76
	B	13·5	59	80
	C	14·0	57	78
	C	12·6	58	78
Annealed, cycled at 16 tonf/in²	A	15·6	25	77
	A	14·8	28	80
	B	15·8	30	68
	B	14·5	34	70
	C	15·2	33	78
	C	15·4	27	66
Cold drawn, uncycled	A	16·0	32	59
	A	16·3	33	74
	B	14·9	32	66
	B	14·6	37	68
	C	15·1	30	62
	C	14·9	33	68
Cold drawn, cycled at 16 tonf/in²	A	16·8	25	49
	A	15·6	24	55
	B	15·4	25	56
	B	15·1	22	60
	C	15·7	23	50
	C	15·4	22	58
Annealed cube extended 24 per cent in direction A by cyclic loading along B and C directions	A	15·7	32	78
	A	16·4	27	78

ZINC

Only two zinc cubes were tested. One was used to obtain the monotonic compression stress–strain curve for direction A. The other cube was given a series of cyclic treatments as follows; it was first cycled progressively up to 7 tonf/in², thence it was cycled down to 3 tonf/in² and again up to 7 tonf/in², and this latter sequence was repeated once again. The resulting stress/strain values are plotted in Fig. 6.

DISCUSSION

The tension tests on the uncycled annealed copper indicated a good measure of isotropy, and curve 1, Fig. 2, shows that cyclical compression does not significantly alter that isotropic state. An important feature of the agreement obtained between the three methods tried for cycling a cube up to a particular value of stress is that the same relation of stable stress and strain is reached regardless of whether the cycles are of constant stress or strain and the size of the stress increments. However, it appears that curve 1 is not the basic cyclical stress–strain relationship, since curves 2 (decreasing) and 3

(increasing again) show further strain hardening. Similar behaviour is also seen in Fig. 6 for zinc (direction A). The most likely explanation for not obtaining a unique curve during the first increasing path is that the value of strain which is considered stable for a particular stress is not so. It has been shown elsewhere[4,5] during low endurance fatigue studies that cyclical hardening or softening to a stable value of strain or stress may take from a few (20) up to several hundred cycles. Although changes are rapid and considerable in the first few cycles, further change still occurs slowly thereafter. It would be impracticable to conduct a large number of cycles in the present type of test to achieve complete stability and a more sophisticated method of strain measurement would be required to determine accurately the final value. However, it appears that up-and-down cycling sequences do to some extent have the same result as applying a larger number of cycles on a single increasing path.

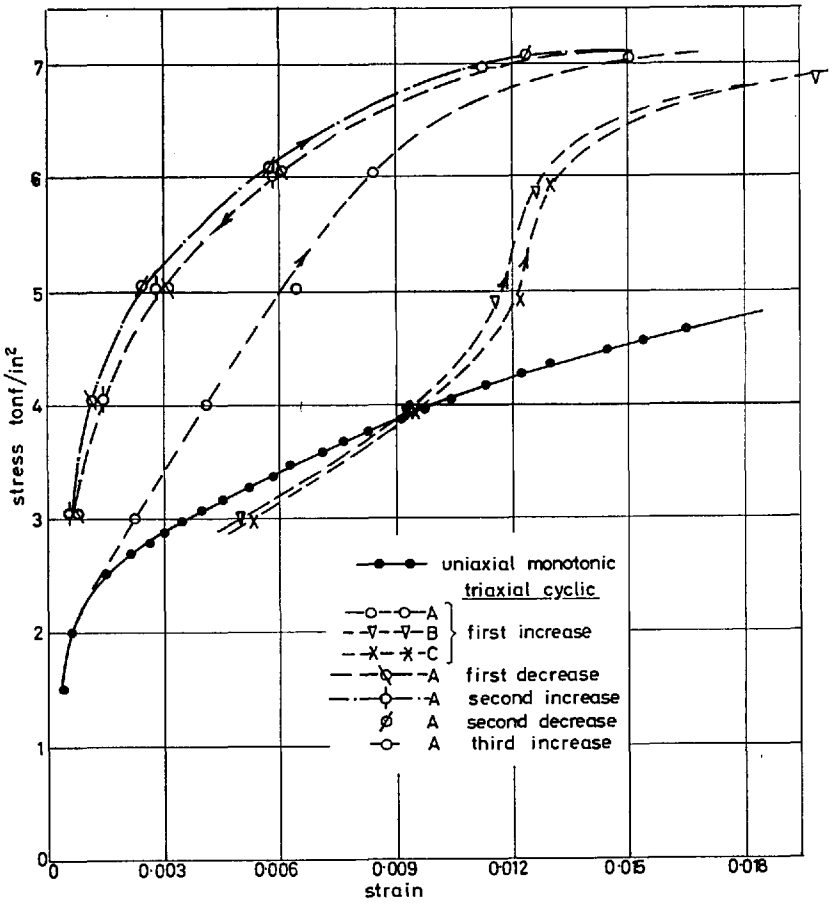

FIG. 6. Monotonic and cyclic compression of cast zinc cubes.

The first increasing stress sequence on the cold drawn copper shows (Fig. 4) some measure of strain softening below 15·9 tonf/in² and the initial anisotropy is still evident during cycling as shown by the A, and B, C curves. A subsequent stress increase sequence shows a further shift of the stress–strain relationship as with the annealed material. It is also noticeable that at the higher stress levels the A and B, C curves approach quite closely, indicating a return to a more isotropic state. A comparison of curve 3, Fig. 2, for the initially soft material, with the second increasing sequence on the cold drawn

material shows close agreement, providing further support for the concept of a basic cyclical stress–strain relationship.

The results for biaxial cycling of annealed material along directions B and C apparently show slightly more hardening than for triaxial cycling and the difference becomes more pronounced at higher stresses (Fig. 3). The most logical cause for this difference is the increasing contact friction caused by the elongation of the specimen in direction A, giving a larger surface area.

In spite of some scatter in the Hounsfield tension test values, there are indications that triaxial cycling retained initial isotropy and reduced previous anisotropy, while achieving a harder or softer state of the material.

In order to compare the cyclic stress–strain relationships from the previous investigation[4] of copper under tension–compression constant load and strain cycles with the present results it is first necessary to consider the form of cycle in the compression test. Stress–plastic strain paths for directions A, B and C are shown in Fig. 7(a), assuming

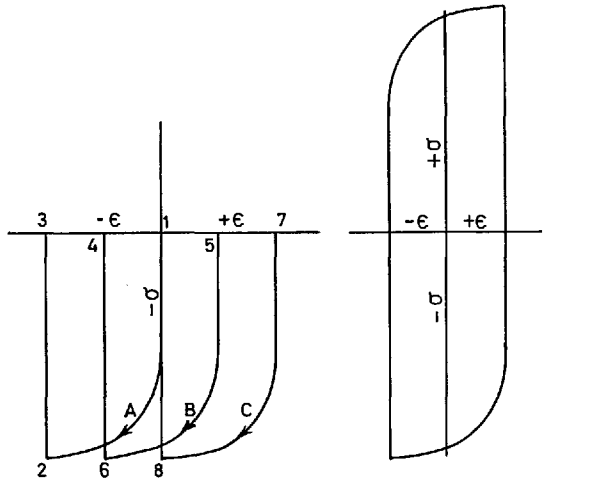

FIG. 7. Stress–plastic strain hysteresis loops.

that loading commences along direction A, which gives the loop 12341, and is entirely in the compression quadrant. The sequence for direction B is 15641 and in this case the strain is equal tension and compression. Finally, direction C follows the path 15781 and strain is on the tensile side of the origin. The stress–strain loop for reversed uniaxial tension–compression is shown for comparison in Fig. 7(b). The monotonic and cyclic stress–strain relations for this and the previous work on copper are illustrated in Fig. 8. The compression and tension monotonic curves agree quite well; however, there is a marked difference between the tension–compression and triaxial compression cyclical curves. Part of this difference may be due to frictional effects and barrelling in compression. On the other hand, the cube is not subjected to tensile stress, and compressive stress is only present for half a cycle (for a particular direction), even though strain is reversed in direction during each cycle, and this may have an important bearing on hardening and softening characteristics.

One of the difficulties of studying cyclical plastic stress–strain behaviour in push–pull, bending or torsion specimens is that at strains greater than, say, 0·05, failure occurs by fatigue after very few cycles, and so potential hardening or softening ability of the material is cut short. Since the present test involves only compressive stresses, the likelihood of fatigue cracking and failure in a cube would be retarded to larger values of strain (barring limitations due to barrelling) than that obtainable in the other tests above.

It is interesting to speculate on the dislocation behaviour during cycling. It has been suggested[7] that when dislocations cut each other, "jogs" in the lattice are formed, and when these are forced to travel with dislocations of the screw type they leave trails of lattice defects which harden the structure. Any kind of cyclic deformation may be assumed to encourage migration of atoms and hence softening. However, in an initially soft (annealed) material subjected to cycling, the to-and-fro movement of dislocations sets up jogs and lattice defects to cause rapid hardening in the early cycles, but then the disordered lattice and cyclic action encourages migration of atoms until an equilibrium state is reached between softening and hardening.

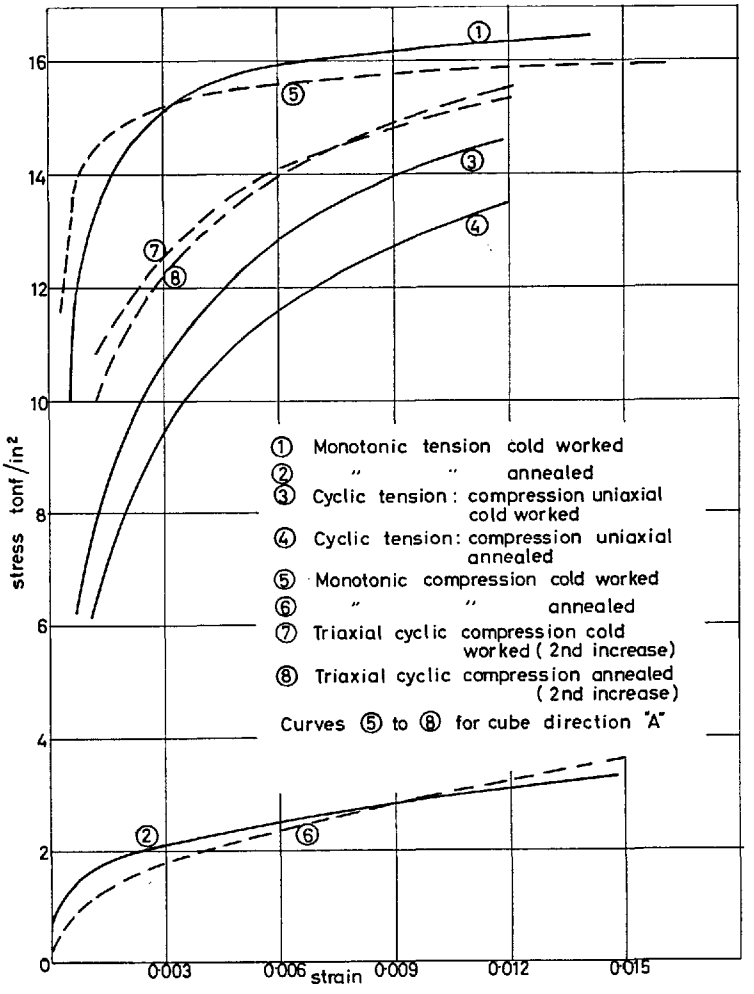

FIG. 8. Comparison of monotonic and cyclic stress–strain behaviour of copper.

It seems that an initially cold-worked material will soften if the cyclic stress is below that which had caused the previous cold work. This is presumably because atoms can migrate to cause softening, but the cyclic stress is not high enough to reinitiate the movement of previous dislocations and jogs to outweigh the softening with hardening. However, with continued cycling and softening it becomes easier for new dislocations to move and eventually there is a balance achieved between softening and hardening.

CONCLUSIONS

(1) Within the limitations imposed by surface friction and barrelling, cubes of copper subjected to cycles consisting of uniaxial compression in turn along each of the three principal axes yield a stable cyclical stress–strain relationship.

(2) When a material is cycled at a given stress it reaches a stable value of hardness. If the cyclic stress exceeds all previous stresses the state reached is unique; however, this is not so if the cyclic stress is not greater than the previous stress.

(3) Initially cold-worked material will strain soften for cyclic stresses of value less than obtained during the initial cold work. Annealed material strain hardens to a stable value at any level of cyclic stress.

(4) Large cyclic stresses cause the initially different materials (cold worked and annealed) to reach the same degree of hardness and have the same cyclic stress–strain relation.

(5) Cycling along two axes of the cube only produces similar stable strain values as cycling along the three axes. Differences may be attributed to increase in frictional effects during biaxial cycling.

(6) Cyclical stress–strain relationships from triaxial compression tests and previous uniaxial tension–compression tests on copper show marked differences, which may be attributed partly to the different stress systems in each type of test, and partly to friction during compression of the cubes.

REFERENCES

1. D. S. DUGDALE, *J. Mech. Phys. Solids* **7**, 135 (1959).
2. R. W. SMITH, M. H. HIRSCHBERG and S. S. MANSON, *Fatigue Behaviour of Materials under Strain Cycling in Low and Intermediate Life Range.* NASA TND–1574 (1963).
3. JoDEAN MORROW, *Cyclic Plastic-strain Energy and Fatigue of Metals.* A.S.T.M. Materials Science Symposium, Chicago, U.S.A. (1964).
4. P. P. BENHAM, *J. Inst. Metals* **89**, 328 (1961).
5. P. P. BENHAM, *J. Inst. Metals* **91**, 404 (1962).
6. A. B. WATTS and H. FORD, *Proc. Instn Mech. Engrs* **169**, 1141 (1955).
7. A. M. COTTRELL, *Dislocations and Plastic-flow in Crystals.* Oxford University Press (1953).

Paper 27

MODIFICATIONS TO AN INSTRON TESTING MACHINE FOR CYCLIC LOADING IN THE PLASTIC RANGE

By P. W. J. Oldroyd*

This paper describes some modifications made to an 'Instron' tension–compression testing machine for an investigation into the behaviour of metal specimens under cycles of plastic deformation.

For tension–compression testing involving plastic deformation a waisted specimen is often used to avoid buckling. The axial strains in this cannot be measured directly; instead they must be obtained from measurements of the diametral strains. It was therefore necessary to construct a diametral extensometer which would caliper the waist of the specimen. As the waist diameter was small greater amplification than that available in existing autographic recording systems had to be provided. Also arrangements for the reversal of crosshead motion at pre-selected values of either stress or strain were necessary to make the operation of the machine automatic.

INTRODUCTION

FOR TENSION–COMPRESSION TESTING involving plastic deformation a waisted specimen is often used to avoid buckling. The axial strains in this cannot be measured directly; instead they must be obtained from measurements of the diametral strains. It is therefore necessary to design a diametral extensometer which will caliper the waist of the specimen. As the waist diameter is small the amplification provided by existing autographic recording systems may not be sufficient. Very little backlash in the recording device, though not important in unidirectional testing, is essential in cyclic testing. Also arrangements for the reversal of crosshead motion at preselected values of either stress or strain are necessary if the operation of the machine is to be automatic.

This paper describes some modifications made to an Instron tension–compression testing machine for an investigation into the behaviour of metal specimens under cycles of plastic deformation.

DESCRIPTION OF THE TESTING MACHINE

General

The machine used for the work described is an Instron universal instrument, model TT-C, having a maximum load capacity of 10 000 lb. The control system incorporates some features which are peculiar to the individual machine (Series No. A/0019).

Drive system

The machine is powered and controlled electrically. The drive system gives a constant velocity of crosshead movement (1)†. The moving crosshead is driven by two four-start screws of 1 in pitch. These screws rotate in nuts attached to the moving crosshead. The machine has been modified by the manufacturers for use in cyclic tension–compression testing. Two special anti-backlash nuts below the main nuts can be adjusted by the user to eliminate any backlash between the crosshead and screws. A modified thrust bearing at the top of each screw eliminates any backlash between the screw and the fixed crosshead of the machine.

A choice of crosshead speeds from 20 to 0·002 in/min is provided; but the very high speeds cannot be used for cyclic tests.

Load-weighing system

The load cell, to which the upper end of the specimen is secured, is bolted to the fixed crosshead of the machine.

The MS. of this paper was first received at the Institution on 3rd March 1965 and in its revised form, as accepted by the Council for publication, on 8th April 1965.

* *Recently Research Assistant at Imperial College of Science and Technology, London.*

† *References are given in Appendix 27.I.*

An electronic load-measuring system with bonded wire strain gauges is used (1). The load is recorded by the movement of the pen across the chart of a Leeds and Northrup high-speed recorder.

A load selector switch allows the full-scale range to be changed in steps from ±200 lb to ±10 000 lb. Calibration is carried out, using dead-weights, with the selector set to the ±200 lb scale. As the switch and its resistances can be checked separately this dead-weight calibration applies to the whole range of load scales.

The recorder sensitivity is adjusted by means of an infinitely variable control. Thus the chart can be made to read in units of nominal stress if so desired.

Strain-measuring system

Strain is recorded by the vertical movement of the chart beneath the pen. There are two alternative systems for controlling the chart:

(1) The movement of the chart is made proportional to the movement of the crosshead. This system is suitable for use with long cylindrical specimens because crosshead displacement is then very nearly proportional to strain; it is useless for waisted specimens.

(2) The movement of the chart is controlled by the electrical signal from an extensometer mounted on the specimen. Various kinds of extensometer element can be used. Only the system which uses a microformer as a measuring element is described here.

A microformer is a small transformer the iron core of which is free to move in the axial direction. Movement of the core varies the voltage output of the transformer. There is a single primary winding to which a constant alternating voltage is applied. There are two secondary windings which are connected in series but with their output voltages opposed to each other. When the core is in a central position the two secondary voltages are equal and the net output is zero. When the core is displaced from the mid-position there is a net voltage output. Over most of the range of core travel the voltage output is sensibly linear in its relation to the displacement.

The system as supplied uses a pair of identical microformers: one is actuated by the lever system of the extensometer and the other by a fine screw, the rotation of which is proportional to that of the chart drum. The secondaries of the two microformers are connected in series with each other. Fig. 27.1 shows, in diagrammatic form, the microformers and the basic circuit. If the cores of the two microformers are not in identical positions the individual microformer outputs differ and there is a net voltage output. This total voltage is passed to the recorder amplifier which controls the motor which drives the chart drum. Thus the out-of-balance signal causes a movement of the chart microformer core towards a position identical with that of the extensometer microformer core. (A phase difference distinguishes between the two directions in which a core may be displaced from its mid-position.) Thus, throughout the test the movements of the chart

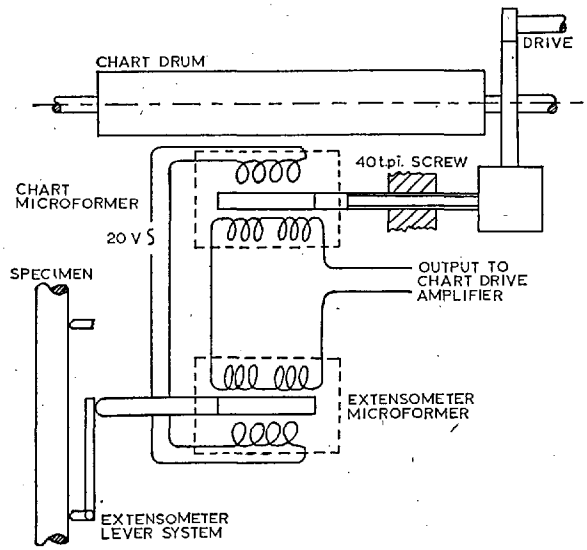

Fig. 27.1. Basic circuit showing principle on which microformer-operated recording system works

microformer core follow those of the extensometer microformer core and the vertical displacement of the chart is proportional to the strain in the specimen.

Fig. 27.2*a* shows the actual circuit used. A potentiometer is connected across the extensometer microformer secondaries. The purpose of this is to provide an infinitely variable calibration control. By reducing the signal from the extensometer the potentiometer reduces the chart displacement for a given strain. A press-button switch enables the potentiometer to be bypassed. When this is pressed the chart microformer adjusts its voltage to zero, i.e. the core takes up its mid-position. It is ideal to operate the microformers with their cores near their mid-positions because this gives equal travel in both directions and avoids any possible non-linearity towards the ends of the range.

USE OF THE MACHINE FOR TENSION–COMPRESSION TESTS

Specimen and end-fittings

The specimen and end-fittings are shown in Fig. 27.3. The upper end-fitting screws on to the nose of the load cell spindle and the lower end-fitting has a flange which is bolted to the upper face of the moving crosshead. This type of end-fitting, in which a split collet is forced against the button end of the specimen, is very satisfactory for tension–compression testing.

The specimen is similar in form to that used by Coffin (2). A neck diameter of 0·250 in was used. This allows the machine to apply a maximum stress of ±91 ton/in^2. In order to have as small a radial stress as possible at the test section it is necessary to make the profile radius as large as possible. After some preliminary tests on En 25 steel a radius of 2 in was decided on. A 2-in radius with a 0·250-in diameter neck gives a Bridgman factor of

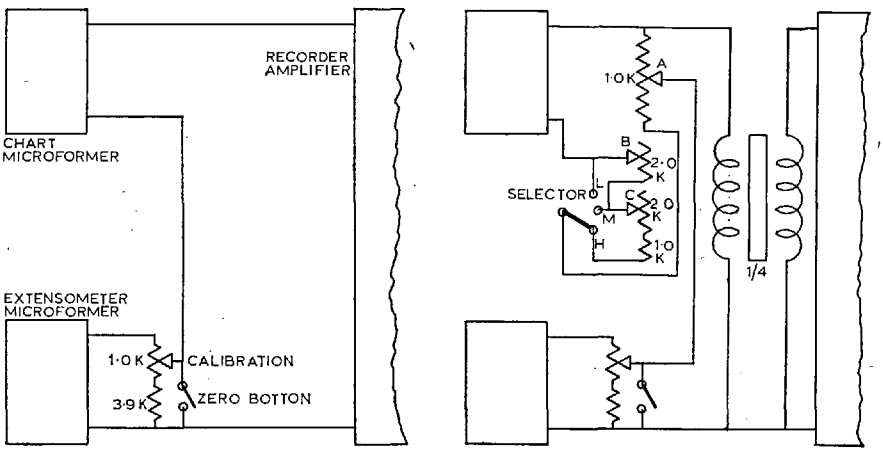

a Original circuit. *b* Modified circuit.

Fig. 27.2

0·985 (3). Thus any error owing to tri-axial stress may be neglected.

Variation of stress across the test section

When load is applied to the specimen it is assumed that a state of uniform tensile or compressive stress will exist at the test section. It follows from this that the specimen must be assumed to be initially free from large-scale internal stresses.

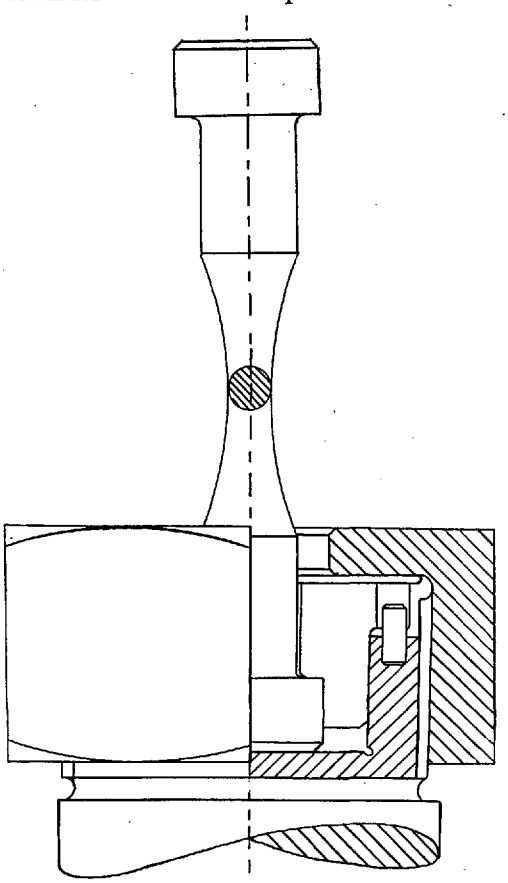

Fig. 27.3. The specimen and an end-fitting

Consider an initially stress-free specimen that has been secured in place in the machine. If the specimen and machine are geometrically perfect the specimen can remain stress-free; but if any misalignment exists internal stresses will be set up in the specimen. The final connection is made by bolting the lower end-fitting flange to the surface of the crosshead. The flange is restrained laterally by the friction of the joint; so a small error in the lateral position of the flange will not cause internal stresses in the specimen. If the flange face is not parallel to the surface of the crosshead a bending moment must be applied to rotate it until it is parallel. It is possible by a simple test to find the value of the bending stresses produced in the test section by this misalignment. The method is to bring the flange slowly into contact with the crosshead and (using the 200-lb load scale) to record the load at which complete surface-to-surface contact occurs. From this value the bending stresses may be calculated. It was estimated that if the gap at the edge of the flange at the instant of first contact was 0·001 in the bending stresses would be: 1 ton/in^2 for aluminium, 1½ ton/in^2 for copper, and 3 ton/in^2 for steel. Normally the gap was considerably less than this. Where a gap existed no attempt was made to pack it with shims; however carefully this is done some misalignment remains.

The influence of any initial stresses in the specimen on the stress–strain curve is always to cause a premature departure from the straight line which represents elastic deformation. As a result low values of proof stress are observed. Fortunately, the effect of plastic deformation is to reduce the magnitude of the residual stresses and this effect occurs also during cycles of plastic deformation. Thus the internal stresses described above will be reduced to negligible values during the first few cycles of plastic deformation.

Lastly, consider a specimen which is known to have no

internal stresses when mounted in the machine but which is not geometrically perfect. The application of load to this may set up bending stresses in addition to the direct stress. These will not be eliminated by cyclic deformation of the specimen.

The serious error that can be caused by a small eccentricity in the force applied to a tensile specimen was pointed out by Unwin in 1887 (4). Even if a specimen is tested using self-aligning shackles an eccentricity which is 1 per cent of the specimen diameter results in a bending stress which is 8 per cent of the mean stress. Examination of some specimens both before and during cyclic testing showed that, except after cycling at very large strain amplitudes, the eccentricity was always considerably less than 1 per cent of the neck diameter.

Calibration of the stress scale

The load scale was set to read in terms of nominal stress. The following settings were used: ± 10 ton/in^2 full-scale deflection for aluminium, ± 25 ton/in^2 full-scale deflection for copper, and ± 100 ton/in^2 full-scale deflection for steel. For the highest setting the voltage across the load-measuring potentiometer had to be raised above the normal value of 1 volt.

The procedure when setting the recorder stress scale was as follows: The zero load position of the pen was brought to the centre of the scale. The scale selector was set to the '200 lb' position and two 25-lb weights suspended from the load cell. The recorder sensitivity control was then adjusted until the pen was displaced 2·28 units from the zero position. In the case of steel 1·14 units had to be used. Each unit is approximately 1 in; there being 10 units in the total width of the chart. It was possible to carry out this setting to an accuracy of ± 1 part in 100.

The stress scale was normally calibrated once a day. This was done because gradual changes in the potentiometer battery voltage occur with time. In order to recalibrate, the specimen was released by disconnecting the flange of the lower end-fitting from the moving crosshead. This could be done with the extensometer still in place.

A calibration of the 10 000-lb load scale using a compression proving ring, followed by a check on the accuracy of the load scale selector, supports the estimate of an accuracy of ± 1 part in 100 of the full scale reading of the stress scale. This degree of accuracy is quite acceptable for the present tests.

Diametral extensometer and the modified chart drive system

A diametral extensometer had to be designed which would use a microformer as a transducer and would operate with the existing chart drive system. It was to be suitable for strain amplitudes from about ± 10 per cent down to $\pm 0{\cdot}1$ per cent axial strain. A scale of 2 in to 1 per cent axial strain was considered suitable.

Axial extensometers used with the Instron machine usually have a 2 in gauge length and a lever system which magnifies the movement imparted to the microformer core. To give the same performance a diametral extensometer working on a neck diameter of 0·250 in needs sixteen times as great a magnification. As the present work is concerned with plastic strains which are quite large compared to the elastic strains it was decided that a smaller increase in magnification ($\times 10$) would suffice. Since the design of a mechanical system of magnification presents considerable problems an attempt was made to provide the magnification by electrical means.

It was required that a small movement of the extensometer microformer core should cause a proportionately

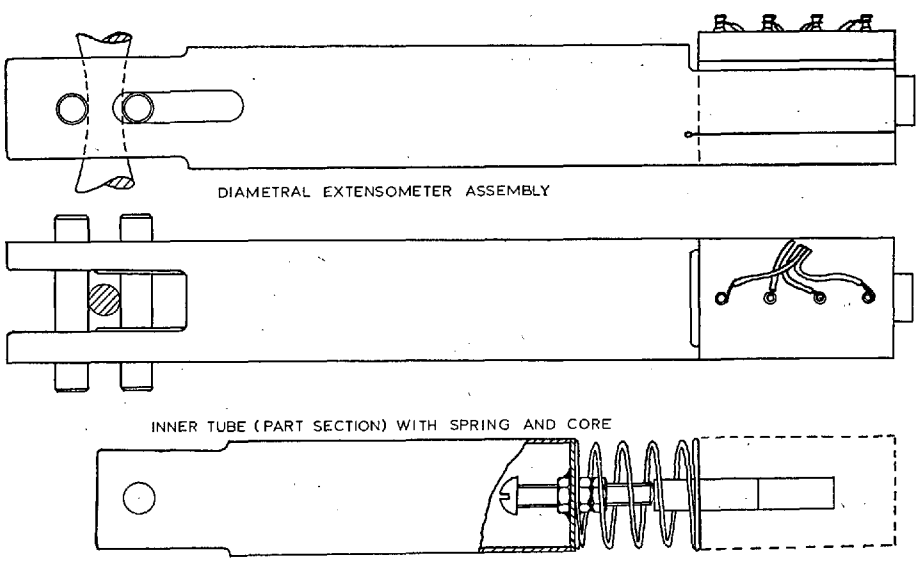

Fig. 27.4. The diametral extensometer, shown in position on a specimen

larger movement of the chart microformer core. To achieve this it was necessary that the microformers should have a linear relationship between output voltage and core displacement. Further, it was necessary either to amplify the signal from the extensometer microformer or to attenuate the signal from the chart microformer. It was decided to obtain the latter with a potentiometer; to achieve the former would need an amplifier with linear characteristics.

Fig. 27.2*b* shows the modifications made to the existing circuit: A is the potentiometer, B and C are two adjustable resistances which may be placed in series with the potentiometer. Thus the selector switch makes available a choice of three scales.

Attenuation of the signal from the chart microformer results in a loss of driving power at the chart. For a given error of chart position the available restoring torque at the chart will be reduced by the same factor as that by which the microformer signal is reduced. Fortunately there was a large reserve of power. The chart drive motor normally drives not only the chart drum but, through friction clutches, the rolls of used and unused paper. The drive to these was disconnected and a free length of paper, weighted to keep it taut, hung over the chart drum. Under these conditions very little torque was needed to rotate the drum. It was found that the performance was further improved by using a transformer to step up the voltage of the signal received by the amplifier.

The diametral extensometer is shown in Fig. 27.4. It consists of two telescopic brass tubes through which are passed two steel pins. One pin is located by one tube and the other by the other tube. When fitting the pins care was taken to make the centre lines parallel. The body of the microformer is gripped by one end of the outer tube and the core of the microformer is in contact with a screw which projects from the flat end of the inner tube. A small spring inside the microformer holds the core in contact with the end of the screw. A spring (the lightest which would overcome the friction between the tubes) is situated between the end of the microformer body and the end of the inner tube. This spring exerts a force which tends to bring the pins together.

When in use the extensometer is mounted on a simple flexible support which is attached to the moving crosshead. Thus the extensometer is kept sensibly horizontal while still being allowed to take up its correct position in relation to the waist of the specimen.

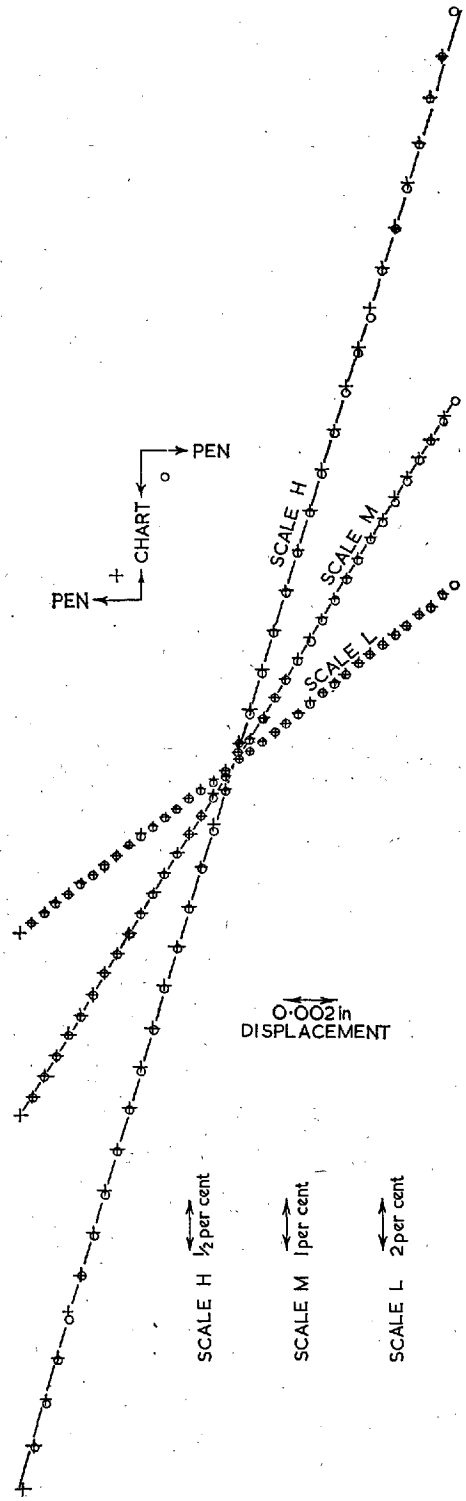

Fig. 27.5. Calibration graph for the three strain scales

Calibration of the strain scale

The strain scale was calibrated in terms of axial strain. It was assumed that no change of volume occurs during plastic deformation and that the axial strain is twice the diametral strain. This involves an arithmetical approximation but for strains of less than 5 per cent the error is negligible.

Elastic strain does not occur at constant volume, so the elastic line of the stress–strain graph produced by the machine will have a false slope. This does not matter if, as in the present work, the graphs are to be used for comparative purposes. If desired the graphs can be converted to a basis of plastic strain by deducting the 'apparent elastic strain' values.

The following calibrations were used: 1 in of chart movement represents ½ per cent (scale H); 1 in of chart movement represents 1 per cent (scale M); and 1 in of chart movement represents 2 per cent (scale L). To obtain these calibrations it was necessary that a relative movement between the tubes of 0·006 25 in should cause chart displacements of 10·00, 5·00, and 2·50 in for scales H, M, and L respectively.

This displacement of 0·006 25 in was used when adjusting potentiometer A and the resistances B and C for the preliminary calibration of the system. It was also used for the periodic checks that were made on the accuracy of the calibration.

In order to calibrate the extensometer its outer tube was held in the clamp of a bench type micrometer. The pin was removed from the outer tube so that the micrometer spindle could contact the pin which is carried by the inner tube. The micrometer drum was marked with 0·0001 in divisions. Thus the micrometer could impose small and accurately measured displacements on the inner tube.

A step by step calibration of each scale was carried out to verify the linearity of the relationship between strain and chart displacement and also to ascertain whether backlash or friction effects were present. At the start of the calibration the micrometer was adjusted to bring the microformer cores to their mid-positions. The extensometer microformer core was then displaced first in one direction and then in the other. For scale H the full range of chart movement possible (about 30 in) was used. Fig. 27.5 shows the three calibration graphs plotted on the

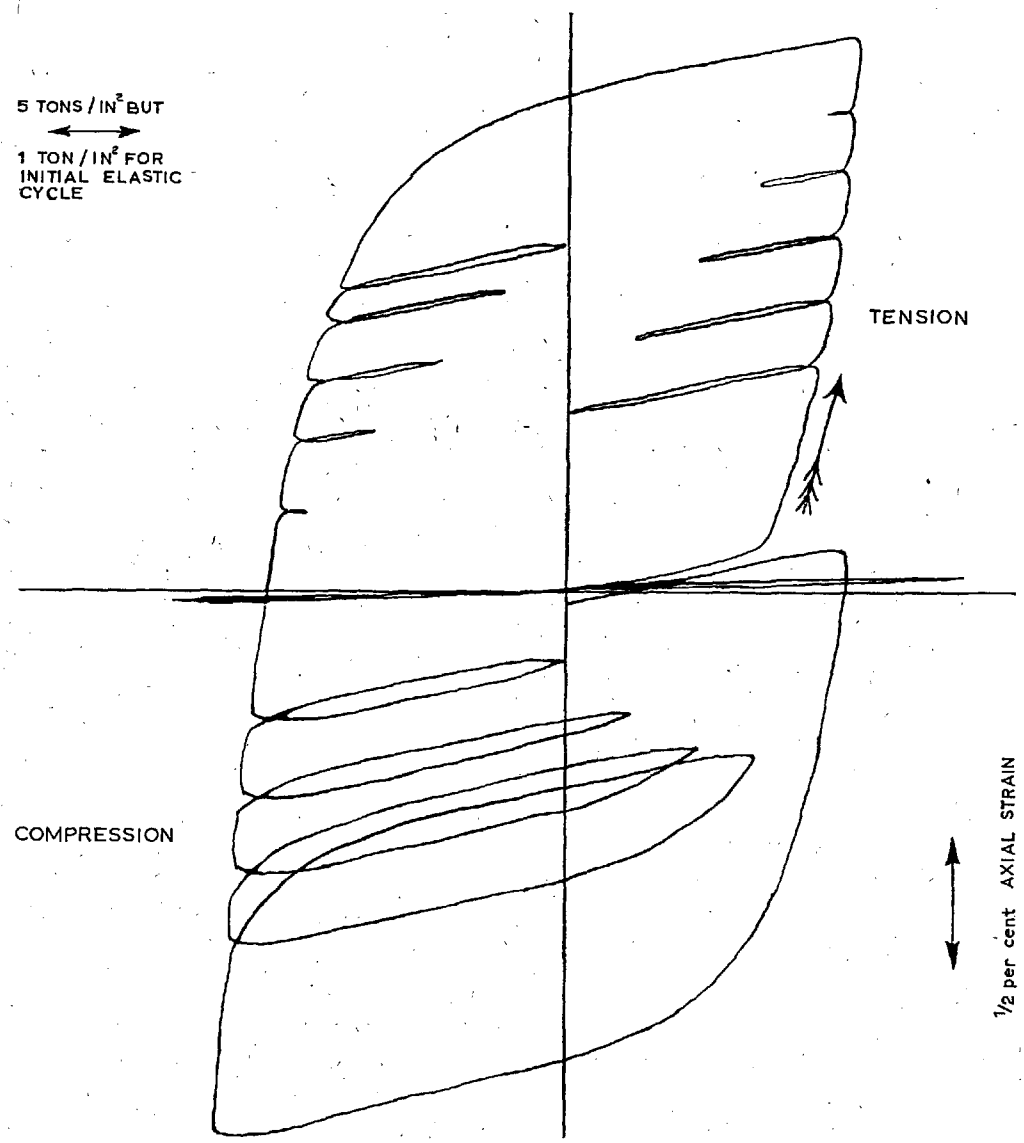

Fig. 27.6. Stress–strain curves for a cold-worked copper specimen, showing Bauschinger effect and hysteresis loops

chart itself. The full range of movement is shown only for scale H. If scale H gives a linear relationship for the full range then the other scales will also give a linear relationship.

Only for strains of more than 6 per cent do the points depart from the straight line. Even at $7\frac{1}{2}$ per cent strain the deviation is only 3 parts in 100 of the recorded value. There is a minute backlash or friction effect observable; at its worst it is 0·05 per cent strain and is usually a lot less. The three calibrations, as determined from the slopes of the lines, show errors of 0, 0, and 3 parts in 100 for scales H, M, and L respectively. The results shown in Fig. 27.5 are for a re-calibration after a period of testing. A reasonable estimate of the accuracy of strain measurement would seem to be ± 1 part in 100.

When using scale L a rapid low amplitude vibration of the pen occurred. No doubt this could have been damped out, but this was not done because the amplitude was less than 0·02 per cent and it seemed to lessen the backlash or friction effect.

Fig. 27.6 shows the performance of the recording system when used with a work-hardened copper specimen. The effects of unloading and reloading and of reversals of loading are illustrated. The Bauschinger effect and various forms of hysteresis loop are shown. Some of the very narrow loops that occur under conditions in which no plastic deformation is expected may be attributable to anelastic effects; but the presence of backlash and friction effects can also cause loops. Likewise, the failure of the pen to follow a straight line when the load in the specimen is slightly reduced from a peak value may be owing to creep occurring; but it is not possible to differentiate between this and the imperfect functioning of the extensometer. Where conditions approaching perfect elasticity can be expected the trace in Fig. 27.6 supports the evidence provided by the calibration test, that backlash and friction effects are very small.

The strain cycling controls

In the existing control system the drive screws are connected to two adjustable cams. Each cam, on reaching a selected position, operates a single-pole two-throw micro-switch. Operation of the switch reverses the direction of motion of the crosshead. One cam controls the upper and the other the lower limit of crosshead movement. The form of control circuit used need not be considered here because the only changes made have been the replacement of the reversing micro-switches by relays.

In the present work it is necessary to be able to cycle between pre-selected values of strain and these bear no simple relation to crosshead position. Chart displacement is proportional to strain and switching devices actuated by the chart drive system are needed if cyclic tests are to be made using pre-selected limits of strain. It was decided to use conducting strips of metal foil attached to the face of the chart to actuate the existing control system.

The additional control equipment provided is shown, in diagrammatic form, in Fig. 27.7. Two narrow strips of aluminium foil are fastened to the surface of the chart. Two spring contacts are associated with each strip: one is a fixed contact attached to the chart platen; this makes contact first and then slides over the vertical portion of the strip. The other is a moving contact attached to the pen carriage; when this makes contact with the strip it closes the circuit which operates one of the reversing relays.

Reversal is not instantaneous and, in order that the pen point shall not reach the metal foil, the two pen contacts are set at a distance of $\frac{1}{4}$ in from the pen, one above and the other below it. When setting up the apparatus the strips are offset by $\frac{1}{4}$ in less the estimated over-run of the chart.

The use of moving contacts mounted on the pen carriage instead of a simpler system of fixed contacts has the advantage that limits of plastic strain can be used instead of limits of total strain. If the foil is placed horizontally across the chart reversals will occur at selected values of total strain; but if the foil is placed parallel to the lines which represent elastic deformation then reversals will occur at selected values of plastic strain. Both kinds of cyclic deformation are of interest; the former to the designer, the latter to the research worker. In the present investigations cycles of plastic strain are used.

Fig. 27.8 shows the stress–strain curves for a work hardened copper specimen tested at a plastic strain amplitude of $\pm 1{\cdot}0$ per cent. A crosshead speed of 0·05 in/min was used; this gives one cycle in 45 seconds. The strain control system does not function satisfactorily at higher speeds: the use of constant crosshead speed does not ensure constant strain rate at the test section; the strain rate increases as the limit is approached. It is the final speed of approach of the pen to the strip which limits the crosshead speed that may be used.

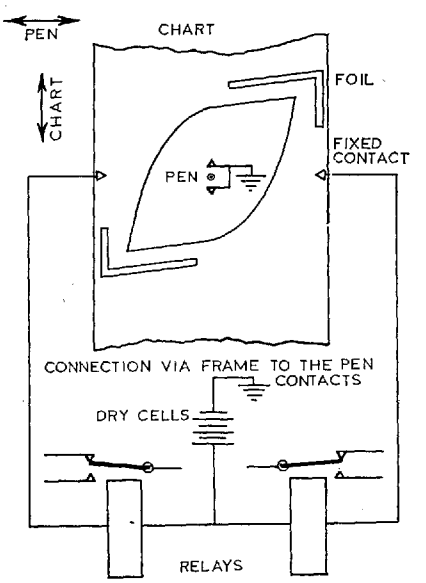

Fig. 27.7. Diagrammatic representation of the strain cycling control system

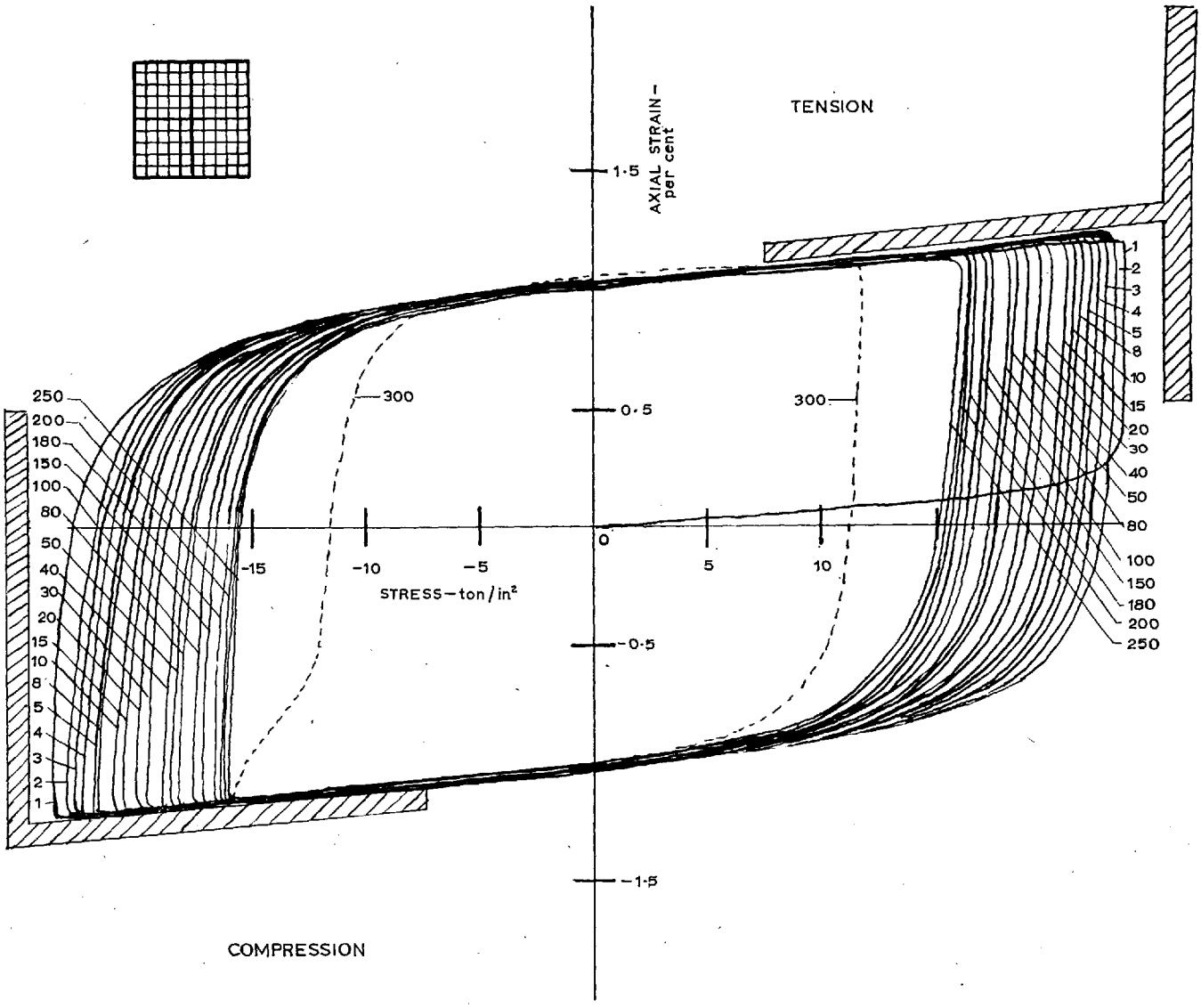

Fig. 27.8. Stress–strain curves for cold-worked copper cycled at ±1 per cent plastic strain, showing the softening caused by cycles of plastic deformation

The progressive decrease of the stress amplitude shows the softening effect of cycles of strain on a work hardened material. When such a large change of stress occurs and the plastic strain limits are held constant the total strain limits alter appreciably.

This specimen was tested until fatigue occurred. The last loop recorded (shown in broken line) reveals the presence of a fatigue crack, which opens under tension and closes under compression.

Under favourable conditions the strain limits can be set and held to an accuracy of ±0·05 per cent strain. If the material creeps the limit cannot be set so accurately. If the top of the curve suffers a considerable change of slope the rate of approach alters and the limit cannot be accurately held.

CONCLUSIONS

Modifications to the recording and control systems of the Instron universal testing machine enable it to be used for cyclic tension–compression tests in which the strain is controlled between selected limits.

ACKNOWLEDGEMENTS

The work described has been carried out at Imperial College, London, as part of a programme of research into the behaviour of metals under cycles of plastic deformation. This work is financed by the Department of Scientific and Industrial Research. The copper was supplied by Imperial Metal Industries (Kynoch) Ltd. The help given by the staff of Instron Ltd, and by the staff, past and present, of

the Mechanical Engineering Department of the College is gratefully acknowledged.

APPENDIX 27.I

REFERENCES

(1) ZAHLER, G. G. 'Inertialess weighing machine for tensile testing a wide range of materials', *Res. and Develop.* 1962 (No. 6), 62.

(2) COFFIN, L. F. jun. 'The influence of mean stress on the mechanical hysteresis loop shift of aluminium 1100', *J. Basic Engng, Trans. Amer. Soc. mech. Engrs* **86** (Series D, No. 4), 673.

(3) BRIDGMAN, P. W. *Studies in large plastic flow and fracture* 1952 1st ed. Ch. 1 (McGraw-Hill, New York).

(4) UNWIN, W. C. 'Measuring instruments used in mechanical testing', *Proc. phys. Soc. Lond.* 1887 **8**, 179.

Ph.D. 1968. P. W. J. OLDROYD.

APPLIED MECHANICS CONVENTION 1966

Cambridge · 4–6th April



PAPER 2

Strain hardening and softening of metals produced by cycles of plastic deformation

P. W. J. OLDROYD, D. J. BURNS, and P. P. BENHAM

Advance copy subject to revision. The paper and discussion will be published in Proceedings 1965–66, Volume 180, Part 3I

PUBLISHED BY THE INSTITUTION OF MECHANICAL ENGINEERS
1 BIRDCAGE WALK · WESTMINSTER · LONDON · SW1

The Convention was arranged by the

APPLIED MECHANICS GROUP

of the

INSTITUTION OF MECHANICAL ENGINEERS

© *The Institution of Mechanical Engineers 1966*

This paper is intended to be presented for discussion at the Convention, in Cambridge, on 4–6th April 1966. Communications, which should be addressed to R. J. Millson, Editor of Proceedings, must reach the Institution by 18th May 1966.

Paper 2

STRAIN HARDENING AND SOFTENING OF METALS PRODUCED BY CYCLES OF PLASTIC DEFORMATION

By P. W. J. Oldroyd*, D. J. Burns*, and P. P. Benham†

When a metal is subjected to cycles of plastic deformation between strain limits the stress range may change significantly, particularly in the first few cycles. The terms cyclic strain hardening and softening are used to describe such increases and decreases in stress range, since these are accompanied by corresponding changes in indentation hardness. The object of the present research was to investigate how these phenomena are related to the initial condition of various metals and the range of cyclic plastic strain.

Cyclic tension–compression tests on OFHC copper suggest that for a given plastic strain amplitude, the stress amplitude tends towards a limiting value which is independent of prior strain history. Tests on this material, En 25 steel, an austenitic stainless steel and commercially pure aluminium support the suggestion of Smith *et al.* that materials with an ultimate/yield strength ratio $> 1{\cdot}4$ cyclically harden and those for which this ratio $< 1{\cdot}2$ cyclically soften. It is concluded that cyclic hardening and softening can be explained in terms of the Bauschinger effect if certain simplifying assumptions are made.

INTRODUCTION

WHEN A METAL is subjected to cycles of plastic deformation between strain limits the stress range may change significantly during cycling, particularly in the first few cycles (1)‡. The terms cyclic strain hardening and softening are used to describe such increases and decreases in stress range, since they are accompanied by corresponding changes in indentation hardness (2). A related effect is the progressive deformation (cyclic creep) which occurs when ductile metals are subjected to cycling between stress limits sufficient to cause plastic deformation (3).

An understanding of the above phenomena is essential for the development of reliable design procedures for the low endurance ($< 10^4$ cycles) fatigue region (4) (5). Studies of these phenomena can be of value in metal-working processes and the work of Coffin and others (6) (7) has led to the development of a rolling mill in which the material is subjected to roll force, strip tension, and cyclic plastic bending simultaneously. Since the cyclic plastic bending leads to work-softening of severely work-hardened materials the mill can be used to produce very large reductions without intermediate annealing.

The MS. of this paper was received at the Institution on 10th November 1965.

* *Imperial College, London.*
† *The Queen's University of Belfast.*

‡ *References are given in Appendix 2.1.*

The object of the present research was to investigate how cyclic strain hardening and softening are related to the initial condition of various metals and the range of cyclic plastic strain. The majority of the work was carried out on OFHC copper and a $2\frac{1}{2}$ per cent nickel–chromium–molybdenum steel (En 25). An 18–8–Ti austenitic stainless steel in the fully soft condition and commercially pure annealed aluminium were also tested.

EQUIPMENT AND SPECIMENS

Cyclic tension–compression tests were carried out between plastic strain limits at room temperature in a 10 000 lbf Instron machine.

In order to avoid buckling a waisted specimen was used, Fig. 2.1. The design of a diametral extensometer to caliper the waist of this specimen and the modification of the Instron machine and its autographic recorder to permit cycling between strain limits have been described in detail in a previous paper (8).

MATERIALS

The copper was supplied as 3-in diameter bar which had been annealed at 650°C for 2 hours. Specimens cut from this bar were either tested in the as-machined condition or

machined with an oversize waist, pre-stretched, finish-machined, and tested. Cylindrical rods were also cut from the bar, and were reduced by various amounts by cold roller or press swaging and/or drawing to give specimen blanks.

The En 25 steel was supplied as 1-in diameter bar which had been annealed at 650–660°C for 2 hours, cooled at 10 degC per hour to 630°C and then air-cooled. Specimens cut from this bar were tested in either the annealed as-machined condition or after oil-quenching from 830° to 850°C and tempering at various temperatures.

The stainless steel was supplied as $2\frac{3}{4}$-in diameter bar in the fully soft condition. The aluminium was supplied as $2\frac{1}{4}$-in diameter extruded (40 per cent reduction) bar and finish-machined specimens were annealed at 350–360°C for $1\frac{1}{2}$ hours.

The chemical compositions of the steels and aluminium are given in the Table 2.1.

DISCUSSION OF RESULTS

OFHC copper

Fig. 2.2 shows the as-recorded stress–strain loops for an annealed copper specimen tested at a plastic strain amplitude of ±1 per cent*. The loops for a cold-worked copper specimen subjected to the same strain amplitude have been shown in a previous paper (reference (8), fig. 27.8). Although the cyclic hardening or softening shown by these specimens was considerable it will be noticed that the change per cycle decreased rapidly.

Autographic records similar to Fig. 2.2 have been used to prepare Figs 2.3–2.8. In some instances the results obtained from more than one specimen have been used to prepare a curve. Both tension and compression stress values are plotted, since in some cases they are appreciably different, cf. Fig. 2.4.

Fig. 2.3 shows the results of testing annealed copper specimens at various plastic strain amplitudes. At strain

* *Axial strain values are used throughout this paper.*

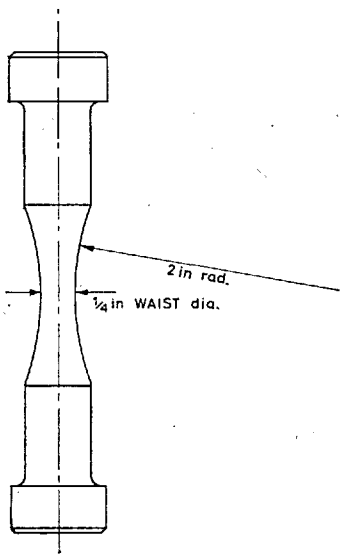

Fig. 2.1. The specimen

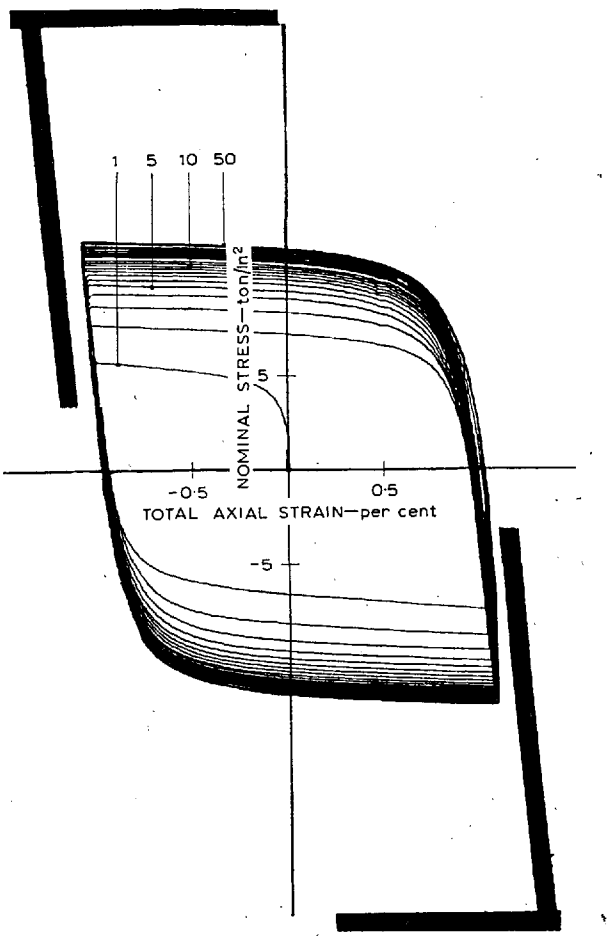

Fig. 2.2. Cyclic hardening of annealed copper; ±1 per cent plastic strain

Table 2.1

	C	Mn	Si	S	P	Ni	Cr	Mo	Ti
En 25 steel	0·32	0·58	0·19	0·016	0·021	2·50	0·65	0·52	—
Stainless steel	0·06	1·56	0·70	0·013	0·034	8·6	18·2	—	0·34
	Fe	Cu	Si	Mn	Mg	Zn	Ti	V	
Aluminium	0·33	0·01	0·09	0·02	0·02	0·01	< 0·01	< 0·01	

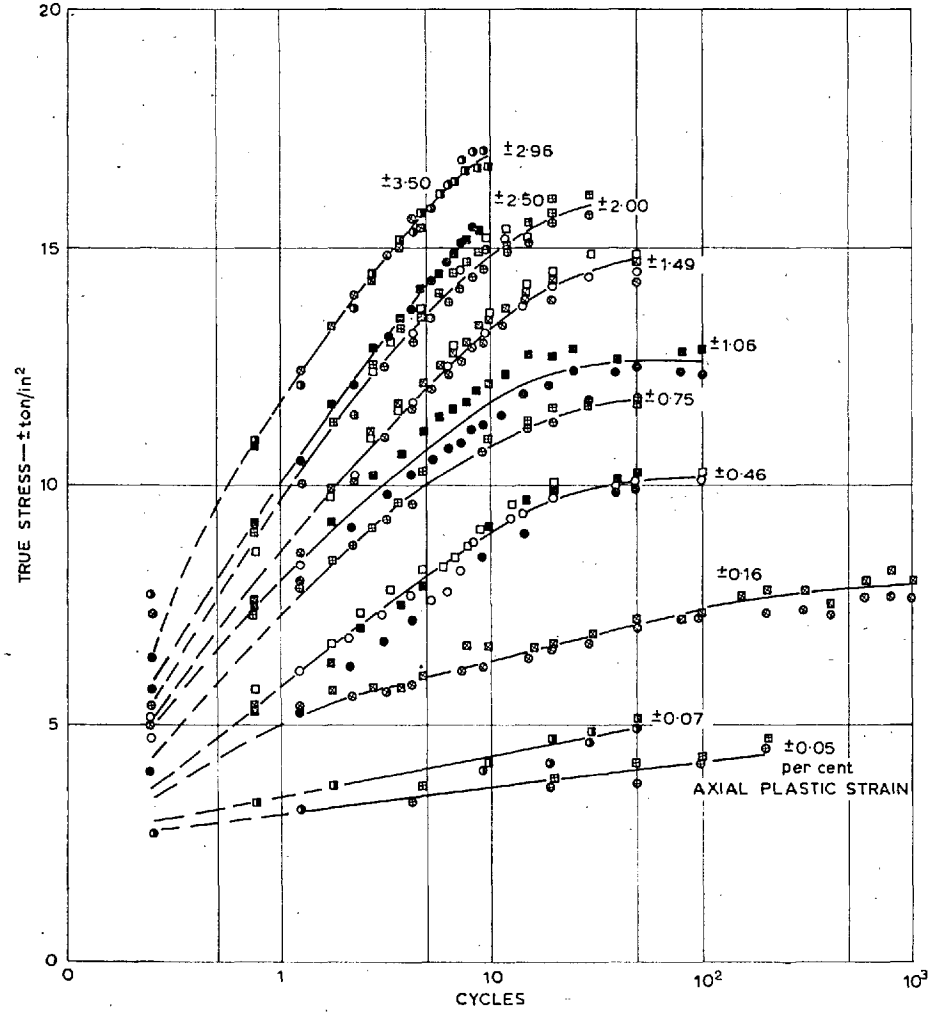

Fig. 2.3. Effect of plastic strain range on the cyclic hardening of annealed copper

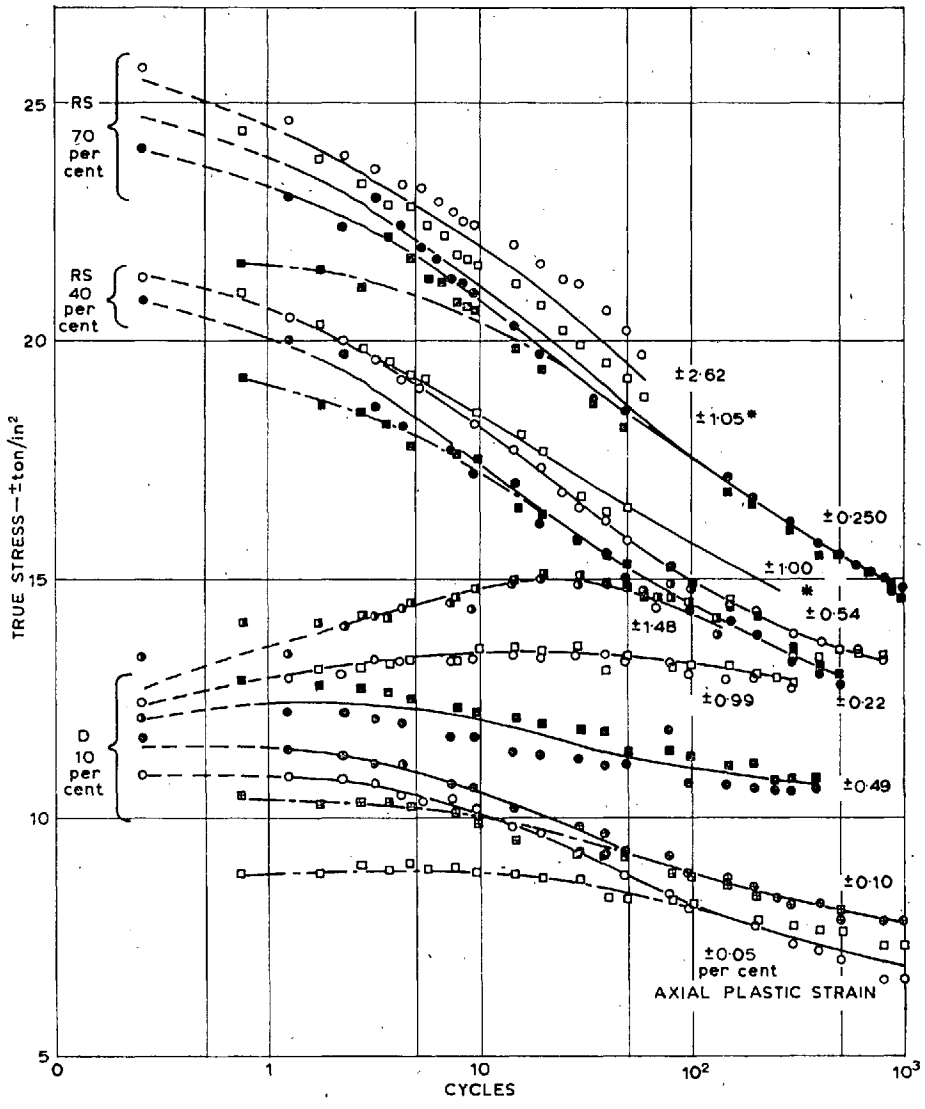

RS Roller swaged.
D Drawn.
* Points shown on another figure.

Fig. 2.4. Cyclic hardening and softening of cold-worked copper

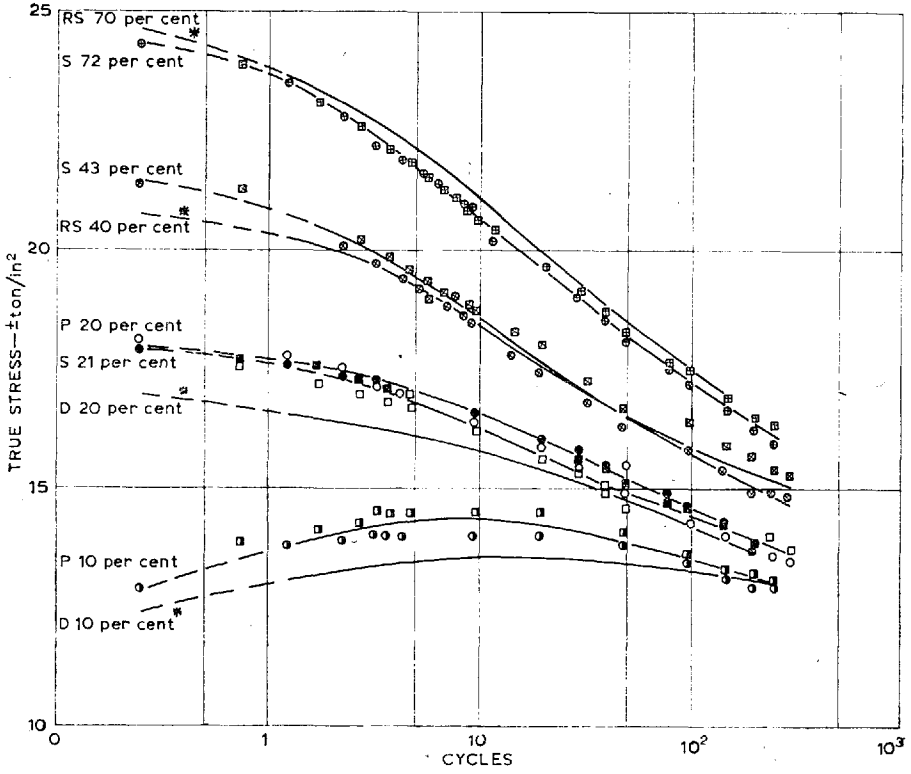

RS Roller swaged.
S Press swaged.
D Drawn.
P Stretched.

* Points shown on another figure.

Fig. 2.5. Effect of method of cold-working on cyclic hardening and softening of copper: ±1 per cent axial plastic strain

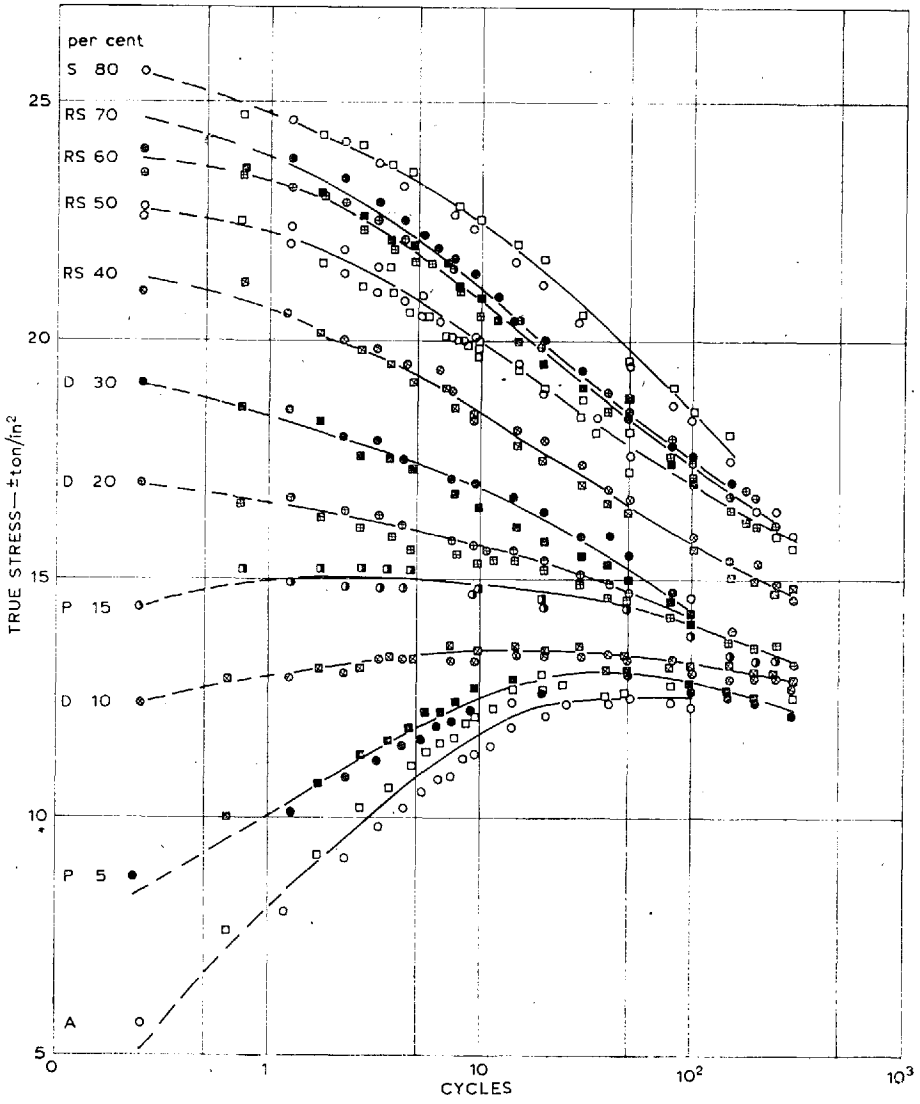

S Press swaged.
RS Roller swaged.
D Drawn.
P Stretched.
A Annealed.

Fig. 2.6. Effect of degree of cold-working on cyclic hardening and softening of copper: ±1 per cent axial plastic strain

amplitudes between 0·5 and 1 per cent there is a definite indication that the stress tends towards a limiting value for each strain range. Tests at higher strain ranges are inconclusive because the specimens failed; the onset of failure was usually shown by differences between the compressive and tensile stresses. Tests at lower strain amplitudes are inconclusive because machine control problems made prolonged tests impossible.

Fig. 2.4 shows the results of tests at various plastic strain amplitudes for work-hardened copper. At small strain amplitudes the differences in tensile and compressive properties produced by cold-working persisted for a number of cycles. It will also be noticed that the 40 and 70 per cent cold-worked material always softened whereas the 10 per cent cold-worked material hardened and/or softened according to the strain amplitude.

The influence of the method of cold-working on the cyclic hardening or softening behaviour of copper cycled at a plastic strain amplitude of ± 1 per cent is illustrated on Fig. 2.5. These results suggest that the method of cold-working has little or no effect on cyclic hardening or softening.

Figs 2.3–2.5 and other data have been used to prepare Fig. 2.6, which shows the influence of the degree of cold-working on the behaviour of copper cycled at a plastic strain amplitude of ± 1 per cent. Fig. 2.6 provides some support for the argument (1) that stress amplitude tends towards a limiting value for each strain range irrespective of the prior strain history.

To investigate further the effect of prior strain history each of a set of annealed copper specimens was tested at a series of strain amplitudes. At each strain amplitude cycling was continued until the stress amplitude tended to a limiting value. When the results of these step-tests are compared with those of single amplitude tests on a basis of cumulative plastic strain, Fig. 2.7, it can be seen that the limiting value of stress amplitude for a given strain amplitude is almost independent of prior strain history.

The data presented in Figs 2.3–2.6 are not in a convenient form for design calculations (5). If stress amplitude is plotted against strain amplitude for given numbers of cycles so-called cyclic stress–strain curves are obtained. These are compared on Fig. 2.8 with the corresponding simple tension curves.

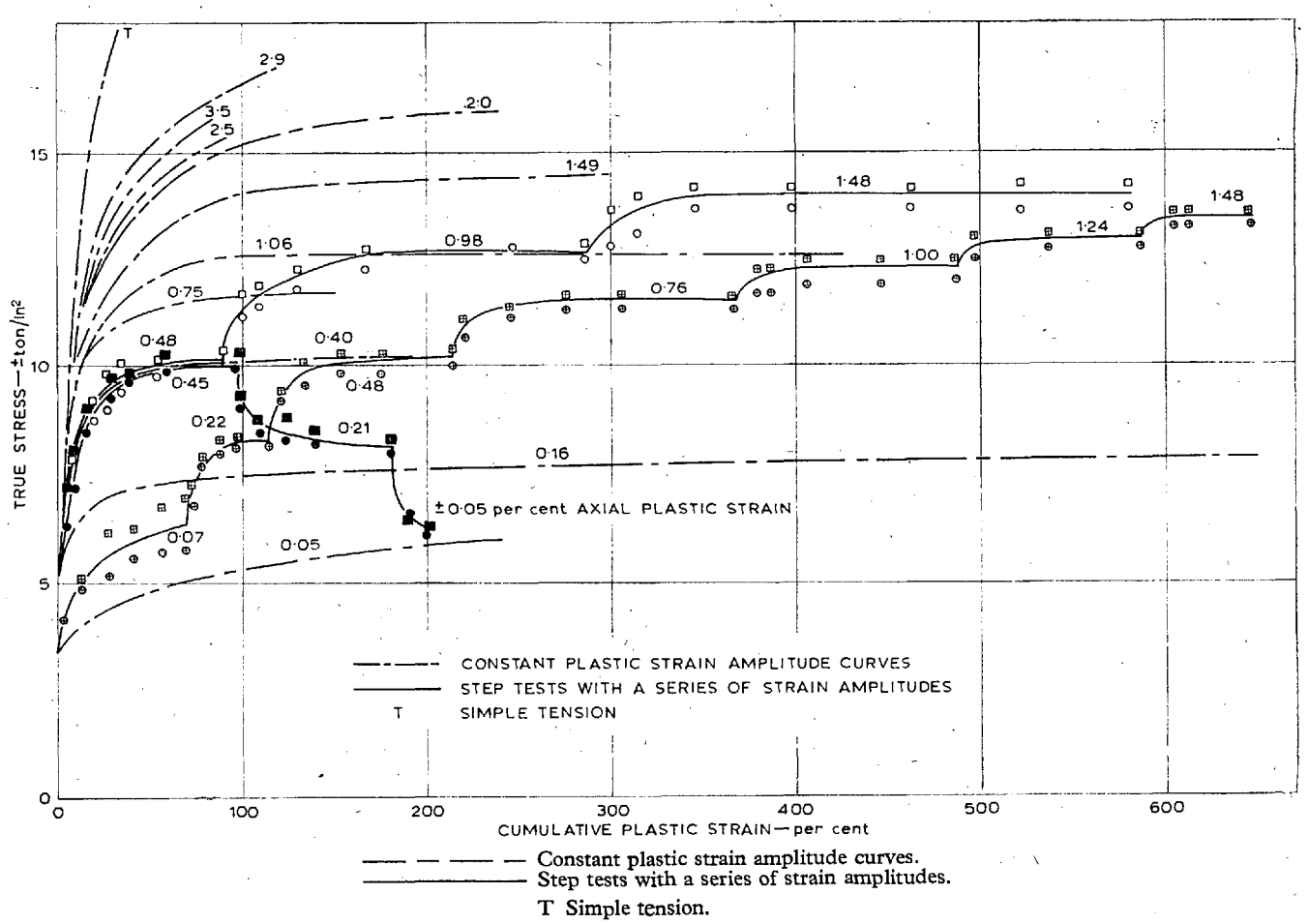

— — — — Constant plastic strain amplitude curves.
———— Step tests with a series of strain amplitudes.
T Simple tension.

Fig. 2.7. Comparison of step and constant strain amplitude behaviour of annealed copper

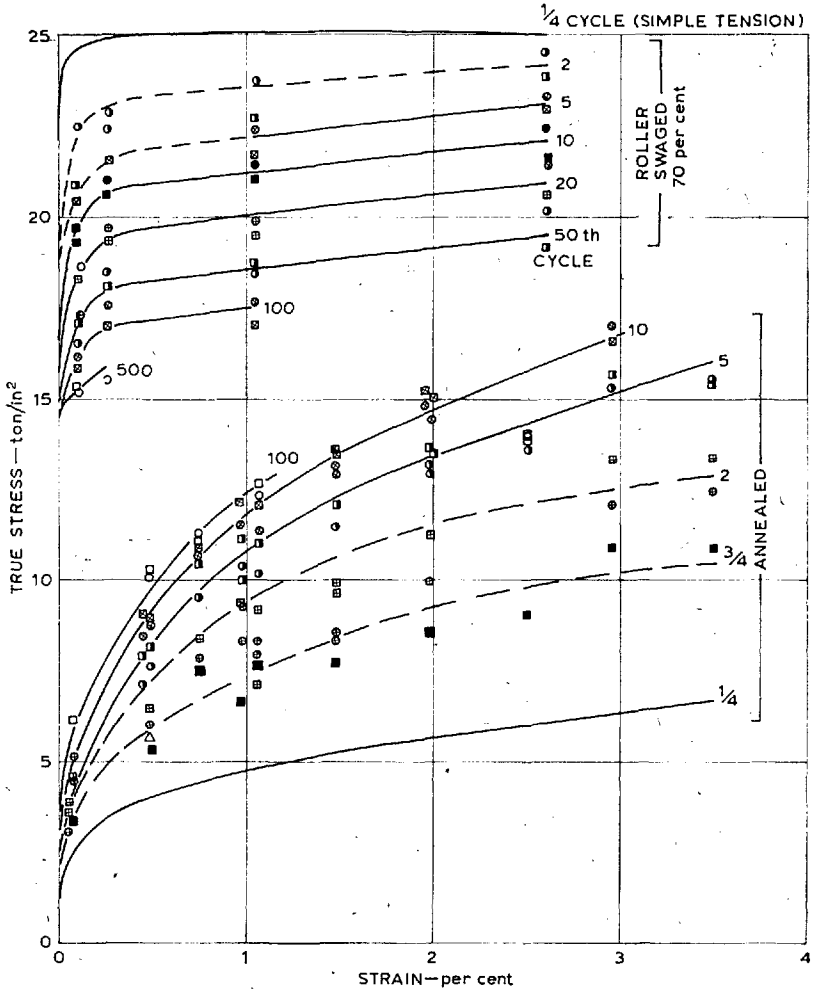

Fig. 2.8. Cyclic and static stress–strain curves for copper

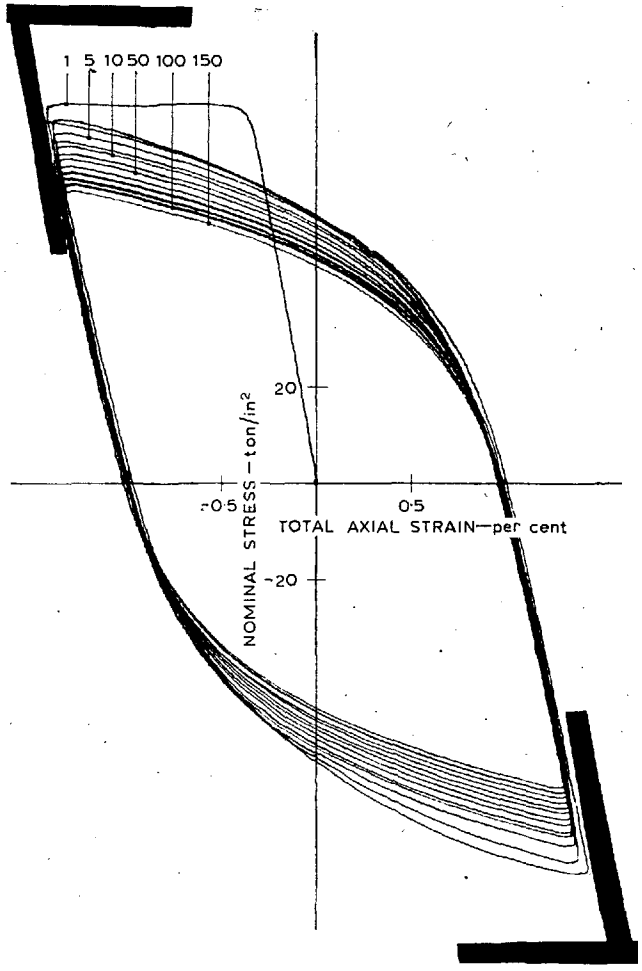

Fig. 2.9. Cyclic softening of En 25 steel (tempered at 450°C); ±1 per cent plastic strain

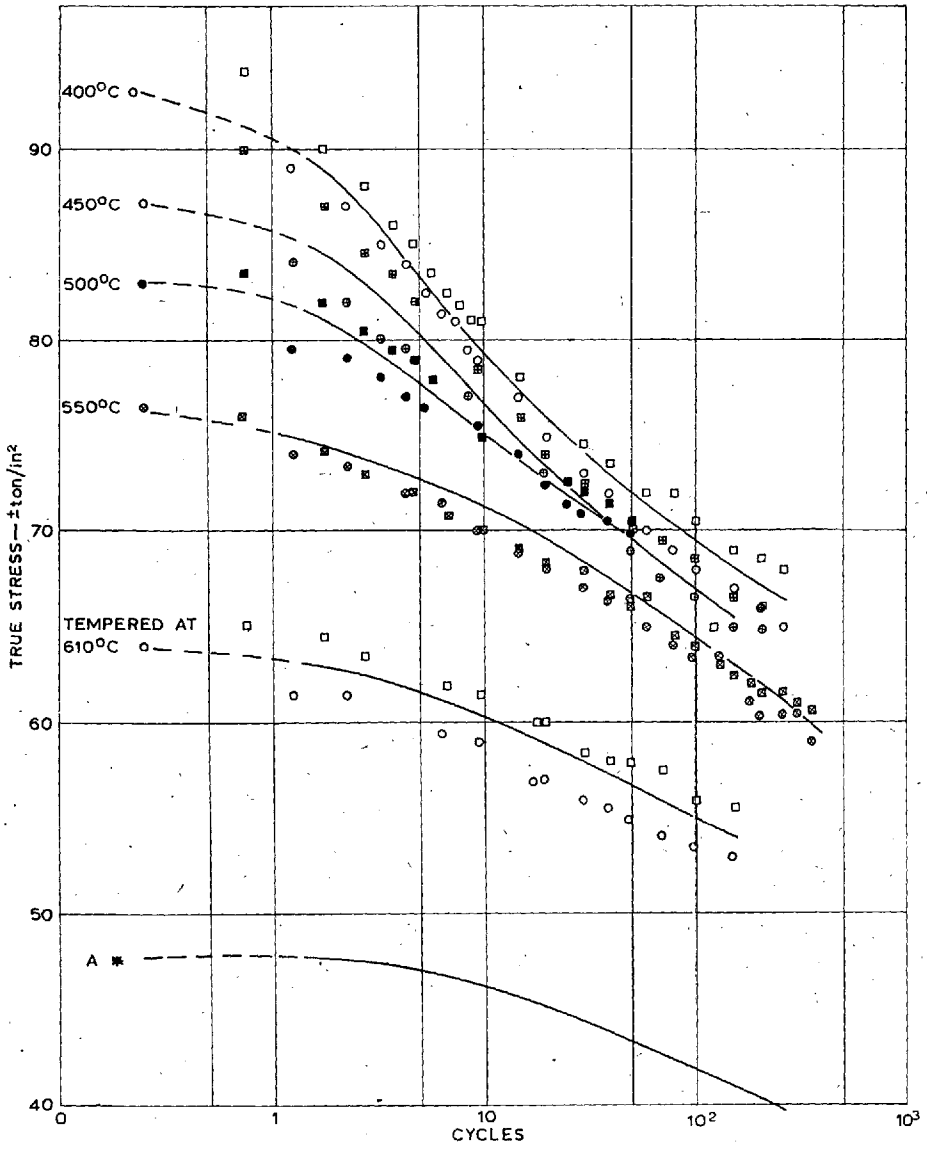

A Annealed.
* Points shown on another figure.

Fig. 2.10. Cyclic softening of hardened and tempered En 25 steel: ±1 per cent axial plastic strain

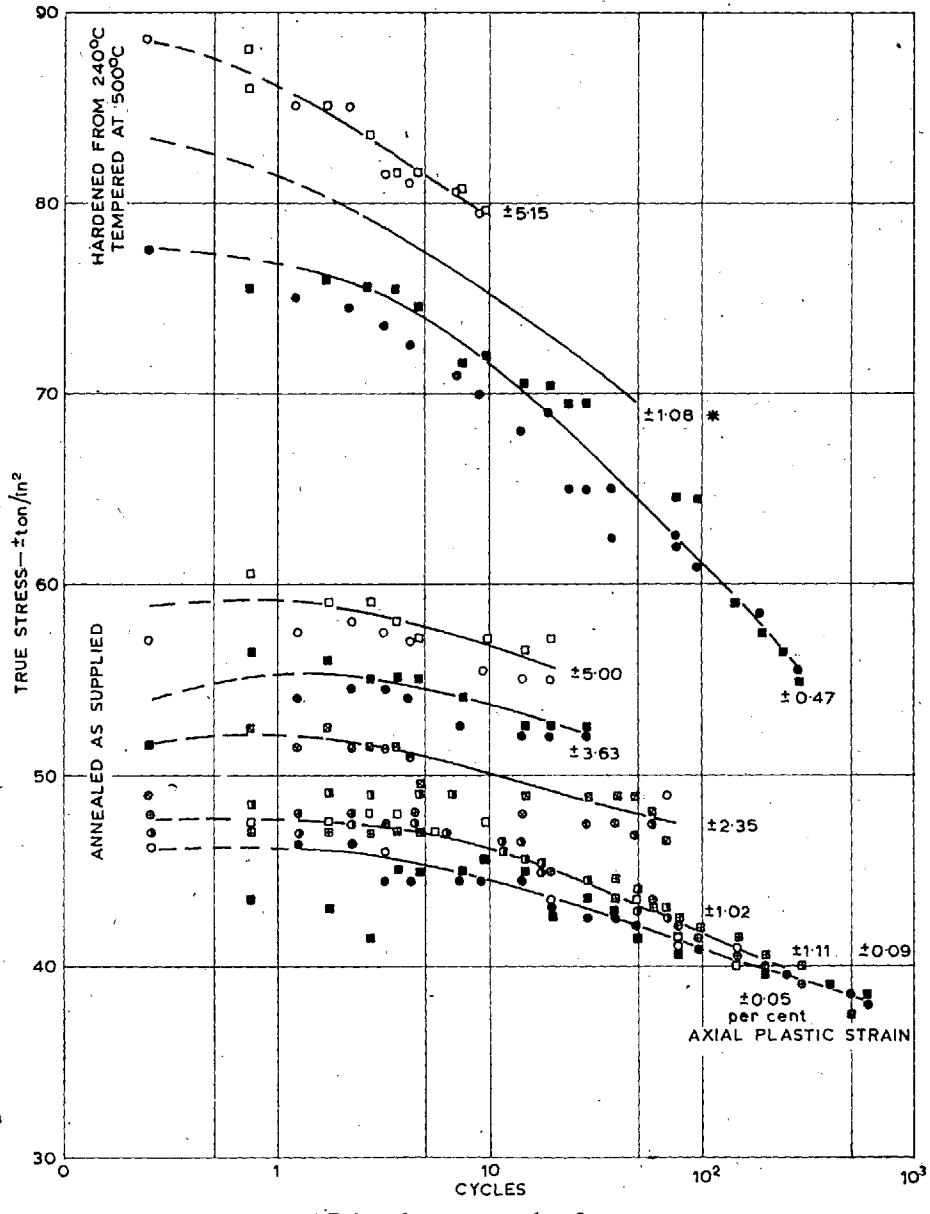

* Points shown on another figure.

Fig. 2.11. Effect of plastic strain range on the cyclic softening of En 25 steel

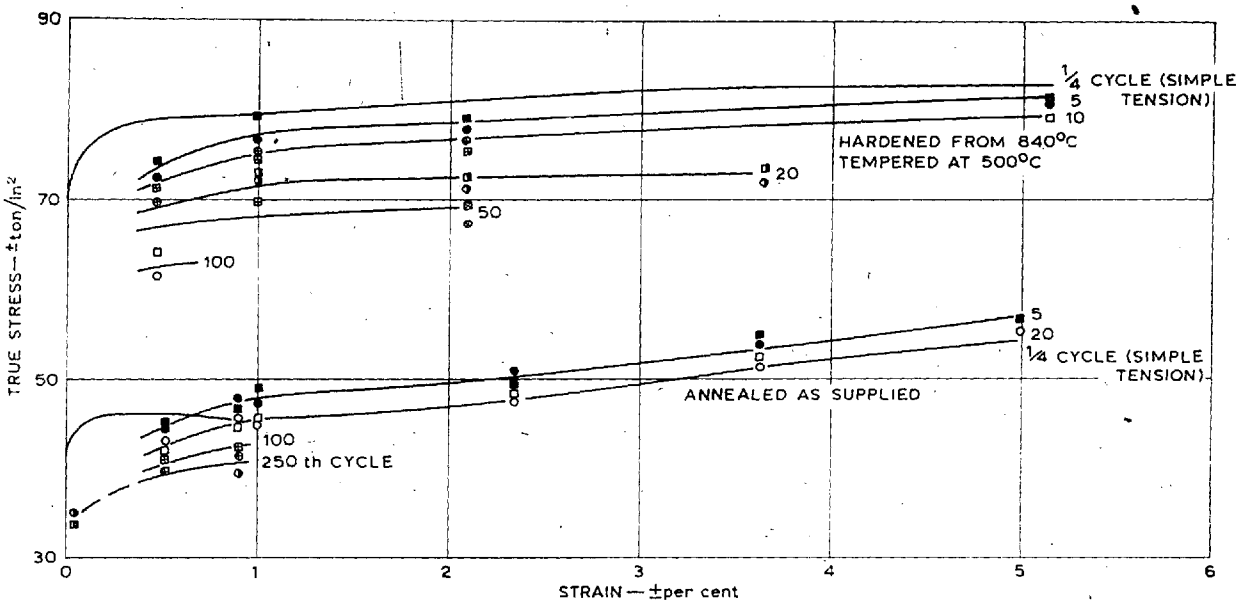

Fig. 2.12. Cyclic and static stress–strain curves for En 25 steel

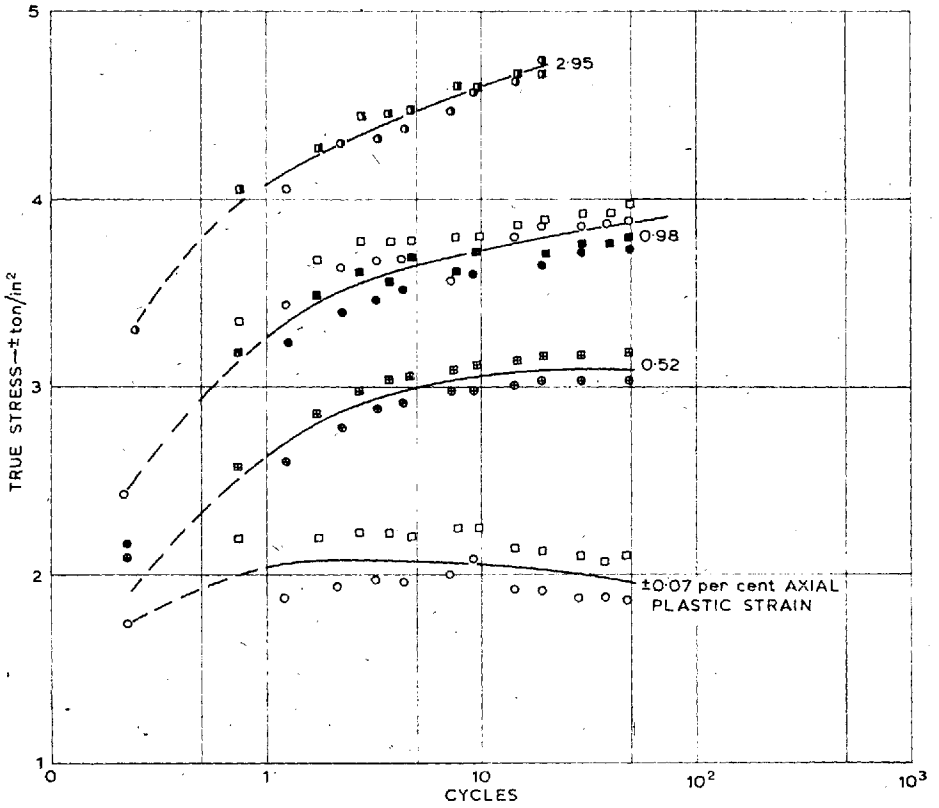

Fig. 2.13. Effect of plastic strain range on the cyclic hardening of annealed aluminium

En 25 steel

Fig. 2.9 shows the as-recorded stress–strain loops for a hardened and tempered En 25 steel specimen tested at a plastic strain amplitude of ±1 per cent. As with copper the change in stress amplitude per cycle decreases rapidly. Autographic records similar to Fig. 2.9 have been used to prepare Figs 2.10–2.12. Fig. 2.10 shows the results of tests at a plastic strain amplitude of ±1 per cent on specimens which were annealed or hardened and tempered at various temperatures. Fig. 2.10 and Fig. 2.11, which show the results of tests at other strain amplitudes, demonstrate that this steel always strain softens. The rate of cyclic softening increases with decrease in tempering temperature.

Fig. 2.11 has been used to prepare cyclic stress–strain curves for comparison with the corresponding simple tension curves, Fig. 2.12. This figure illustrates that significant strain softening only occurs in the annealed material when the strain amplitude is less than ±1 per cent and is associated with the elimination of the yield step.

Aluminium and stainless steel

Reversed strain cycling tests were also carried out on annealed aluminium and an austenitic stainless steel in the fully soft condition. As might be expected the aluminium results, Fig. 2.13, show the same trend as those for annealed copper, Fig. 2.3, but the rate of cyclic hardening is much lower.

The behaviour of the stainless steel, Fig. 2.14, is very different from that of the annealed En 25 steel, Fig. 2.11. However, similar results have been obtained by Smith *et al.* (**9**) for A.I.S.I. 304 E.L.C. stainless steel. The delayed hardening of these steels at low strain amplitudes is associated with the transformation of austenite to the body-centred lattice (**10**).

GENERAL DISCUSSION

An explanation of cyclical strain hardening and softening from a metallurgical viewpoint involving dislocation theory has been suggested elsewhere (**11**). However, it is also pertinent to attempt an explanation in terms of

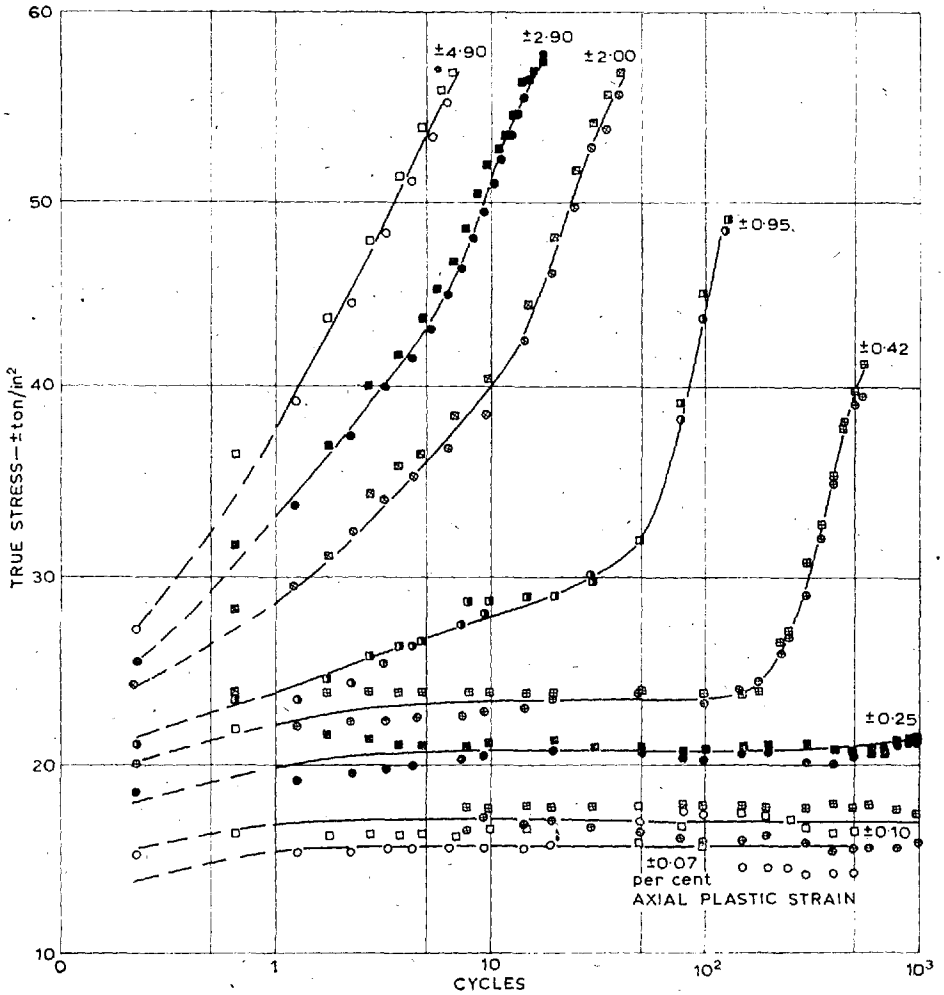

Fig. 2.14. Effect of plastic strain range on the cyclic hardening of austenitic stainless steel

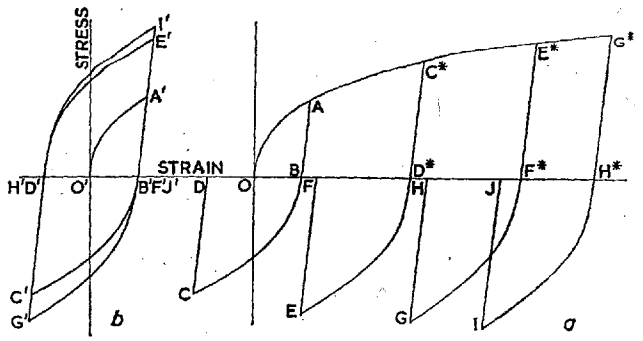

Fig. 2.15. Diagrammatic illustration of the use of simple Bauschinger curves to derive cyclic hardening hysteresis loops

experimentally determined stress–strain relations. First, the term Bauschinger effect will be used, but in this instance it will be defined as the difference in *shape* between a stress–strain curve determined in one loading direction to that obtained for loading in the opposite direction. For example, referring to Fig. 2.15*a*, the difference in shape between the curve OA and BC will be termed the Bauschinger effect and it will be assumed that this is the same either in tension or compression although it is not essential to the hypothesis. It will also be assumed that the Bauschinger effect is dependent on the last maximum stress prior to stress reversal and not on the stress–strain history.

Referring to Fig. 2.15*a*, let it be supposed that the curve OAC*E*G* is the stress–strain curve in simple tension for a material which would cyclically strain harden. If a specimen were subjected to a single reversal of plastic strain range BD it would traverse the path OABCD, in which BC would be different to OA owing to the Bauschinger effect and C would be higher than A. Next a further specimen is loaded monotonically in tension to C*, which has the same stress value as C, and then unloaded and reloaded in compression to E to give the plastic strain range FD* which is the same as BD. Again E will have a higher value than C* owing to the Bauschinger behaviour. Let the above process be repeated on, say, two further specimens for the cyclic paths OE*F*GH and OG*H*IJ, in each case keeping a constant plastic strain range during reversal, i.e. JH* = HF* = BD and E* = E, G* = G. The curves of Fig. 2.15*a* are now redrawn to give Fig. 2.15*b*. Curve OABC becomes O'A'B'C', curve C*D*EF is up-ended to become C'D'E'F'; curve E*F*GH becomes E'F'G'H' and so on. The result in Fig. 2.15*b* may be compared in form with the experimental behaviour for cyclical hardening in Fig. 2.2. If a series of single cycle tests such as in Fig. 2.15*a* are used to construct the stress–strain behaviour of Fig. 2.15*b* and the latter then agrees with the continuous cycling tests, then it is apparent that it is the last maximum stress before reversal and not the stress–strain history which is influencing the Bauschinger effect. In the example described above it was assumed that

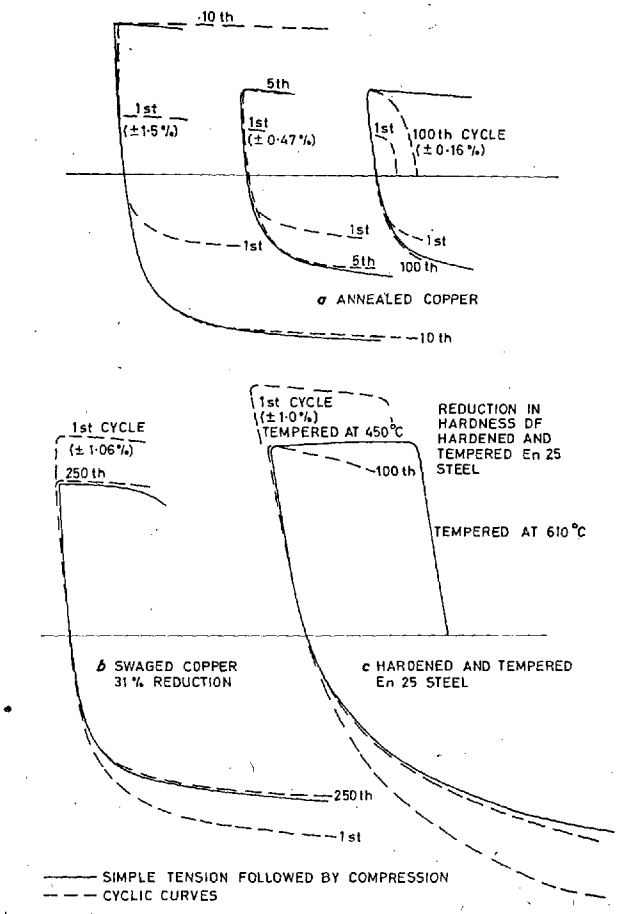

Fig. 2.16. Bauschinger effect in copper and En 25 steel

the Bauschinger effect always gave a peak compressive stress greater than the preceding peak tensile stress which leads to cyclic strain hardening. If the peak compressive stress was always less than the preceding peak tensile stress the material would cyclically strain soften. If the difference between the peak compressive and tensile stresses decreases as they increase in magnitude the material will harden or soften as explained above, but the rate of hardening or softening will decrease with cycling. If the difference between the peak compressive and tensile stresses becomes zero, hardening or softening ends.

The validity of the assumption that the Bauschinger effect is dependent on the magnitude of the last maximum stress and not on the stress–strain history has been examined for copper and En 25 steel. In Fig. 2.16 the Bauschinger effect is illustrated for specimens which have (*a*) been loaded in simple tension to a particular stress level followed by reversal into compression and (*b*) strain cycled to the same stress level as in (*a*). The relevant parts of the stress–strain curves from (*a*) and (*b*) above have been plotted for comparison. To show how the Bauschinger effect varies with cycling, Fig. 2.16 also shows part of the first loop for each cyclic specimen.

Although the agreement between the curves in Fig. 2.16 supports the assumption on which the explanation of cyclic strain hardening or softening is based, it must be emphasized that there are limits to the validity of the assumption. In particular the Bauschinger effect will almost certainly depend on stress–strain history if the tensile (compressive) stress prior to the Bauschinger reversal is considerably smaller than the preceding compressive (tensile) stress. Fortunately, this objection is not relevant to most of the strain-cycling tests described in this paper.

Finally it is interesting to note that the present tests support the suggestion by Smith (**9**) that materials with an ultimate/yield strength ratio greater than 1·4 cyclically harden and those with a ratio less than 1·2 cyclically soften.

CONCLUSIONS

Cyclic tension–compression tests between plastic strain limits show that:

(1) OFHC copper will cyclically strain harden or soften according to its initial state and the strain amplitude. The method by which this material is cold worked has little influence on its cyclic hardening or softening behaviour.

(2) En 25 steel always cyclically strain-softens; the degree of strain softening increasing with decrease in tempering temperature.

(3) Austenitic stainless steels may exhibit delayed cyclic hardening at small amplitudes.

(4) Cyclic hardening or softening of metallurgically stable materials can be explained principally in terms of the Bauschinger effect if certain simplifying assumptions are made.

(5) The aforementioned materials and annealed aluminium follow the rule proposed by Manson that materials with an ultimate/yield strength ratio greater than 1·4 cyclically harden and those for which this ratio is less than 1·2 cyclically soften.

ACKNOWLEDGEMENTS

The work was carried out in the Department of Mechanical Engineering, Imperial College, and was supported by the Department of Scientific and Industrial Research. The authors wish to thank Imperial Metal Industries (Kynoch) Ltd and Alcan Industries Ltd for processing the copper and aluminium.

APPENDIX 2.I

REFERENCES

(1) MORROW, JODEAN. 'Cyclic plastic strain energy and fatigue of metals', *Symposium on Internal Friction, Damping, and Cyclic Plasticity Phenomena*, Am. Soc. Test. Mater. Annual Meeting (Chicago) 1964 (June).

(2) POLAKOWSKI, N. H. and PALCHOUDHURI, A. 'Softening of cold-worked metals under the action of fatigue loads', *Proc. Am. Soc. Test. Mater.* 1954 **54**, 701.

(3) COFFIN, L. F. 'The influence of mean stress on the mechanical hysteresis loop shift of 1100 aluminium', *J. basic Engng, Trans. Am. Soc. mech. Engrs* 1964 **86** (Series D), 673.

(4) LANGER, B. F. 'Design of pressure vessels for low-cycle fatigue', *ibid.*, 1962 **84**, 389.

(5) MANSON, S. S. 'Thermal stresses in design. Pt. 18: Working stresses for ductile materials', *Machine Design* 1960 **32** (June 23, No. 13), 153; also Pt. 19, 1960 **32** (July 7, No. 14), 139.

(6) SUITS, G. 'Steel—and its opportunities', *The Charles M. Schwab Memorial Lecture*, 71st General Meeting American Iron and Steel Institute 1963.

(7) COFFIN, L. F. 'Contact–bend–stretch rolling process', *Engineer, Lond.* 1964 **217**, 678.

(8) OLDROYD, P. W. J. 'Modifications to an Instron testing machine for cyclic loading in the plastic range', Paper 27, Jt Conv. on Machines for Materials and Environmental Testing (Manchester) 1965, *Proc. Instn mech. Engrs* 1965–66 **180** (Pt 3A).

(9) SMITH, R. W., HIRSCHBERG, M. H. and MANSON, S. S. 'Fatigue behaviour of materials under strain cycling in low and intermediate life range', *N.A.S.A. tech. Note D* 1574, 1963 (April).

(10) BRICK, R. M. and PHILLIPS, A. *Structure and properties of alloys*, 1942, 160 (McGraw-Hill Book Co. Inc., New York).

(11) OLDROYD, P. W. J. and BENHAM, P. P. 'Stress–strain behaviour of copper and zinc cubes subjected to cyclical compression', *Int. J. mech. Sci.* (to be published).

MADE AND PRINTED IN GREAT BRITAIN BY WILLIAM CLOWES AND SONS, LIMITED, LONDON AND BECCLES